PHYSICAL CONDITIONS OF THE CIRCUMGALACTIC MEDIUM

Hsiao-Wen Chen

The University of Chicago

Department of Astronomy & Astrophysics

Kavli Institute for Cosmological Physics

International Summer School on the ISM of Galaxies.

GISM 2023, July 25th-August 2nd, Banyuls-sur-Mer, France

<u>PHYSICAL CONDITIONS</u> OF THE CIRCUMGALACTIC MEDIUM

Thermodynamics, ionization, and chemical enrichment

Hsiao-Wen Chen

The University of Chicago

Department of Astronomy & Astrophysics

Kavli Institute for Cosmological Physics

OUTLINE

1. Background motivation
2. A brief review of line profile physics
3. Physical properties of the diffuse circumgalactic medium from emission maps
4. Physical properties of the diffuse circumgalactic medium from absorption spectroscopy
5. Connections to the ISM and star formation histories

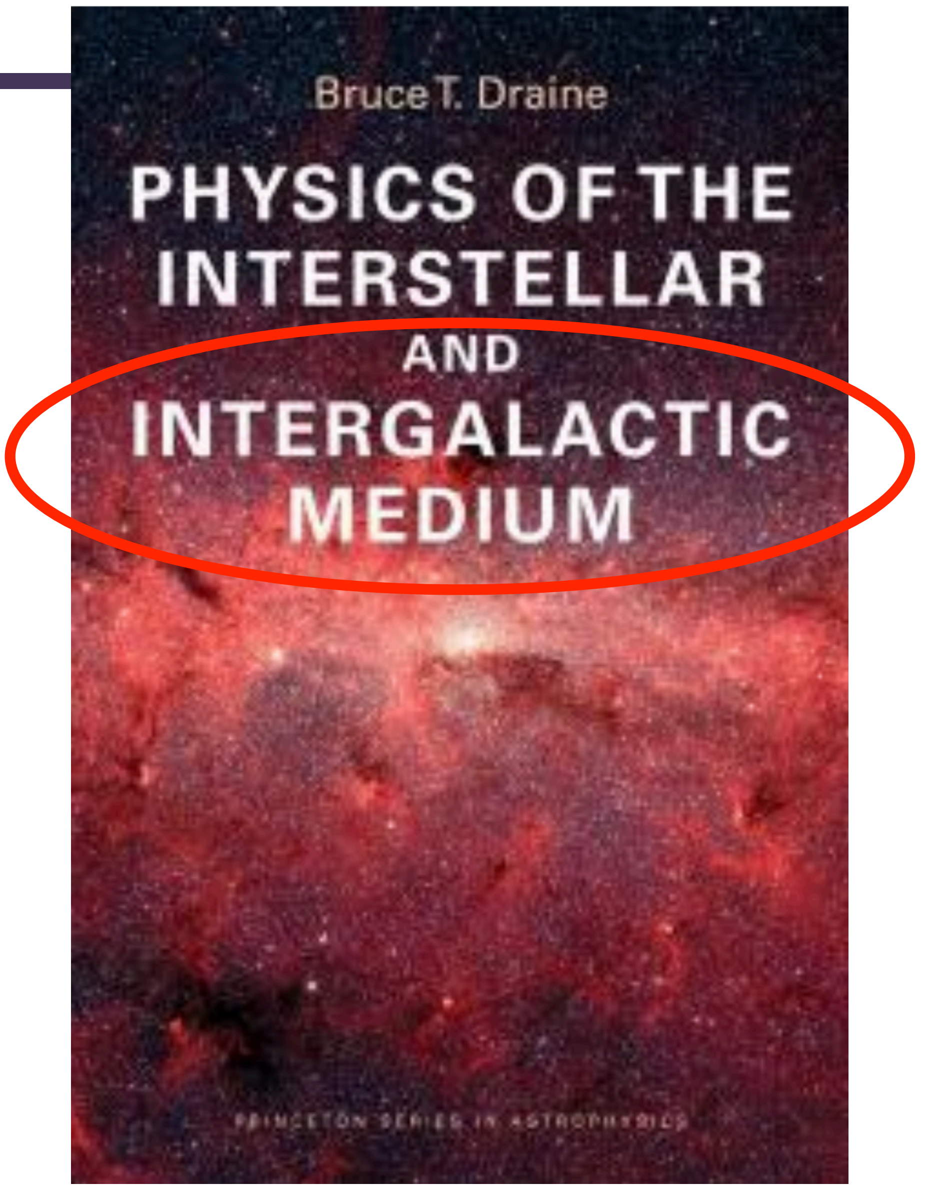

OUTLINE

1. Background motivation
2. A brief review of line profile physics
3. Physical properties of the diffuse circumgalactic medium from emission maps
4. Physical properties of the diffuse circumgalactic medium from absorption spectroscopy
5. Connections to the ISM and star formation histories

REFERENCES

1. "Key Physical Processes in the Circumgalactic Medium" ARA&A (2023), Claude-André Faucher-Giguère & Peng Oh

2. "Baryon Cycles in the Biggest Galaxies" Physics Reports (2022), Megan Donahue & G Mark Voit

3. "The Circumgalactic Medium" ARA&A (2017), Jason Tumlinson, Molly Peeples, & Jessica Werk

4. "Outskirts of Distant Galaxies in Absorption", Outskirts of Galaxies, Astrophysics and Space Science Library (2017), Hsiao-Wen Chen

5. "The Circumgalactic Medium in Massive Halos", Gas Accretion onto Galaxies, Astrophysics and Space Science Library (2017), Hsiao-Wen Chen

WHAT IS THE CIRCUMGALACTIC MEDIUM (CGM)?

From the "edge" of the stellar body to the "edge" of the DM halo

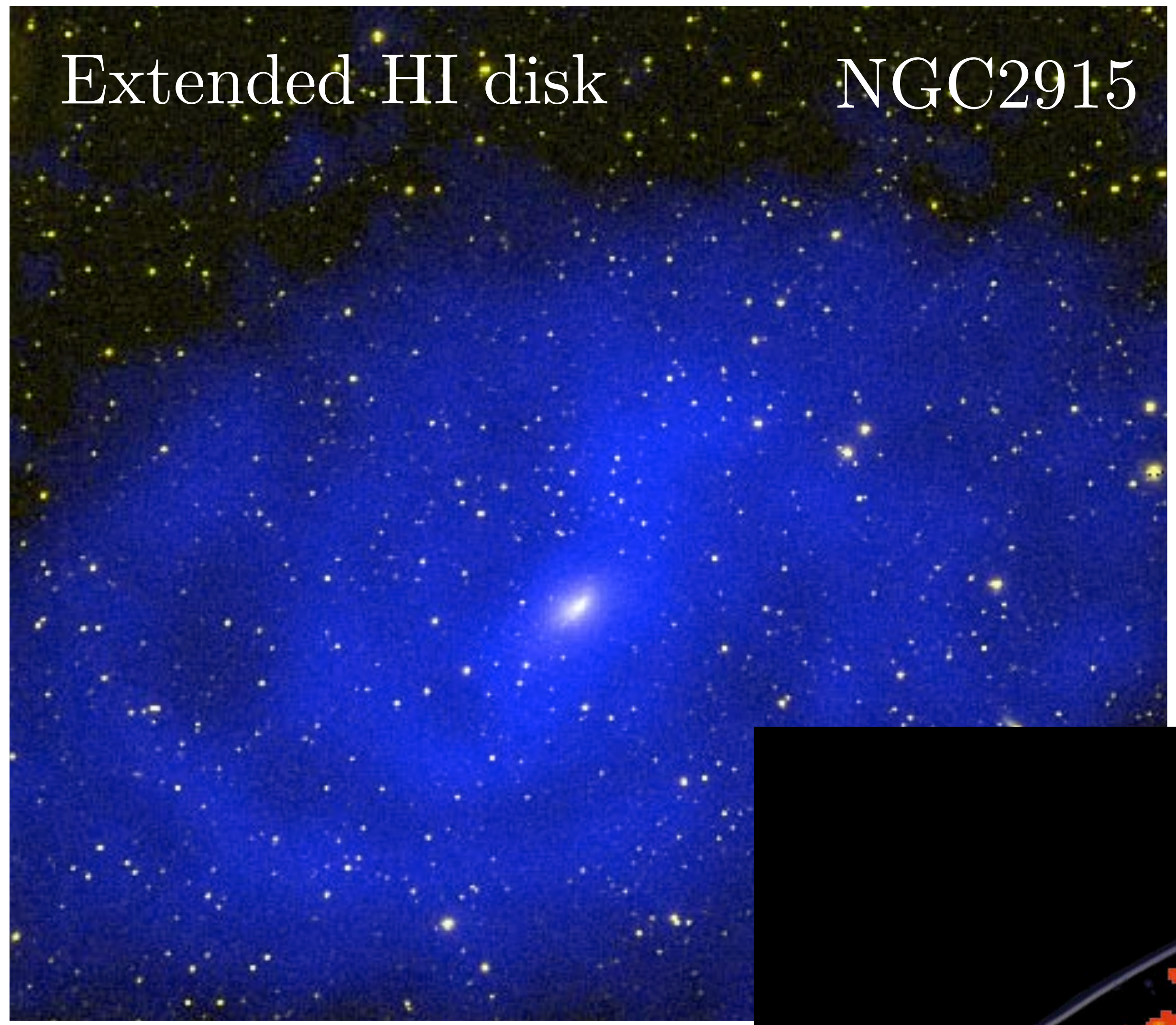

High velocity clouds

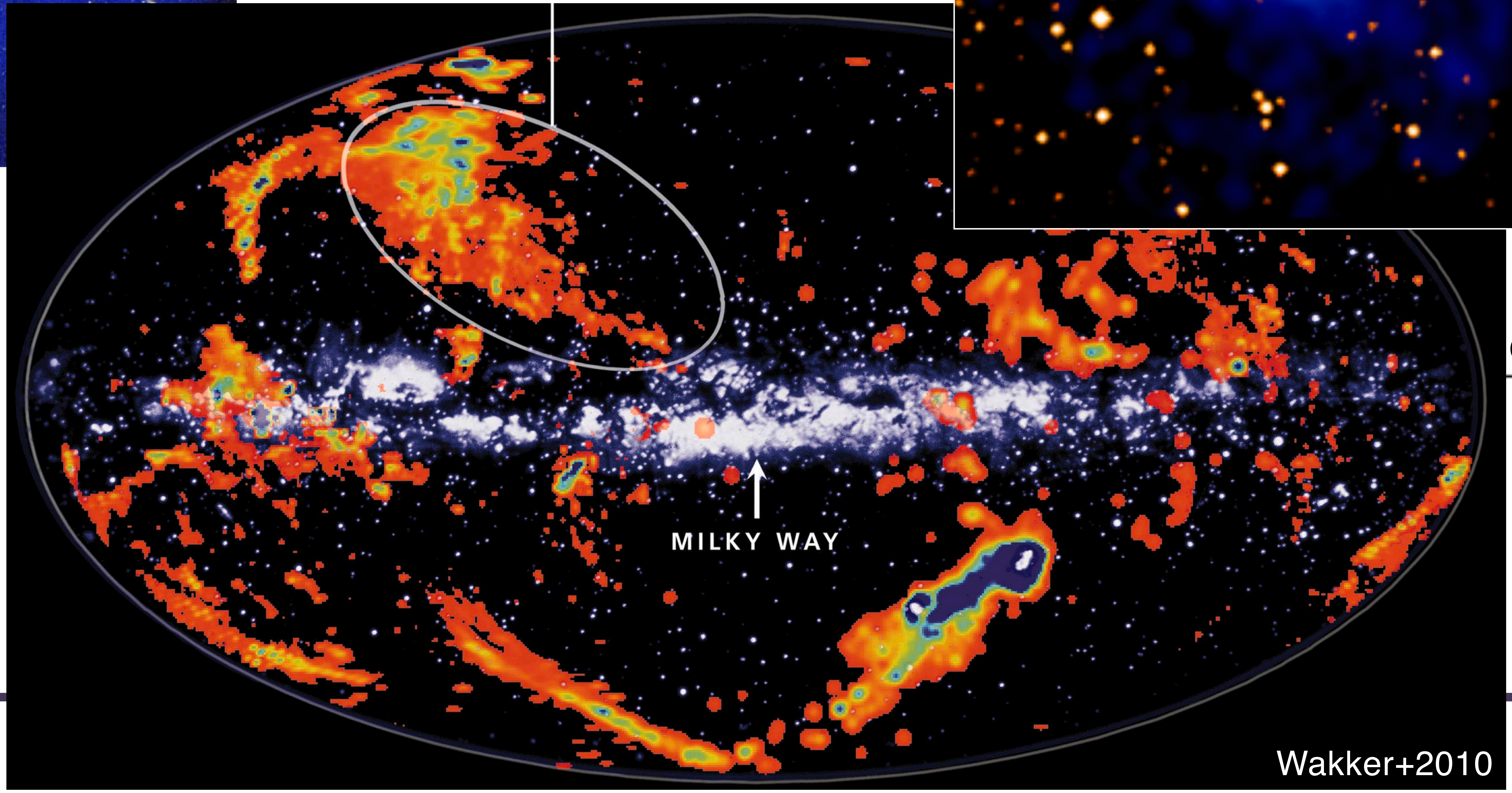

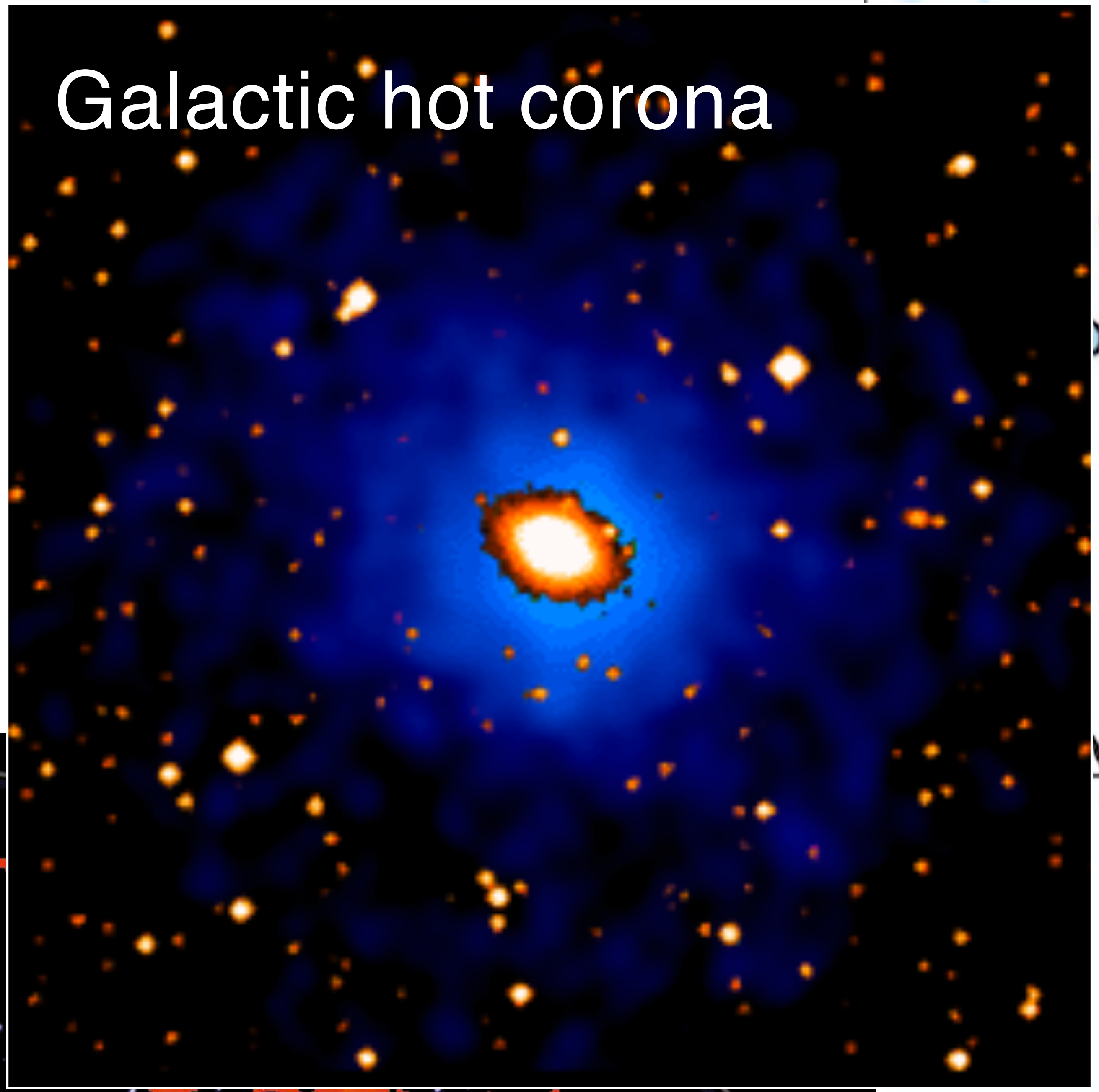

Extraplanar gas

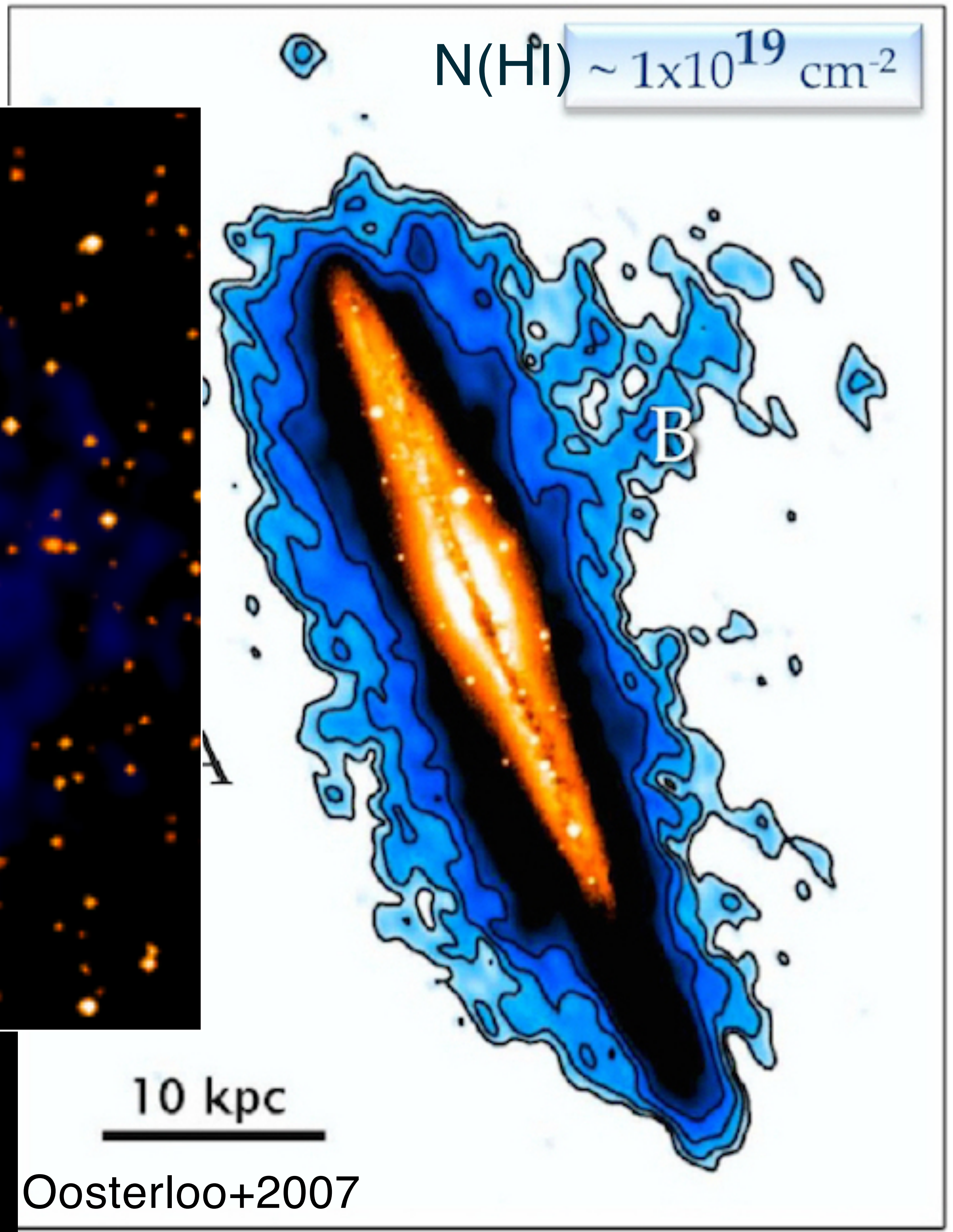

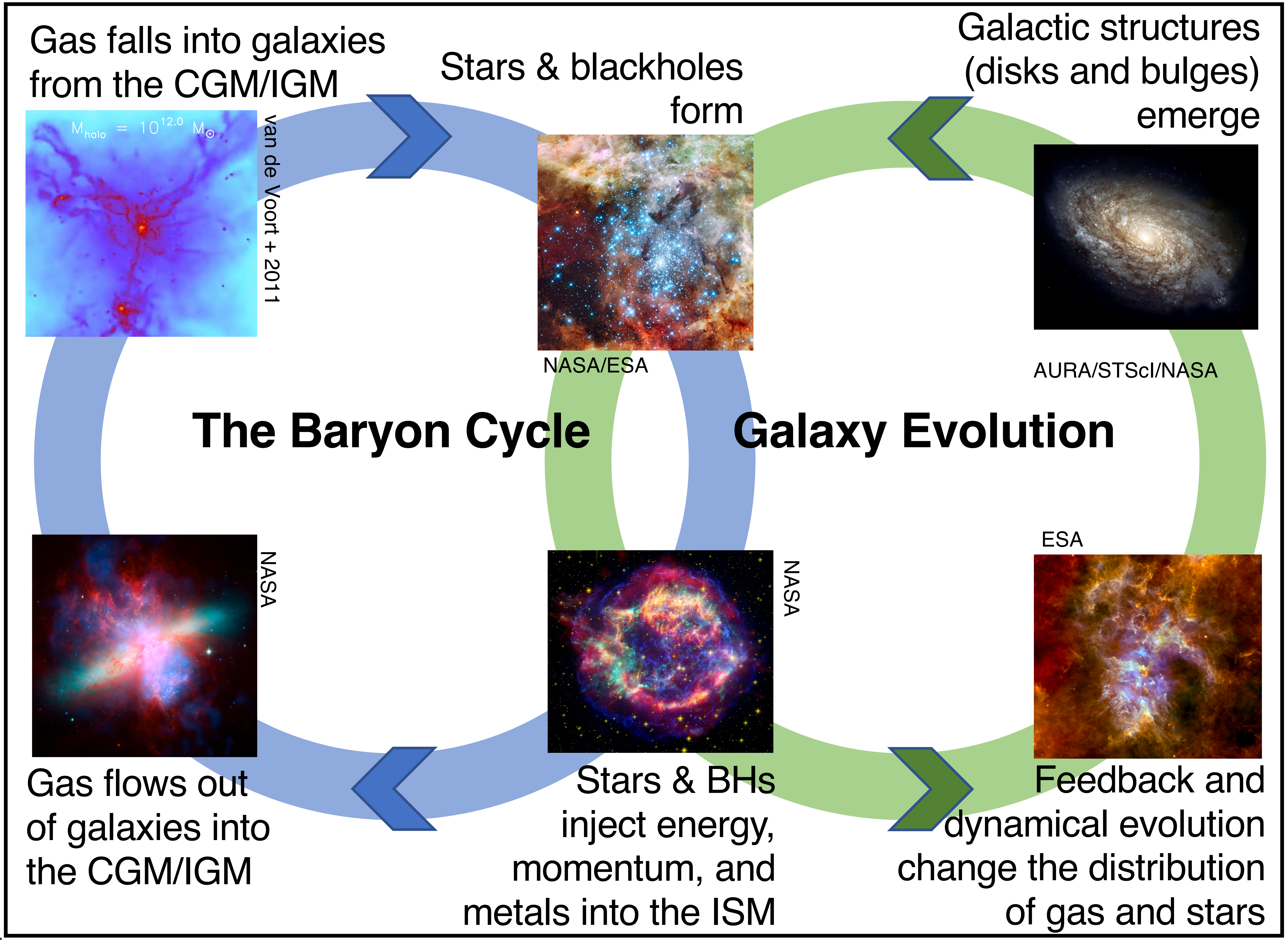

Adapted from Newman+2019

COSMIC BARYON BUDGET

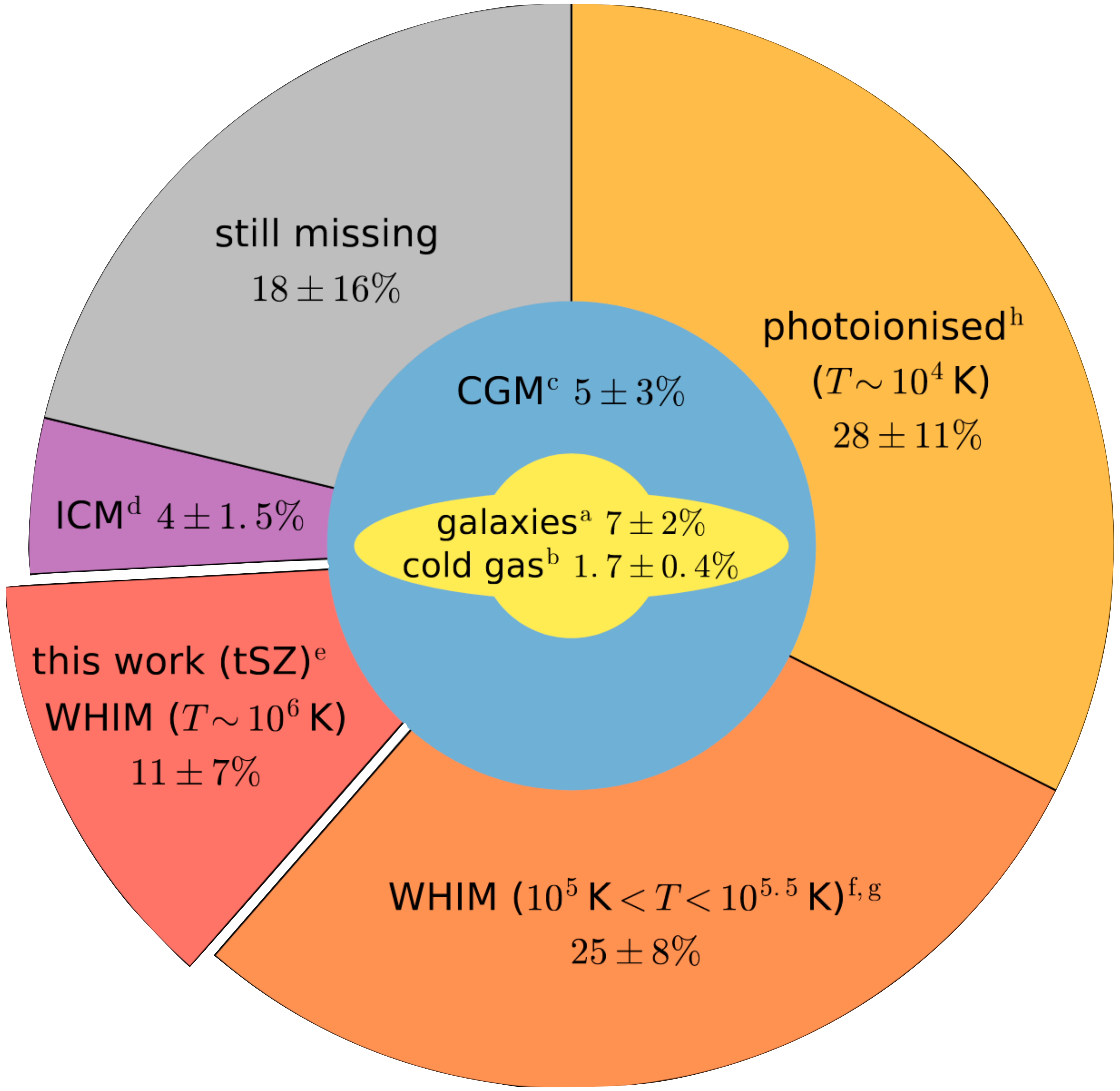

de Graaff, Cai, Heymans, Peacock (2019)

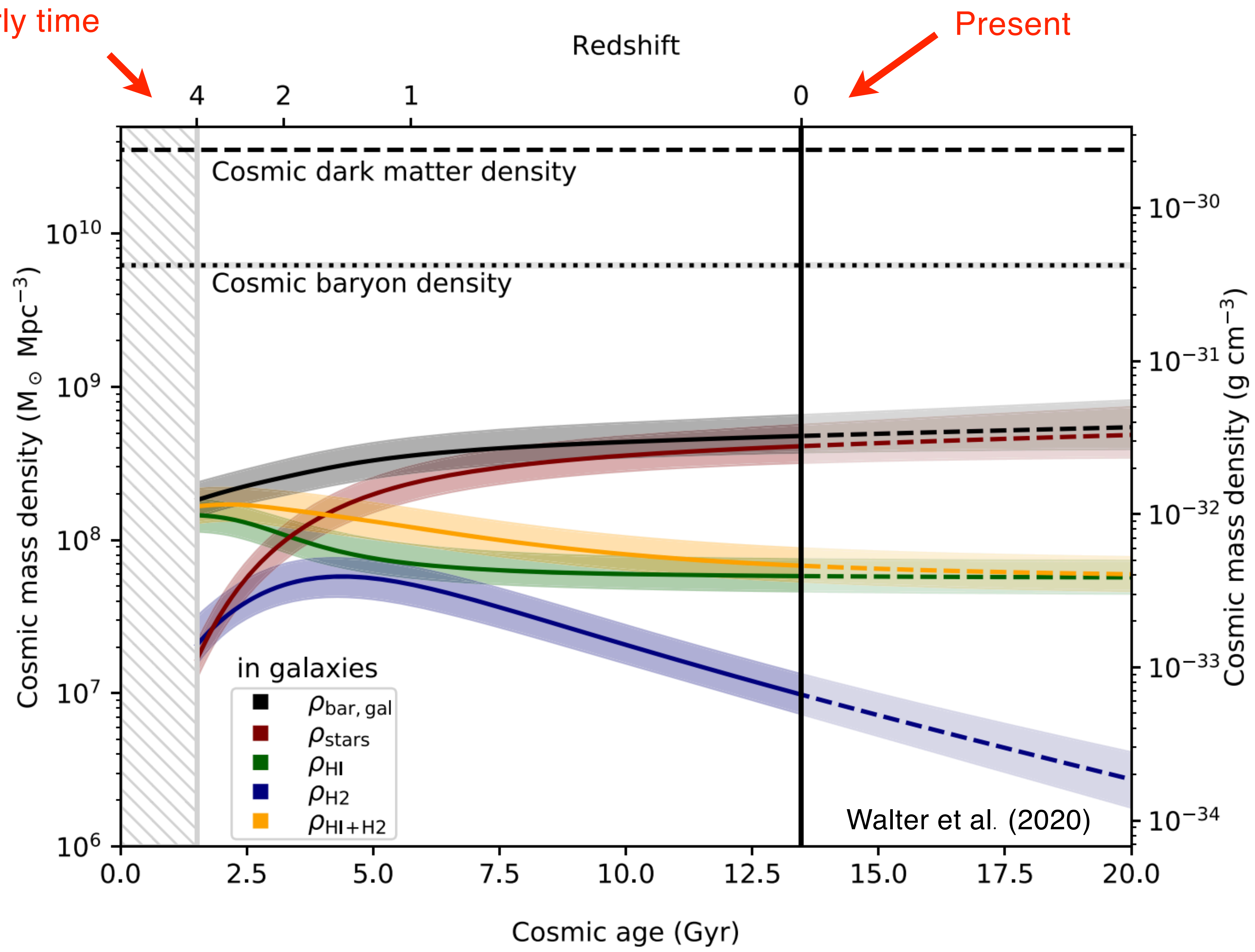

THE MULTI-SCALE & MULTIPHASE CHALLENGE OF TRACKING THE BARYON CYCLE

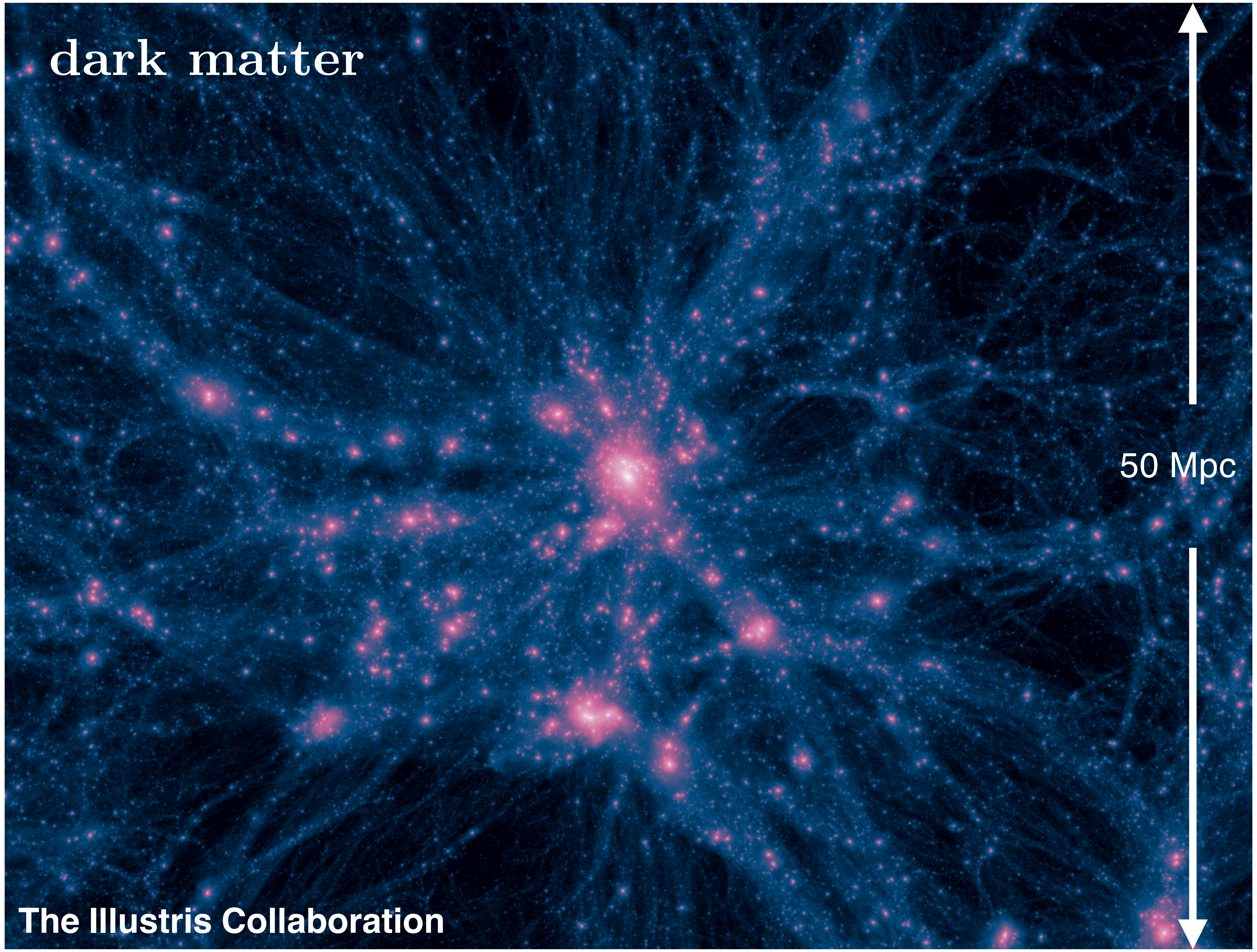

THE MULTI-SCALE & MULTIPHASE CHALLENGE OF TRACKING THE BARYON CYCLE

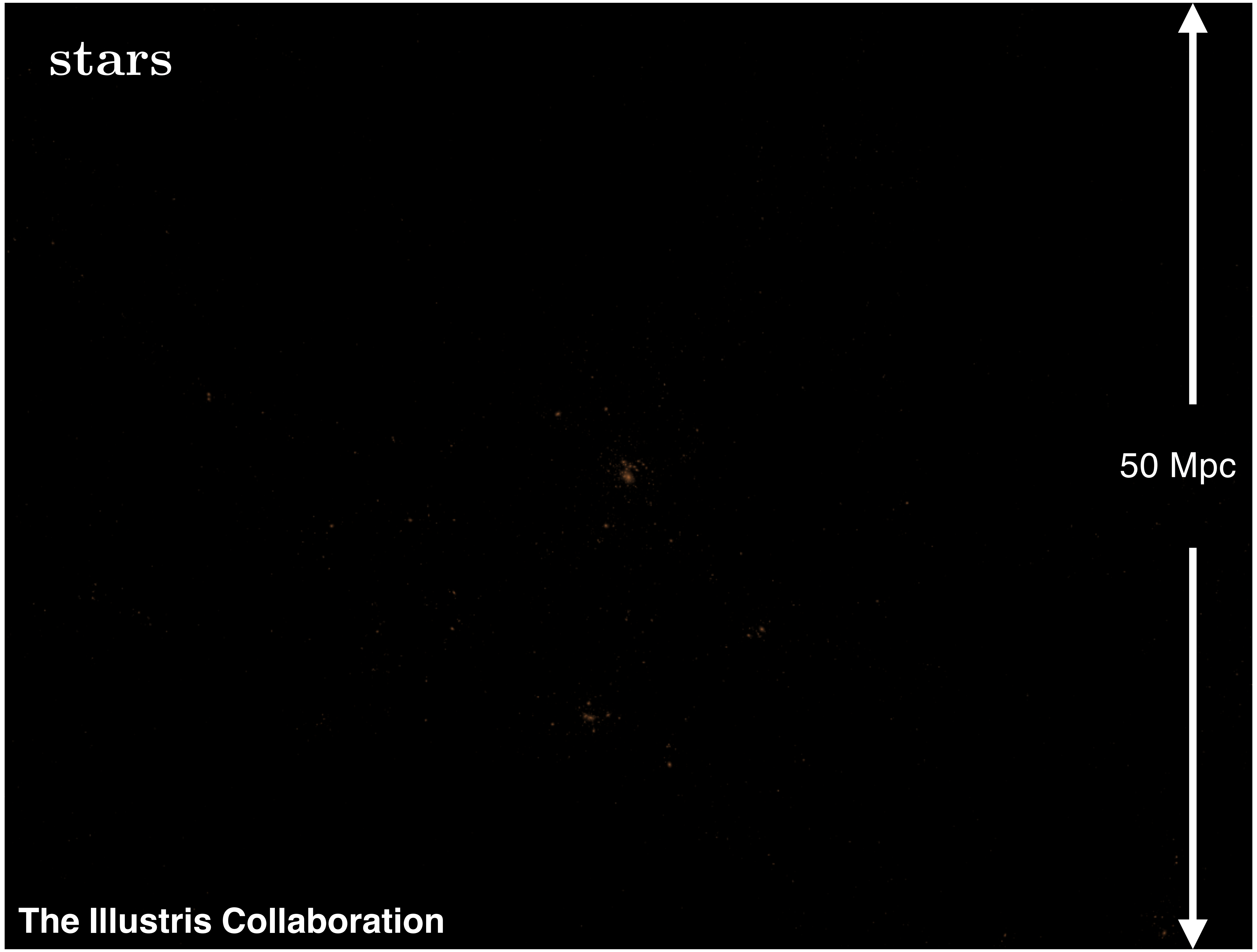

THE MULTI-SCALE & MULTIPHASE CHALLENGE OF TRACKING THE BARYON CYCLE

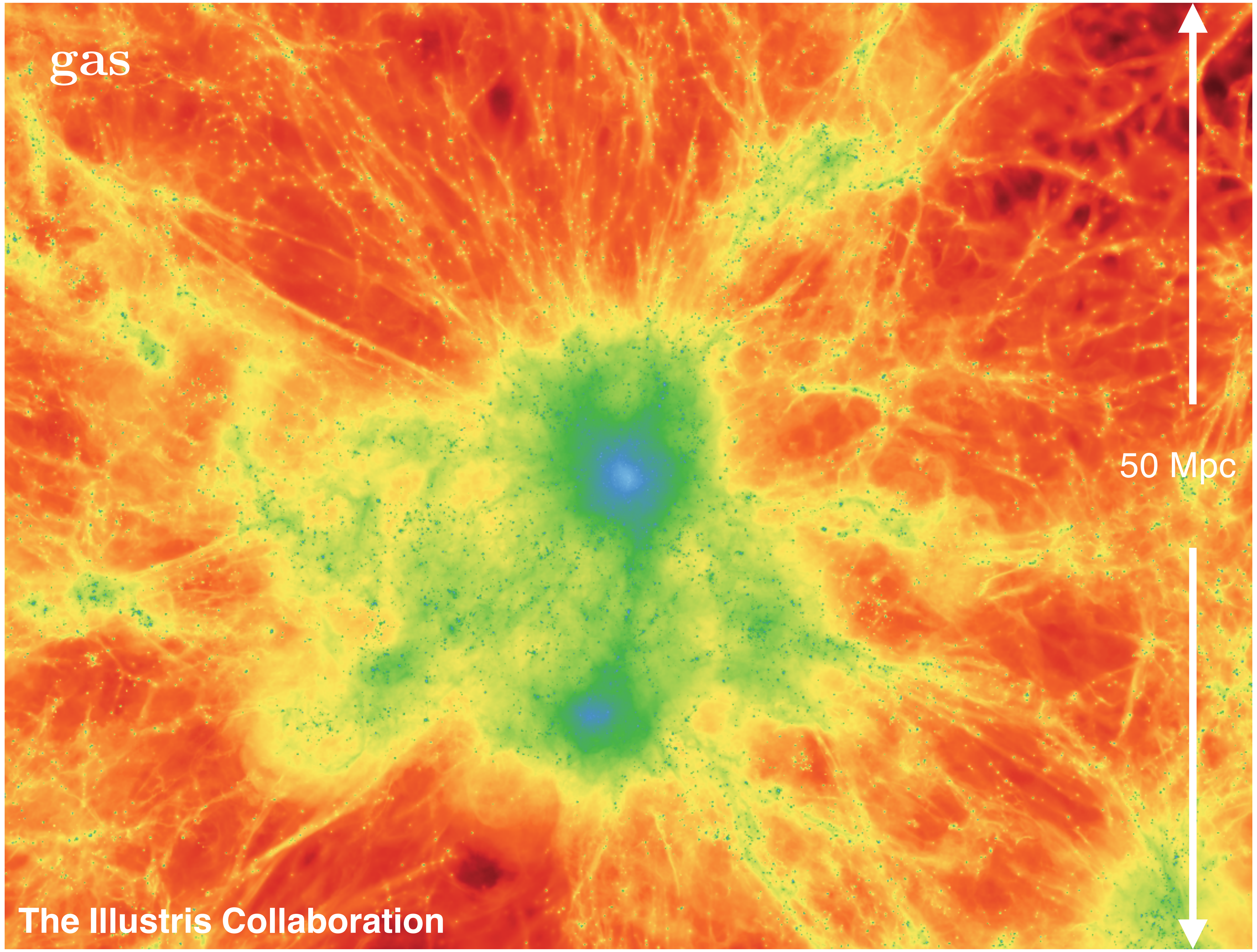

THE MULTI-SCALE & MULTIPHASE CHALLENGE OF TRACKING THE BARYON CYCLE

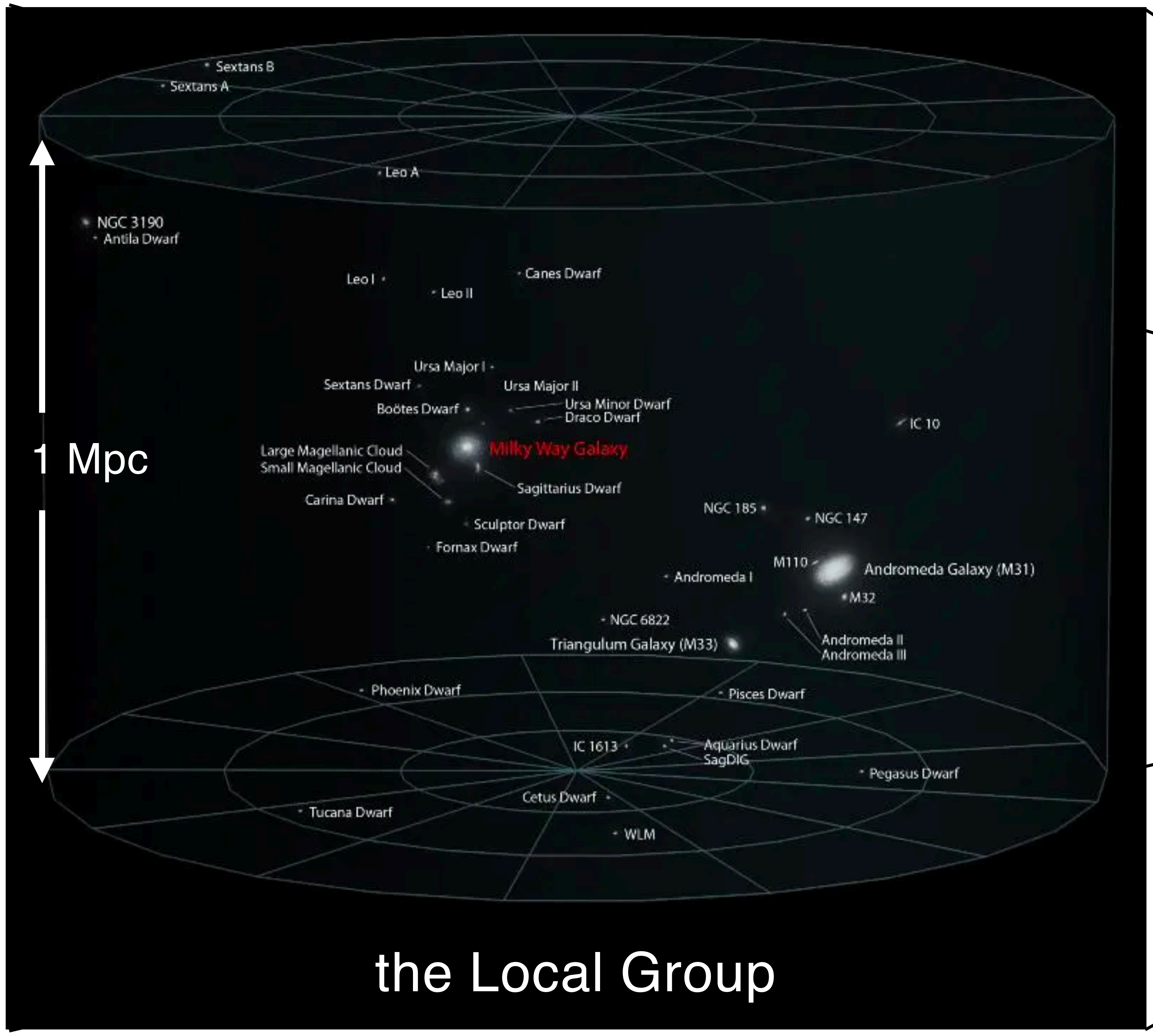

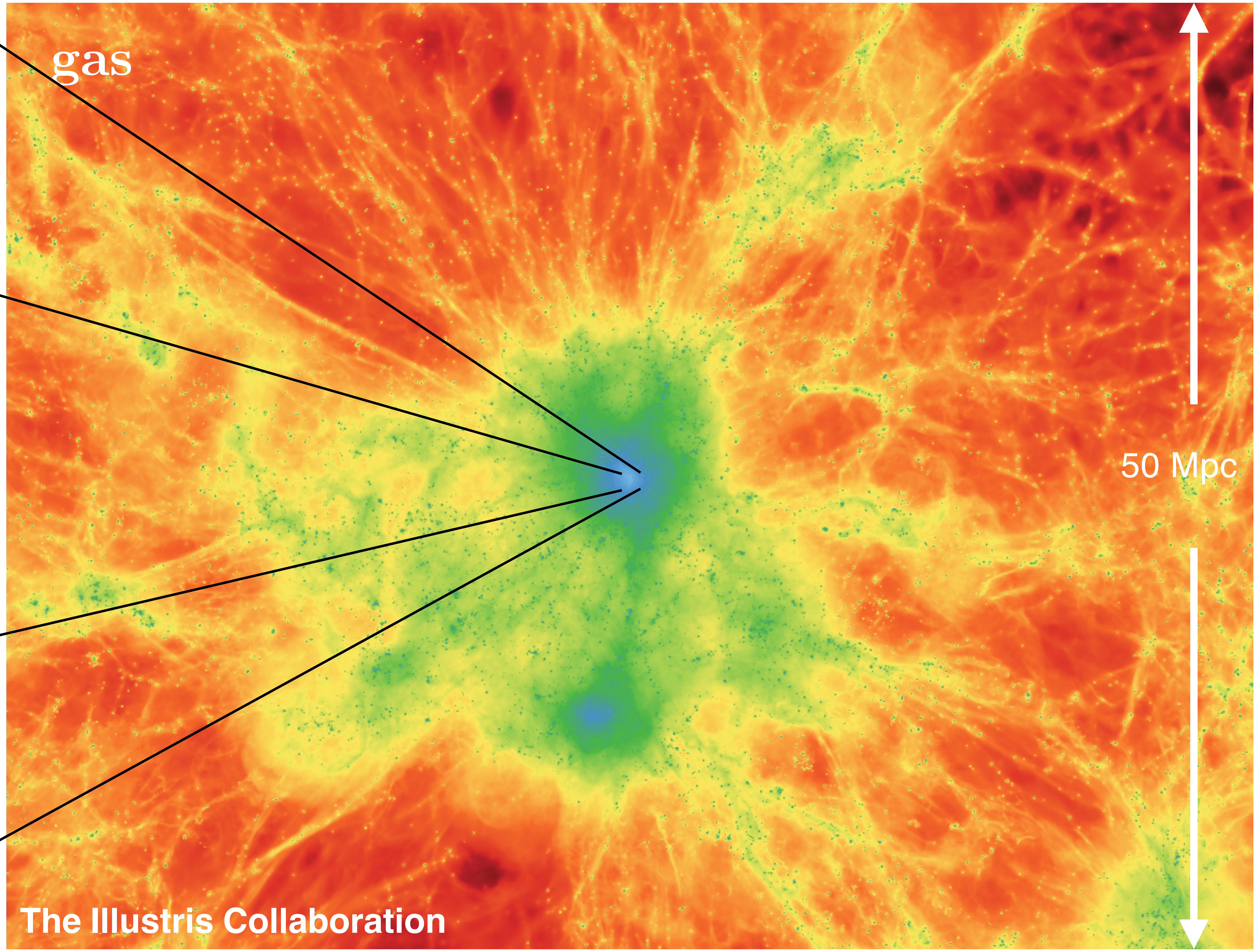

THE MULTI-SCALE & MULTIPHASE CHALLENGE OF TRACKING THE BARYON CYCLE

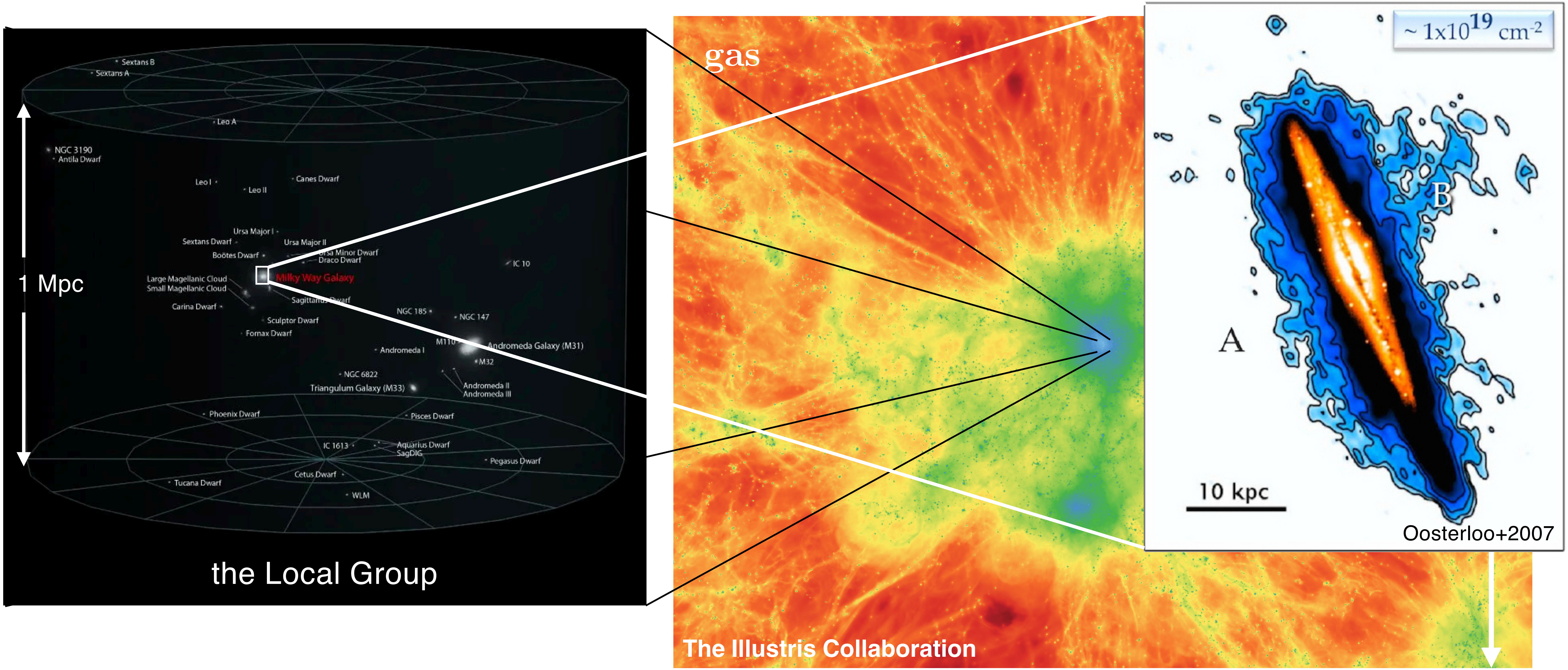

THE MULTI-SCALE & MULTIPHASE CHALLENGE OF TRACKING THE BARYON CYCLE

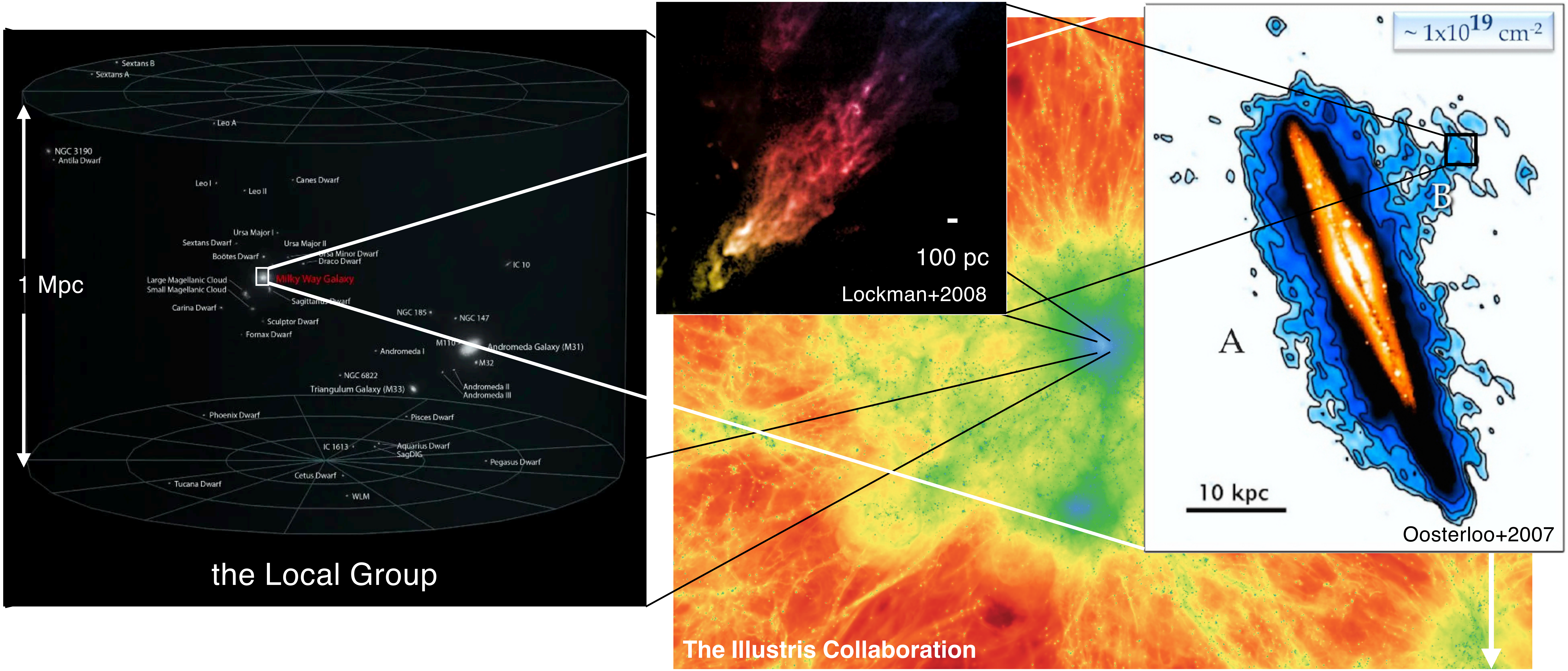

THE MULTI-SCALE & MULTIPHASE CHALLENGE OF TRACKING THE BARYON CYCLE

DIFFICULTIES IN MAPPING THE DIFFUSE COSMIC WEB

Simcoe (2004)

Line profiles

From radiative transfer, $\frac{dI_\nu}{ds} = -n_X\sigma_\nu I_\nu + j_\nu$ with optical depth $\tau_\nu(s) = \int n_X\sigma_\nu\, ds = N_X\,\sigma_\nu$

Considering a resolved line profile $\phi(\Delta\nu)$, $\tau_\nu = N_X\,\sigma_\nu\,\phi(\Delta\nu)$ and $\phi(\Delta\nu) \neq \delta(\nu - \nu_{ij})$

What are possible line broadening mechanisms?

(1) Intrinsic line width (wings): finite life time of the upper level acts like a damping term

The solution takes the form of Lorentz profile $\Phi(\Delta\,\nu) = \frac{\Gamma/4\pi^2}{(\Delta\,\nu)^2 + (\frac{\Gamma}{4\pi})^2}$, where Γ is the damping coefficient

(2) Doppler motion (line core) : Maxwellian distribution $\Phi(\Delta\nu) = \frac{1}{\sqrt{\pi}}\frac{\lambda_{jk}}{b}\exp\left[-\left(\frac{\Delta\nu}{\Delta\nu_D}\right)^2\right]$ $\propto \exp\left[-\frac{mv_z^2}{2kT}\right]$

The Doppler width is $\Delta\,\nu_D = b\,\frac{\nu_{ij}}{c} = \frac{b}{\lambda_{ij}}$ and therefore the Doppler parameter and line-of-sight velocity dispersion are related according to $b = \sqrt{2}\,\sigma_v$

In principle, the observed line width constrains the gas temperature $b = \sqrt{\frac{2kT}{m}} = 1.29 \times 10^4 \sqrt{\frac{T}{A}}\ \mathrm{cm\,s^{-1}}$

But turbulent motions and bulk flows are also expected to contribute to the observed line width $b = \sqrt{\frac{2kT}{m} + b_{\rm bulk}^2}$

Lyα emission

For photoionization, absorption of ionizing photons is accompanied by recombination, generating a series of recombination lines.

In the case of Lyα, the recombination emissivity $j_\nu = \frac{h\nu_{\mathrm{Ly}\alpha}}{4\pi}\eta\, n_e n_p \alpha(T)$, where $\eta = 0.68$ (0.41) is the fraction of recombinations that result in a Lyα photon under optically thick (thin) conditions

The observed Lyα surface brightness of optically-thin (highly-ionized) gas is

C : clumping factor $C \equiv \frac{\langle n^2 \rangle}{\langle n \rangle^2}$

$$\mathrm{SB}_{\mathrm{Ly}\alpha} = \frac{\eta_{\mathrm{thin}} h\nu_{\mathrm{Ly}\alpha}}{4\pi(1+z)^4}\alpha\left(1+\frac{Y}{2X}\right) n_{\mathrm{H}} N_{\mathrm{H}} = 7.7\times10^{-19}\left(\frac{1+z}{3}\right)^{-4}\left(\frac{n_{\mathrm{H}}}{0.1\,\mathrm{cm}^{-3}}\right)\left(\frac{N_{\mathrm{H}}}{10^{20}\,\mathrm{cm}^{-2}}\right)\mathrm{erg\,s^{-1}\,cm^{-2}\,arcsec^{-2}}$$

Under photo-ionization equilibrium, $n_{\mathrm{HI}}\Gamma = n_e n_p \alpha(T)$ where $\Gamma = \frac{1}{4\pi r^2}\int_{\nu_{\mathrm{LL}}}^{\infty}\frac{L_\nu}{h\nu}\sigma_\nu\, d\nu$ is the photo-ionization rate, ν_{LL} is the frequency of at the Lyman edge, and σ_ν is the hydrogen photo-ionization cross-section.

Lyα emission

Photo-ionization equilibrium implies that $j_{\mathrm{Ly}\alpha} \propto n_{\mathrm{HI}}\,\Gamma$. At the same time, neutral fraction $x_{\mathrm{HI}} \approx \alpha\, n_{\mathrm{H}}\left(1+\frac{Y}{2X}\right)\Big/\Gamma$.

In the optically-thin regime, Lyα emission is <u>independent</u> of the strength of the ionizing source, leading to

$$\langle N_{\mathrm{HI}}\rangle = 2.2\times10^{17}\left(\frac{1+z}{3}\right)^{-4}\left(\frac{L_{\mathrm{LL}}}{10^{30}\,\mathrm{erg\,s^{-1}cm^{-2}\,arcsec^{-2}}}\right)^{-1}\left(\frac{R}{100\,\mathrm{kpc}}\right)^{2}\left(\frac{\mathrm{SB}_{\mathrm{Ly}\alpha}}{10^{-17}\,\mathrm{erg\,s^{-1}\,cm^{-2}\,arcsec^{-2}}}\right)\mathrm{cm^{-2}}$$

In the optically-thick regime, self-shielding becomes important and Lyα emission scales with the strength of the ionizing source $\mathrm{SB}_{\mathrm{Ly}\alpha} = \frac{\Theta\,\eta_{\mathrm{thick}}\,h\nu_{\mathrm{Ly}\alpha}}{4\pi(1+z)^4}\frac{\Phi}{\pi} = 4.0\times10^{-17}\left(\frac{1+z}{3}\right)^{-4}\left(\frac{\Theta}{0.5}\right)\left(\frac{R}{100\,\mathrm{kpc}}\right)^{-2}\left(\frac{L_{\mathrm{LL}}}{10^{30}\,\mathrm{erg\,s^{-1}\,Hz^{-1}}}\right)\mathrm{erg\,s^{-1}\,cm^{-2}\,arcsec^{-2}}$

<u>What happens to a Lyα photon after it is generated?</u>

the resonant absorption cross section for Lyα in 10^4 K gas is 10,000 times larger than ionizing cross section

Lyα photons from 2p to 1s will be scattered (re-absorbed & re-emitted) many times. Because of random motion of particles at ~ 10 km/s, each scattered photon undergoes random walk in frequency. The photons that are scattered into the wings of the line profile will have a higher probability to escape.

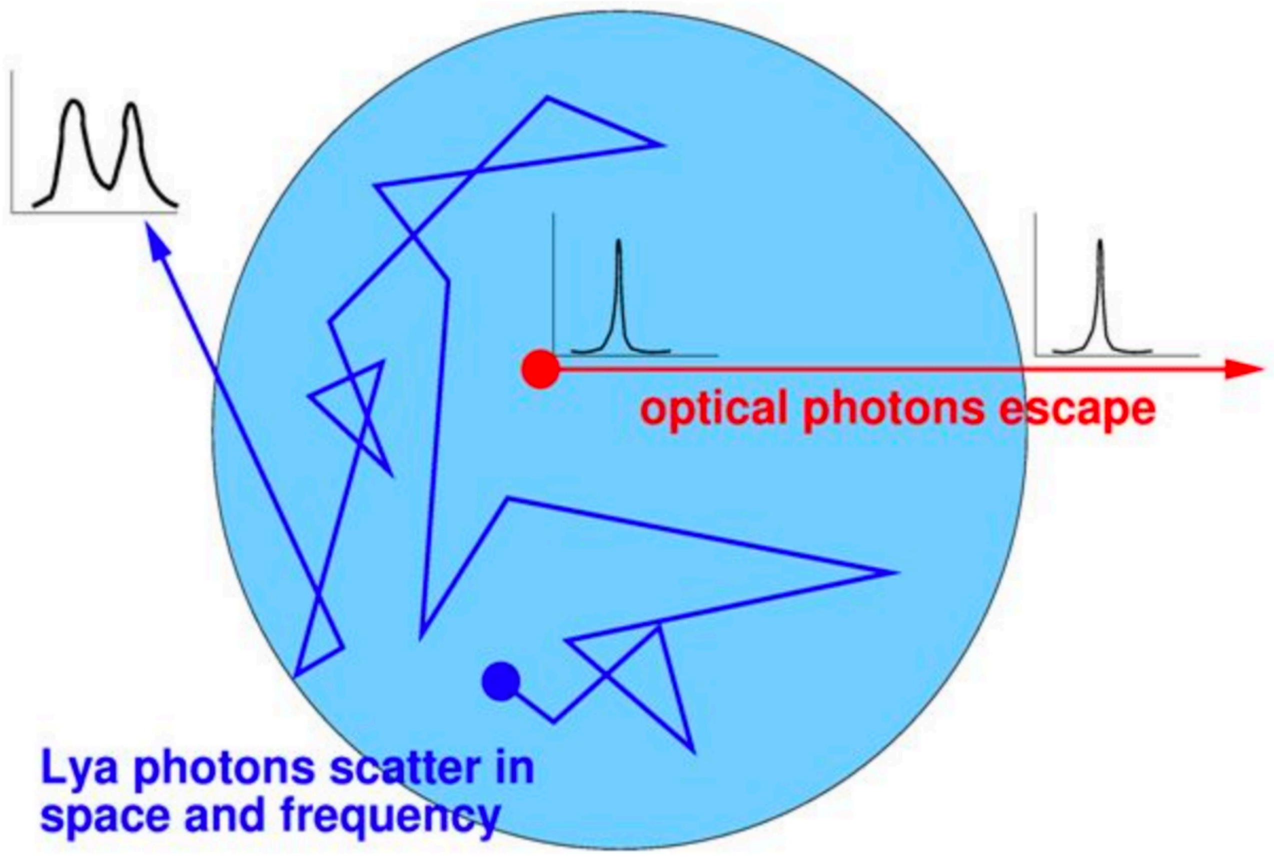

Lyα line profile: a measure of the underlying gas kinematics

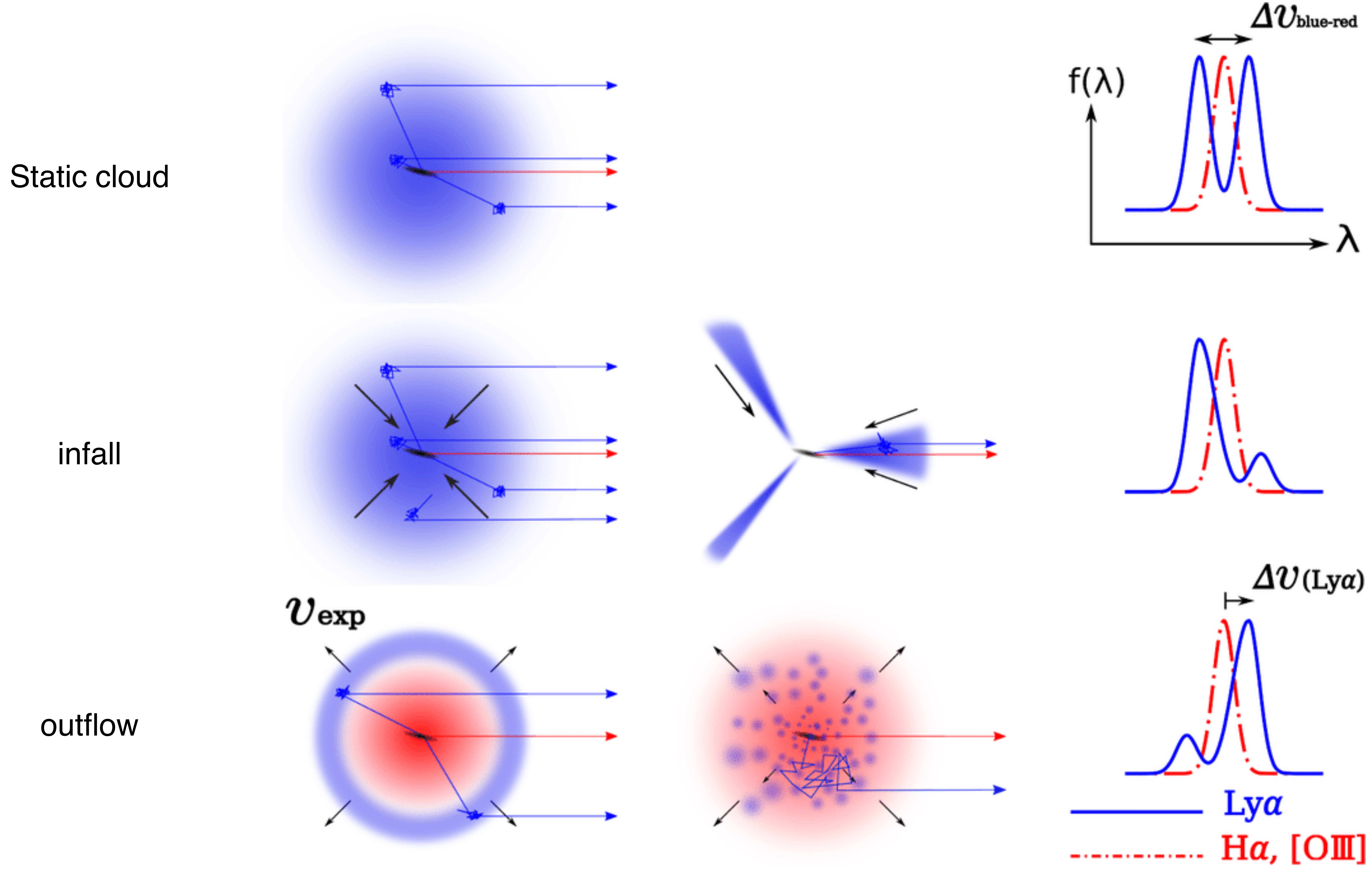

Roughly speaking
Peak separation $\propto N_{HI}$
while peak ratio $\propto v_{exp}$

(see Verhamme et al. 2006; Dijkstra 2017; Gronke et al. 2015)

Adapted from Yang et al. (2014)

Lyα line profile: a measure of the underlying gas kinematics

What about Hα?

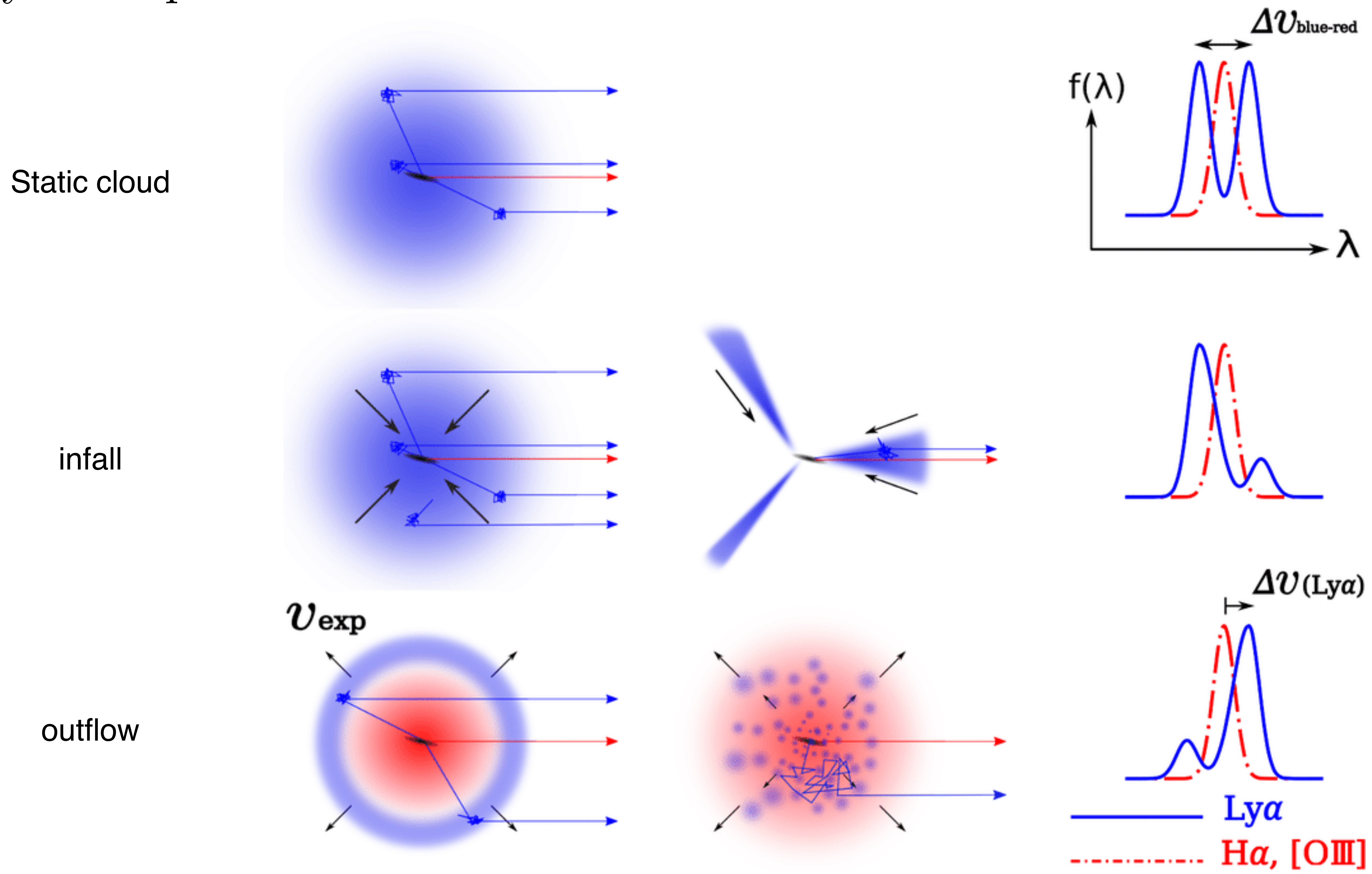

Roughly speaking
Peak separation $\propto N_{HI}$
while peak ratio $\propto v_{exp}$

(see Verhamme et al. 2006; Dijkstra 2017; Gronke et al. 2015)

Adapted from Yang et al. (2014)

Emission

1. Extraplanar diffuse ionized gas around nearby galaxies
2. Line-emitting nebulae in galaxy groups and quasar host halos
3. Lyα nebulae around distant star-forming galaxies/quasars
4. Turbulence in the CGM

Spectral features of star-forming galaxies from far-uv to optical

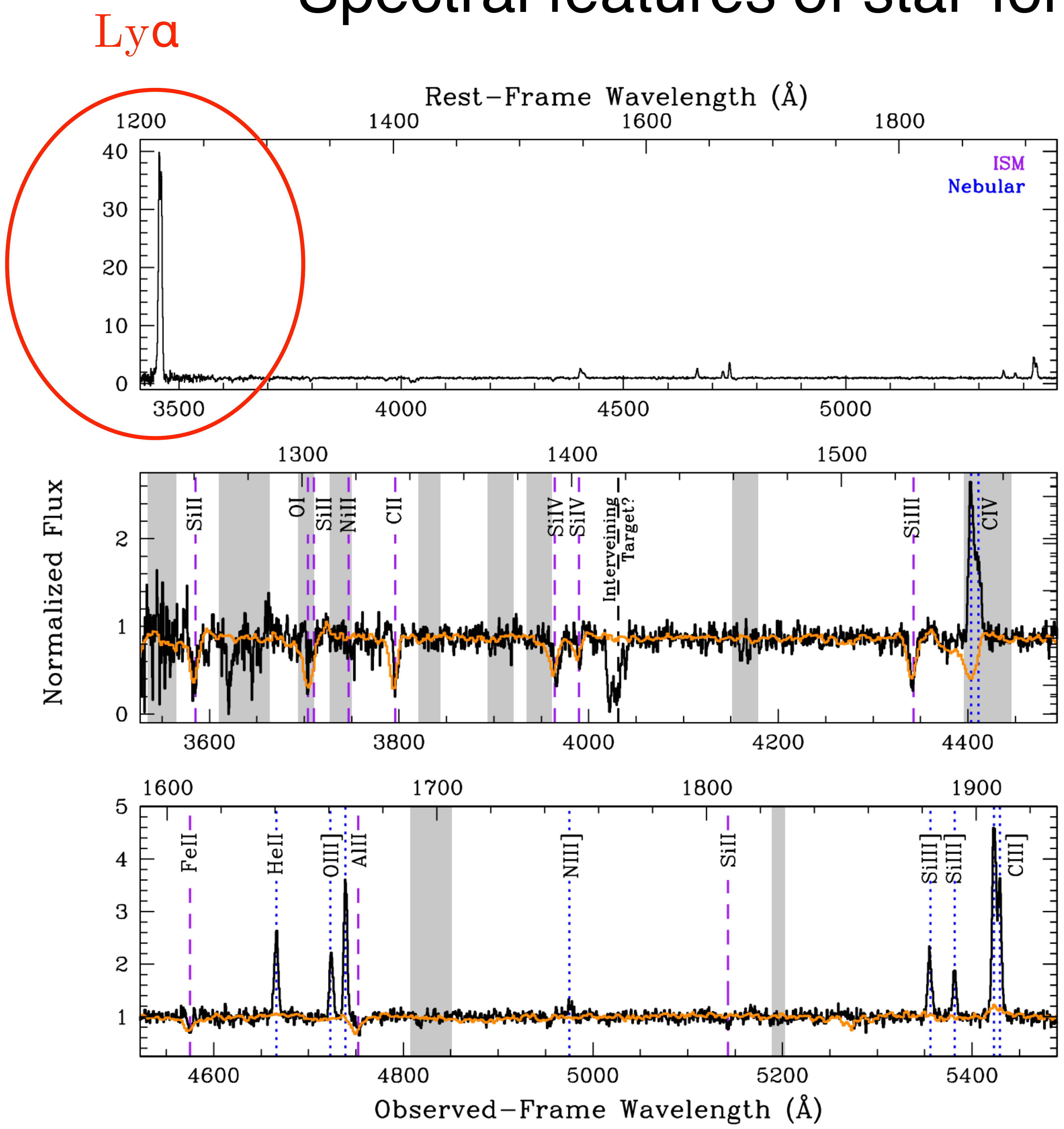

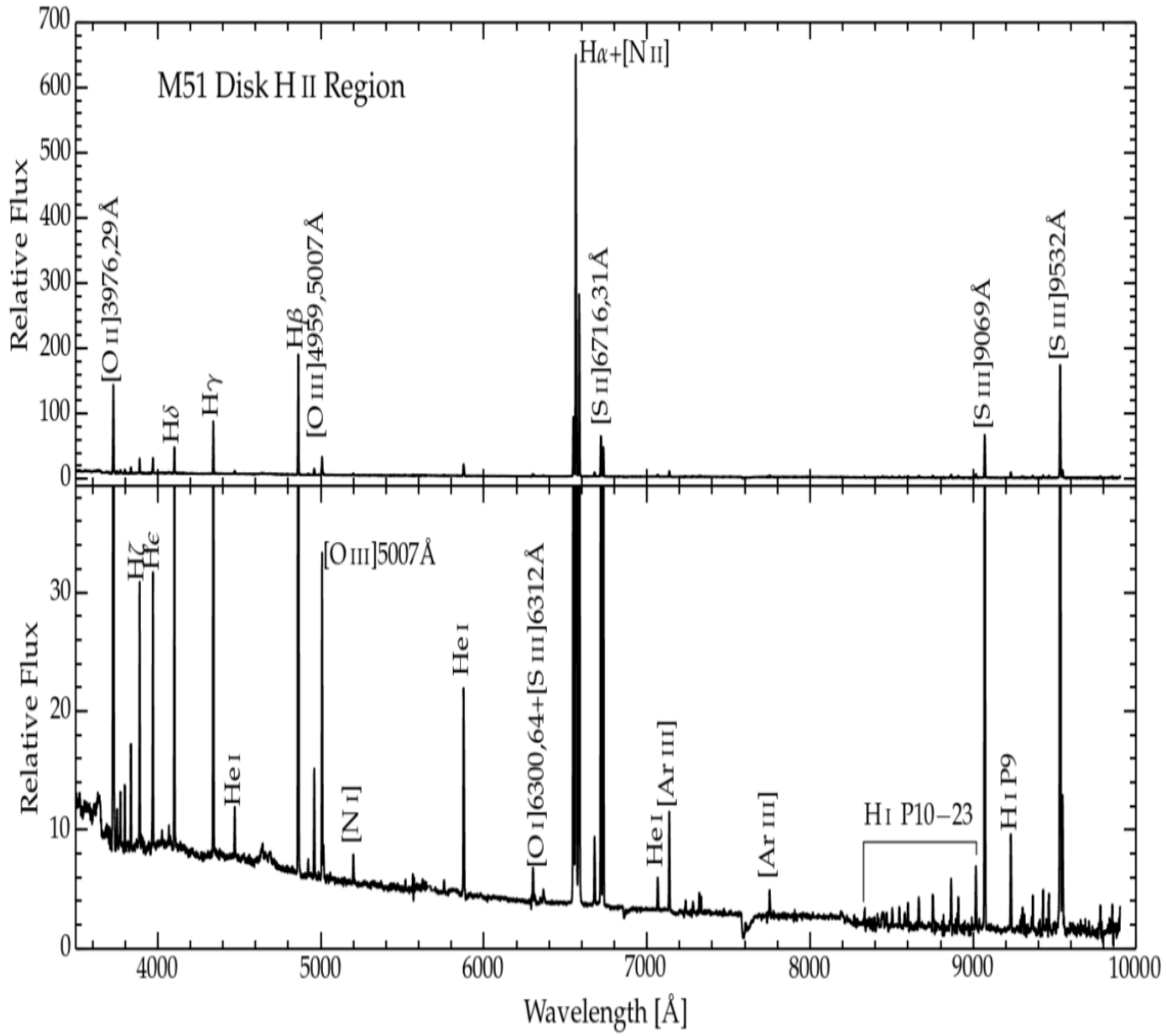

Extraplanar Diffuse Ionized Gas (eDIG)

disk-halo interfaces with structural, kinematic, and chemical clues about the feedback and accretion processes

A velocity-integrated Hα map of the Milky Way
(WHAM-SS; PI: L. M. Haffner)

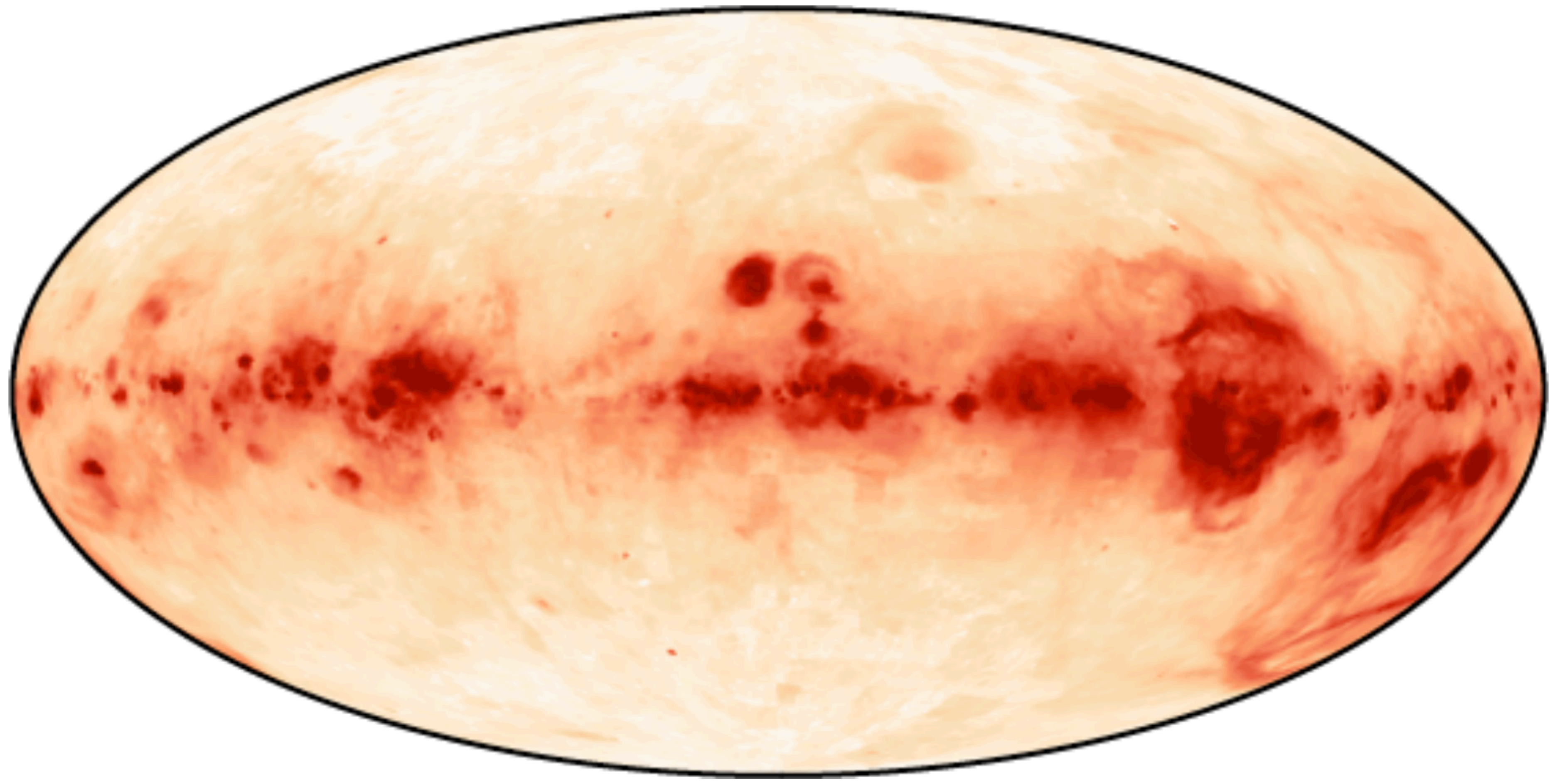

Reynolds et al. (1973); Reynolds (1991); Lehnert & Heckman (1995); Rossa & Dettmar (2003)

Physical properties:

- $T \sim (0.6\text{-}1.5) \times 10^4$ K
- $\langle n_e \rangle \sim 0.03\text{-}0.08$ cm^{-3}
- $H^+/H \sim 1$
- $f_V \sim 0.2\text{-}0.4$ within $|z| \sim 2\text{-}3$ kpc
- eDIG tends toward systemic velocity (Δv = -50 km/s in projection)
- Large scale height, $h_z \sim 1$ kpc, compared to what can be supported by thermal pressure, $h_z \sim 0.3$ kpc
- Elevated line ratios, e.g., [NII]/Hα, [SII]/Hα,

Extraplanar Diffuse Ionized Gas (eDIG)

Under hydrostatic equilibrium

$$\frac{\partial P(z,R)}{\partial z} = -\rho(z,R)\frac{\partial \Phi}{\partial z}$$ and P can have contributions from $P_{\rm gas}$, P_B, and/or $P_{\rm cr}$

$P_{\rm gas}$ and ρ are related according to

$$P_{\rm gas}(z,R) = \sigma^2(z)\,\rho(z,R),$$

velocity dispersion, $\sigma^2 = \sigma_{\rm th}^2 + \sigma_{\rm turb}^2$, constrained using optical emission lines

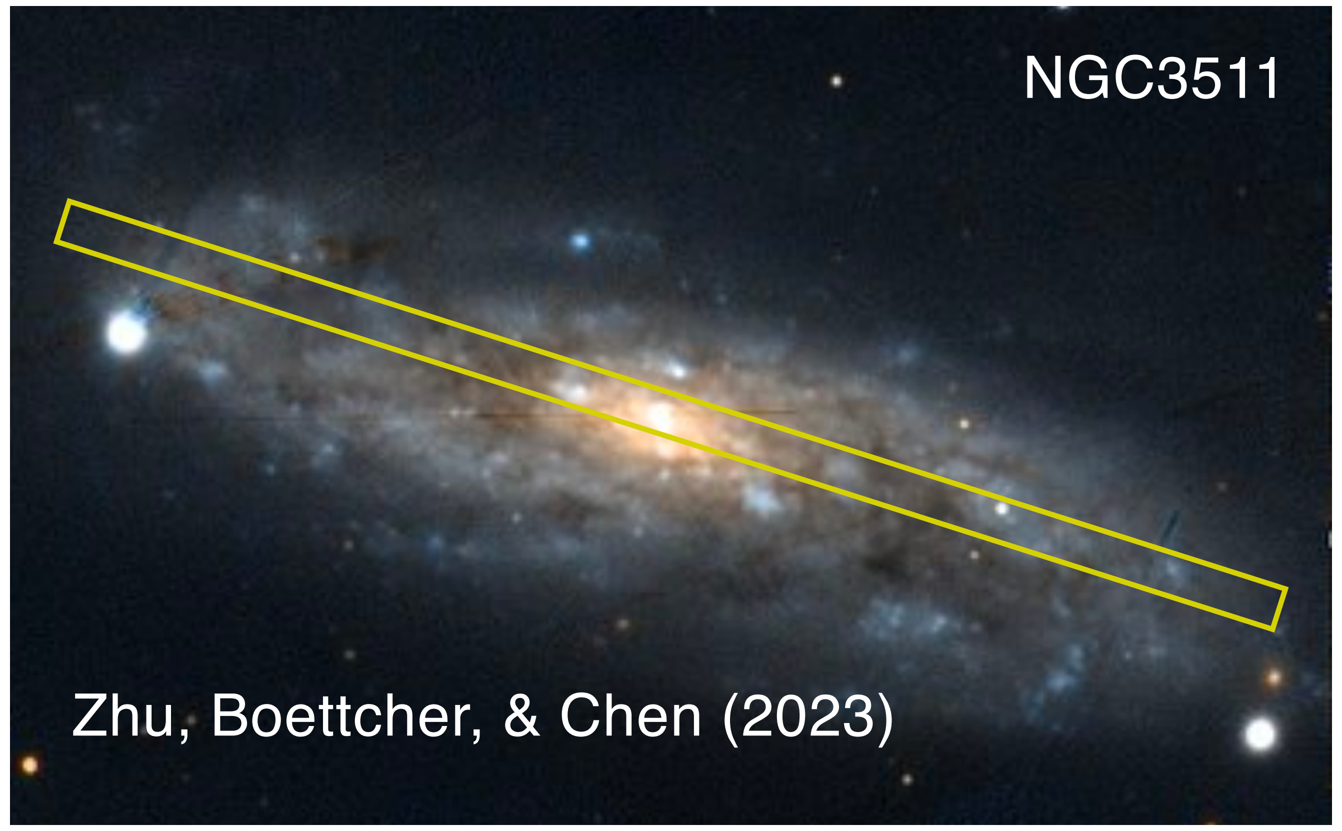

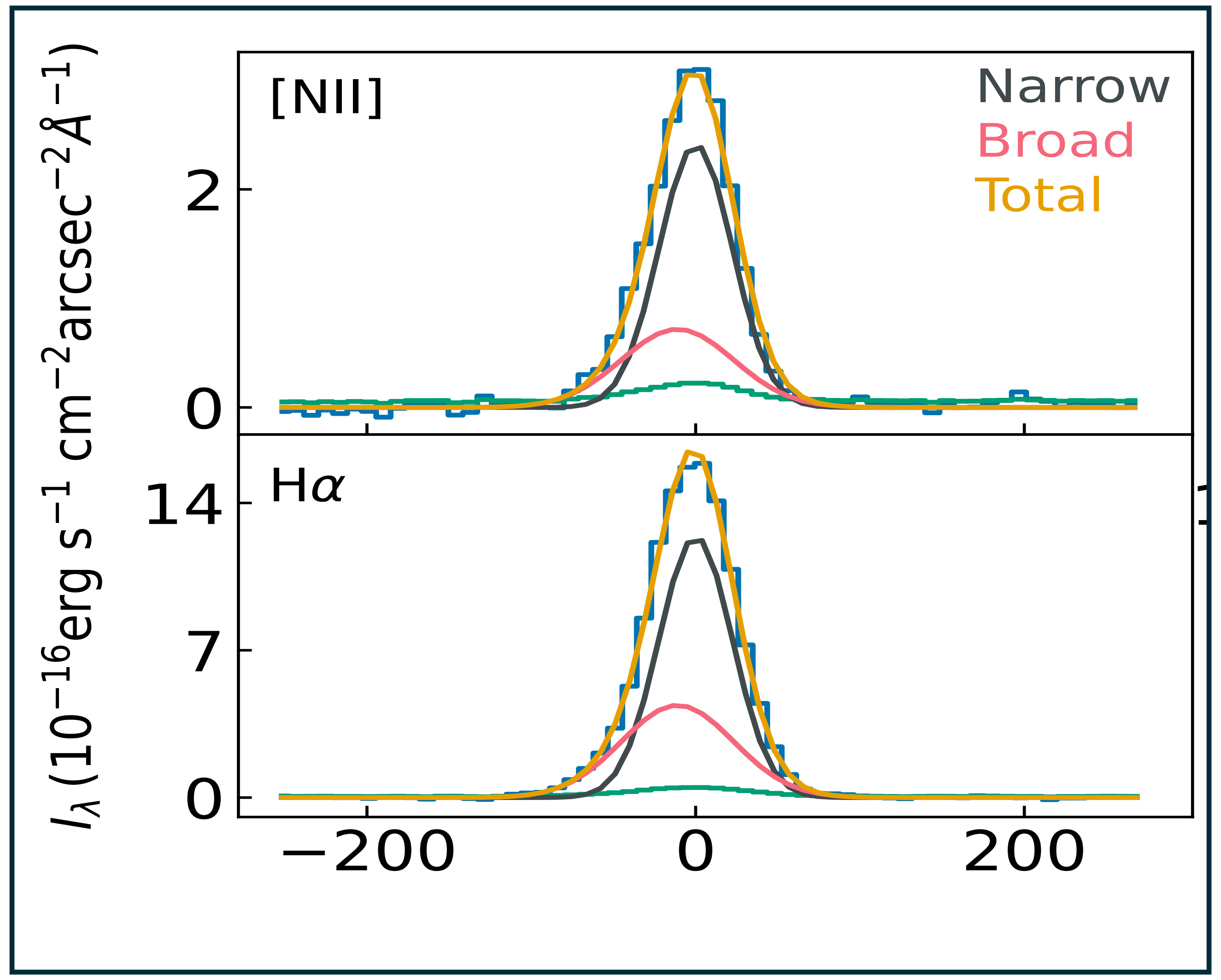

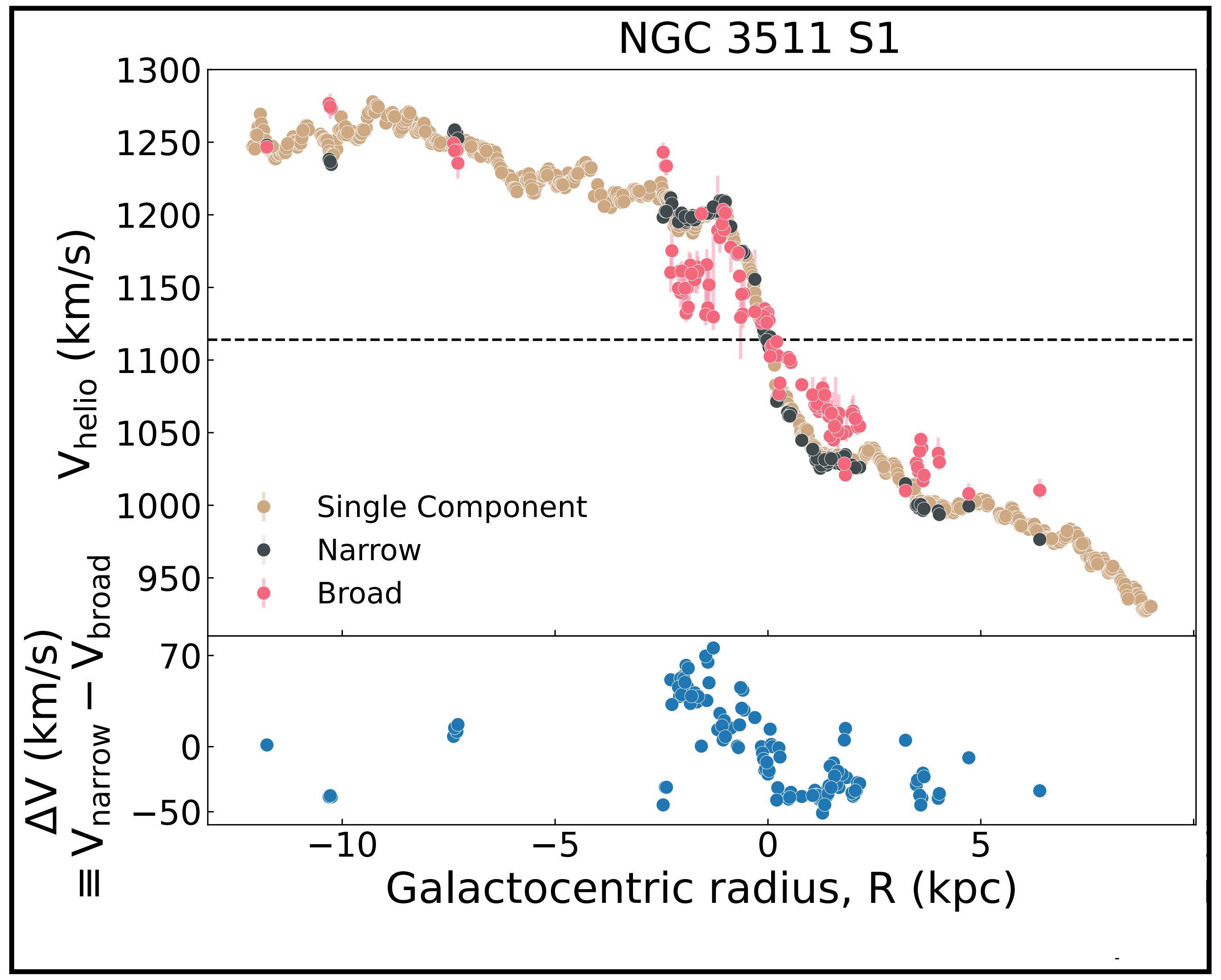

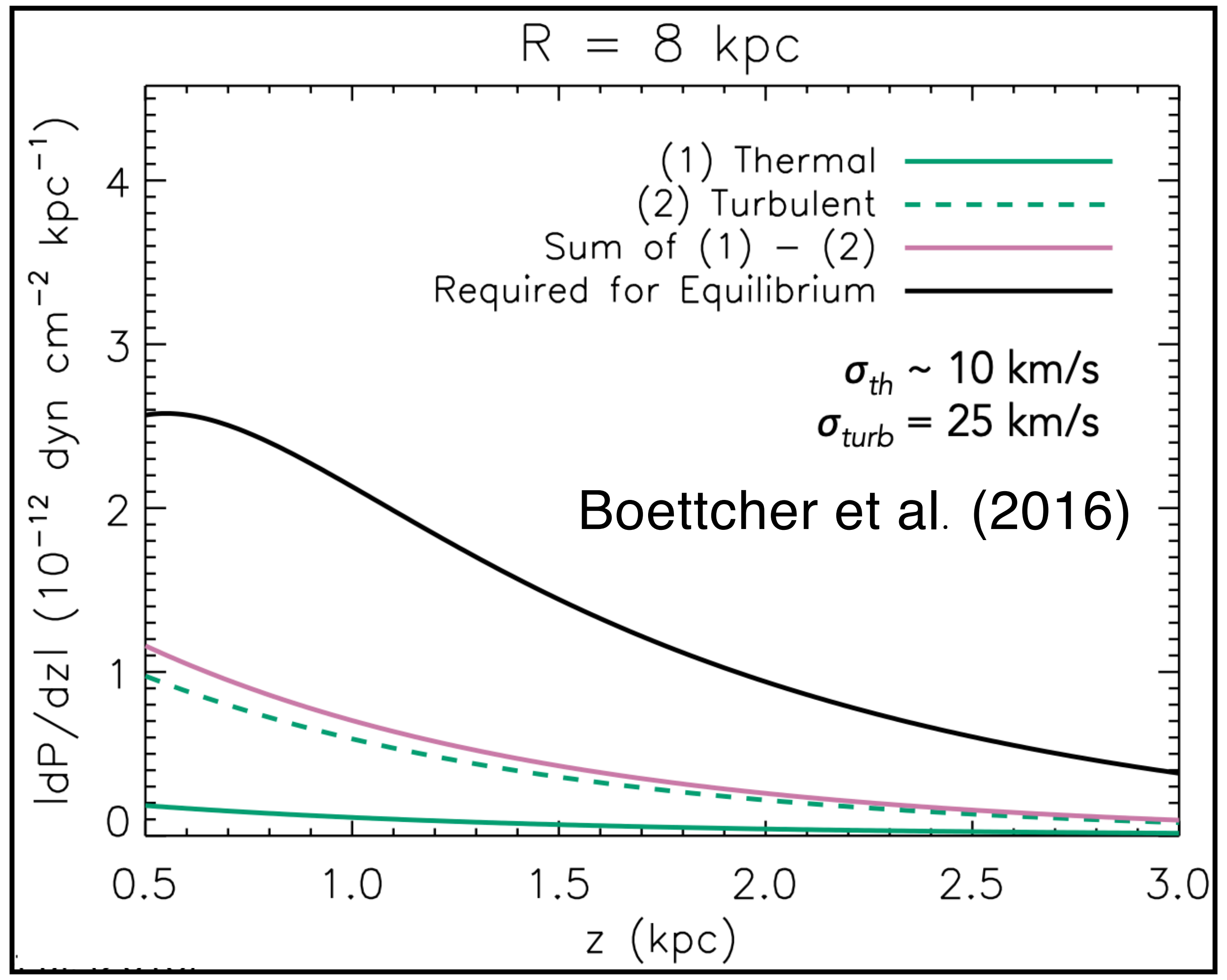

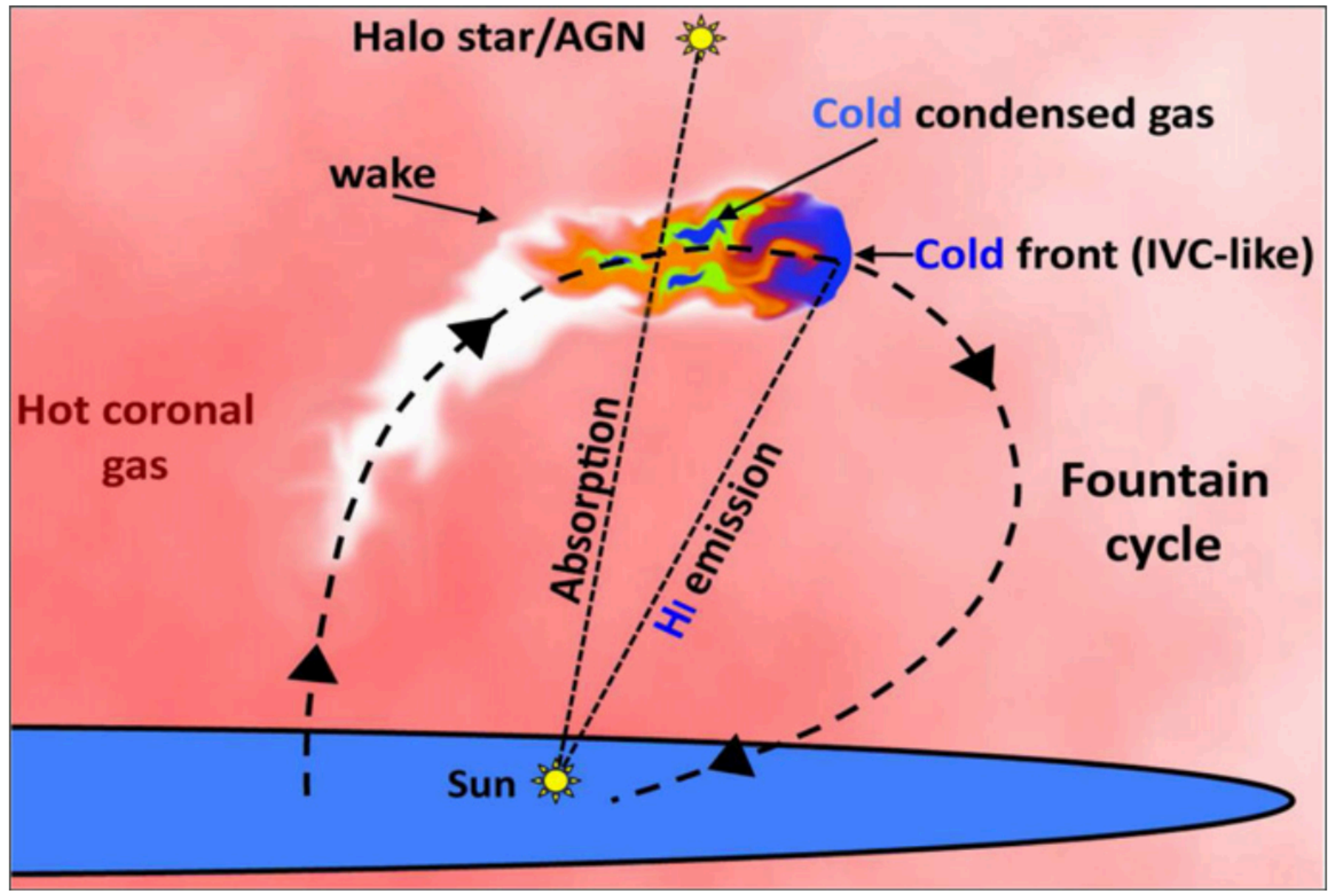

See review by Fraternali (2017)

See Beck 2015 and Boettcher et al. (2016) for discussions on the contributions from magnetic field and cosmic rays

Mapping Cool Intragroup Gas in Emission

A previously known damped Lyα absorber of $N(\mathrm{HI}) = 5 \times 10^{21}\,\mathrm{cm}^{-2}$ and $[\mathrm{M/H}] = -0.8 \pm 0.1$at z=0.313

(e.g., Bergeron & Boisse 1991; Lane+1998; Rao & Turnshek 2000; Chen & Lanzetta 2003; Kacprzak+2010; Kanekar+2014; Guber+2018; Peroux+2019)

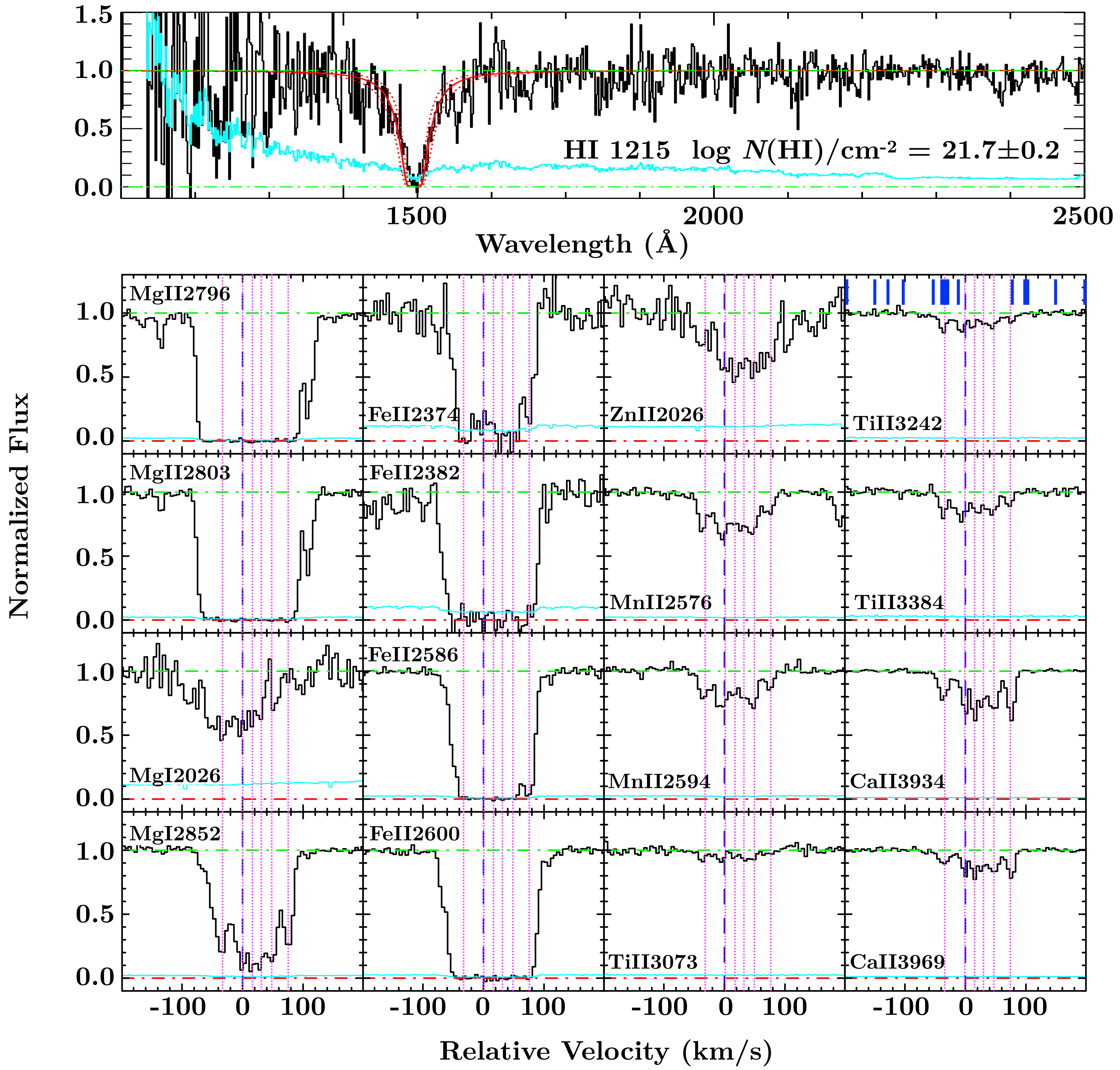

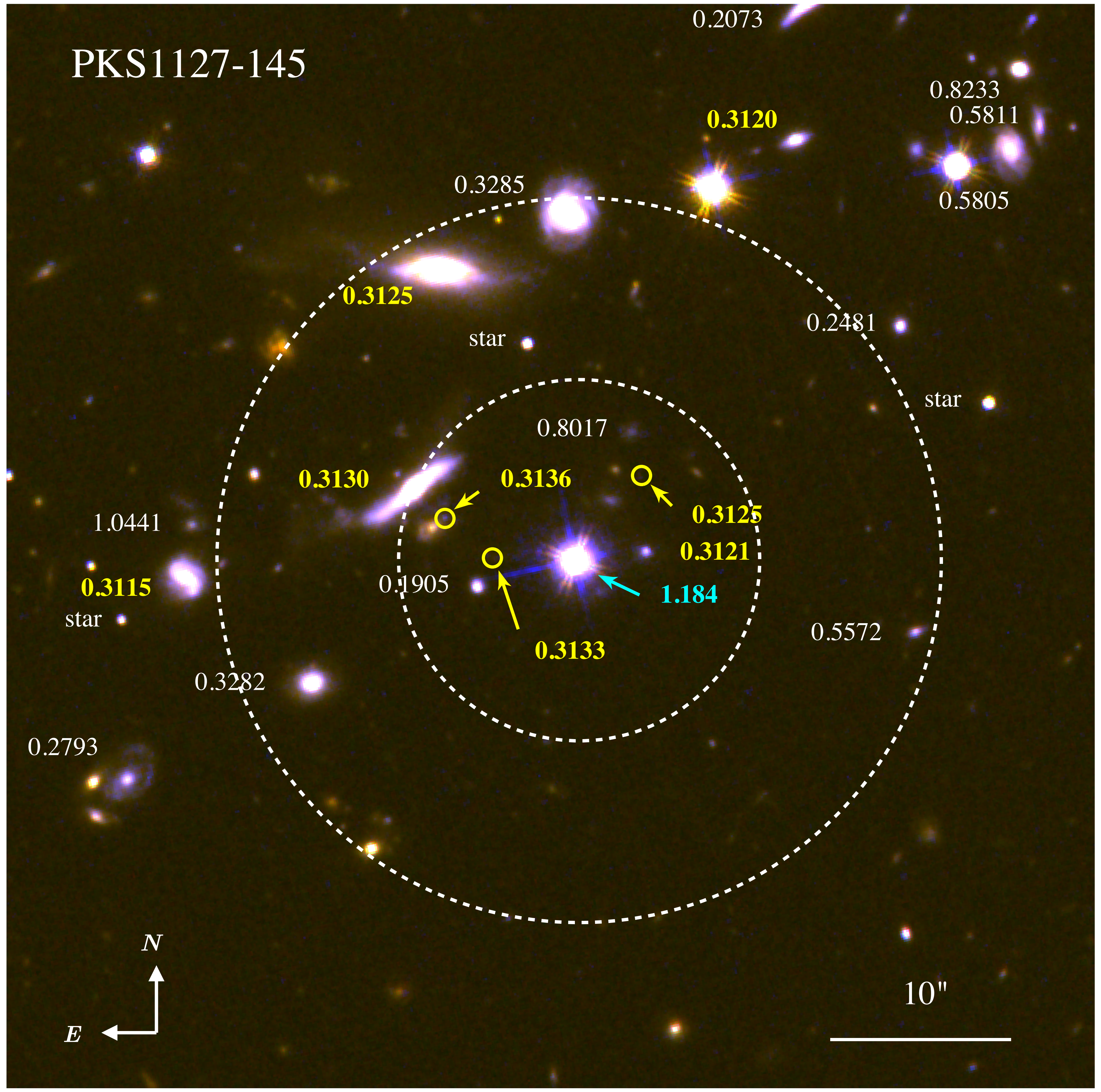

Mapping Cool Intragroup Gas in Emission

New MUSE observations confirm the presence of a galaxy group at z = 0.313 with σ_v = 128 km/s, $M_h \sim 3 \times 10^{12}\ M_\odot$

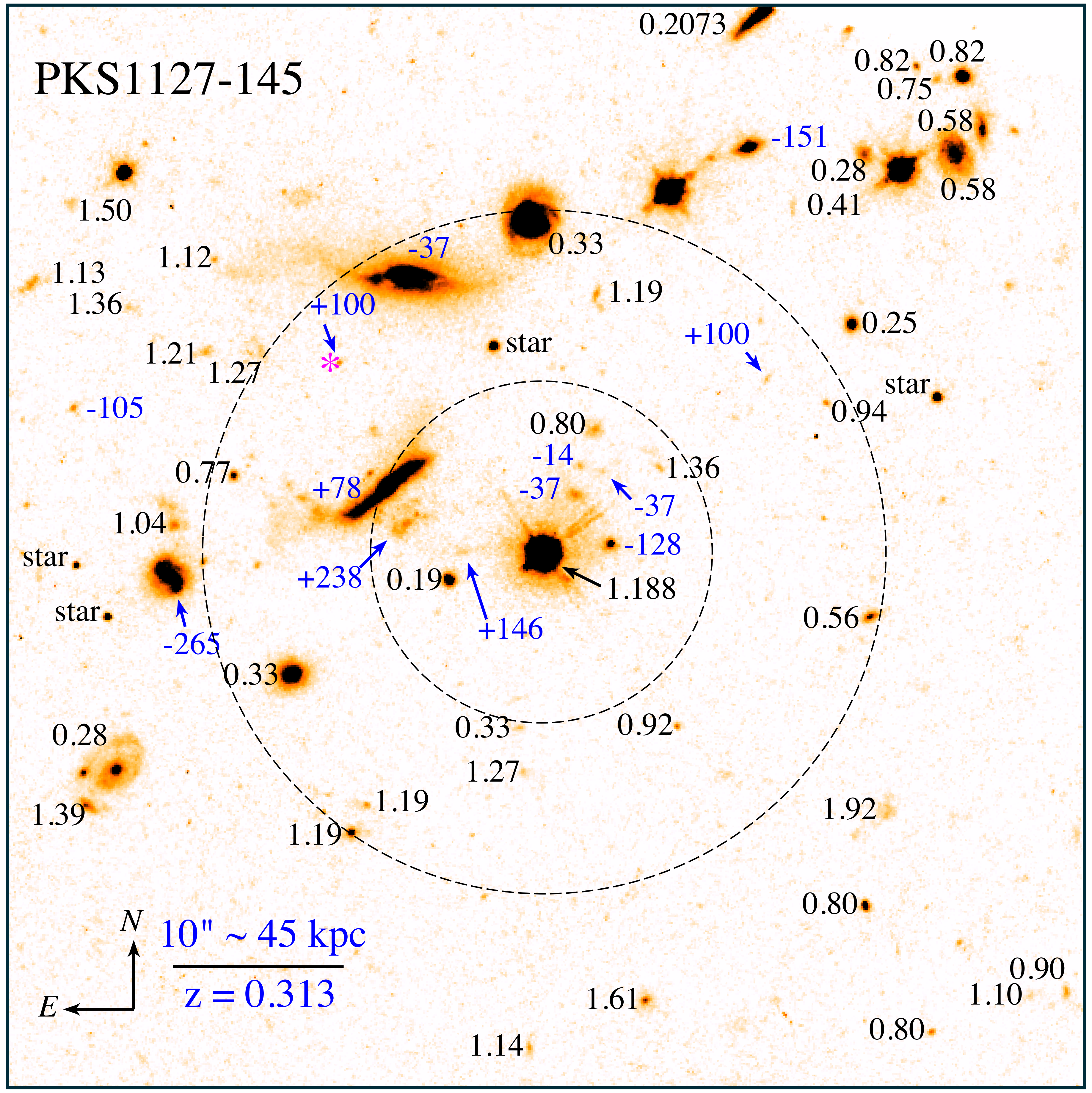

But also reveal wide-spread gaseous streams, connecting between group members

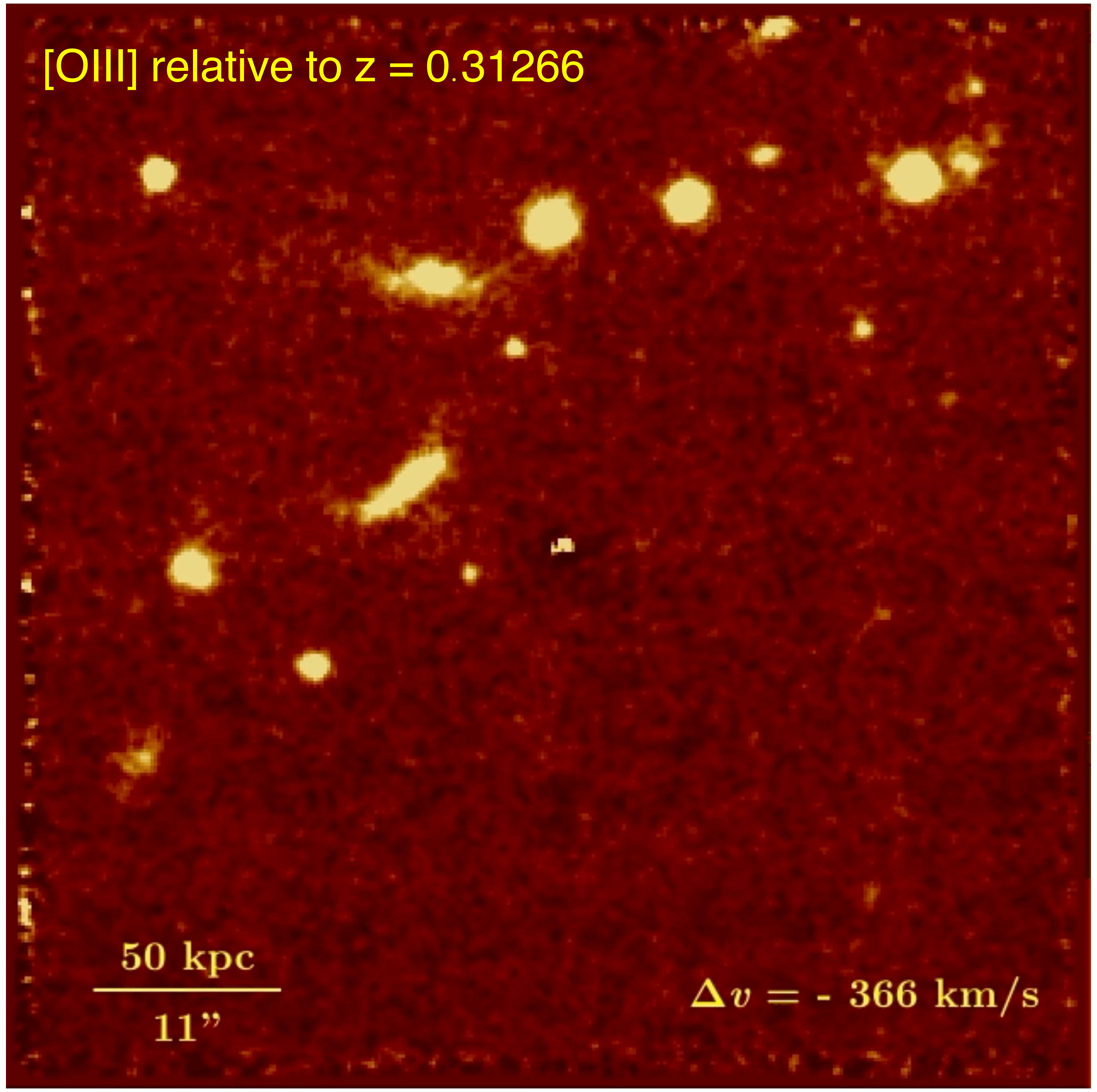

Chen et al. (2019)

Mapping Cool Intragroup Gas in Emission

$$\mathrm{SB_{H\alpha}} \approx 2.5\times10^{-17}\,C\left(\frac{\langle n_e\rangle}{0.2\,\mathrm{cm^{-3}}}\right)^2 \frac{l}{\mathrm{kpc}}\left(\frac{1+z}{1.313}\right)^{-4}\ \mathrm{erg\,s^{-1}\,cm^{-2}\,arcsec^{-2}}$$

Chen et al. (2019)

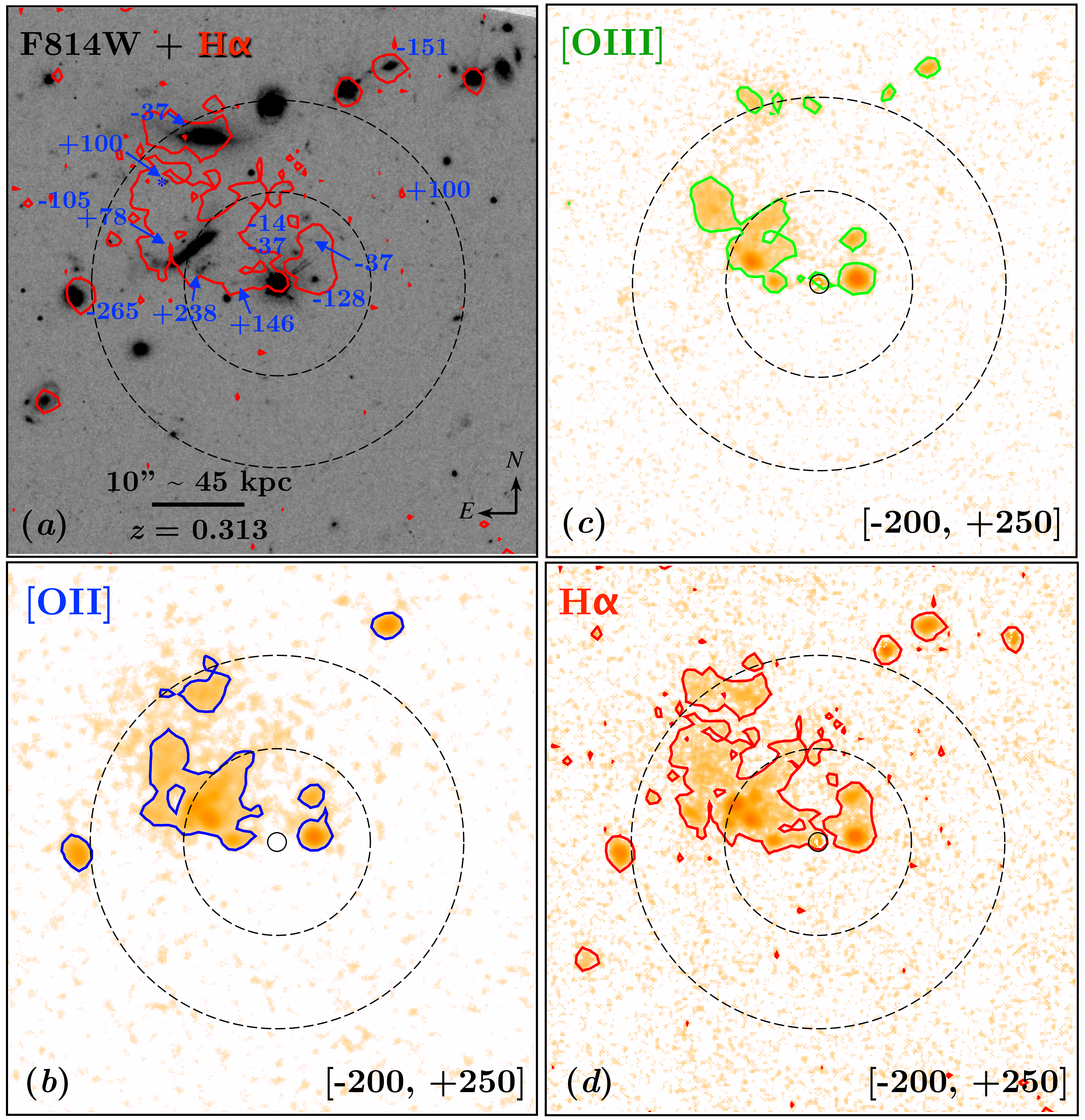

both line-emitting morphology and kinematic show that the DLA originating in streams of gas stripped from sub-L_* group members at $d \lesssim 25$ kpc from the QSO sightline

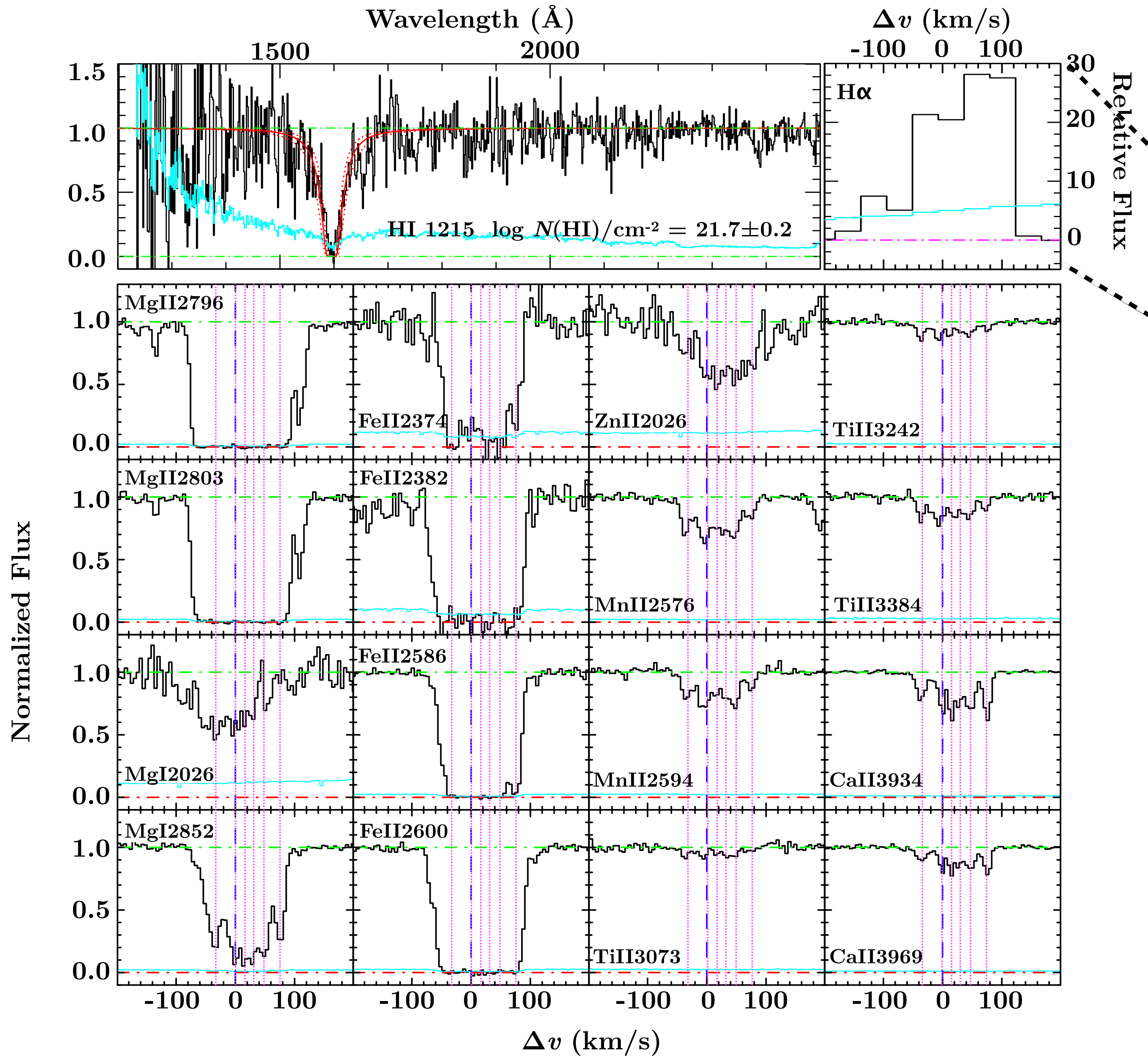

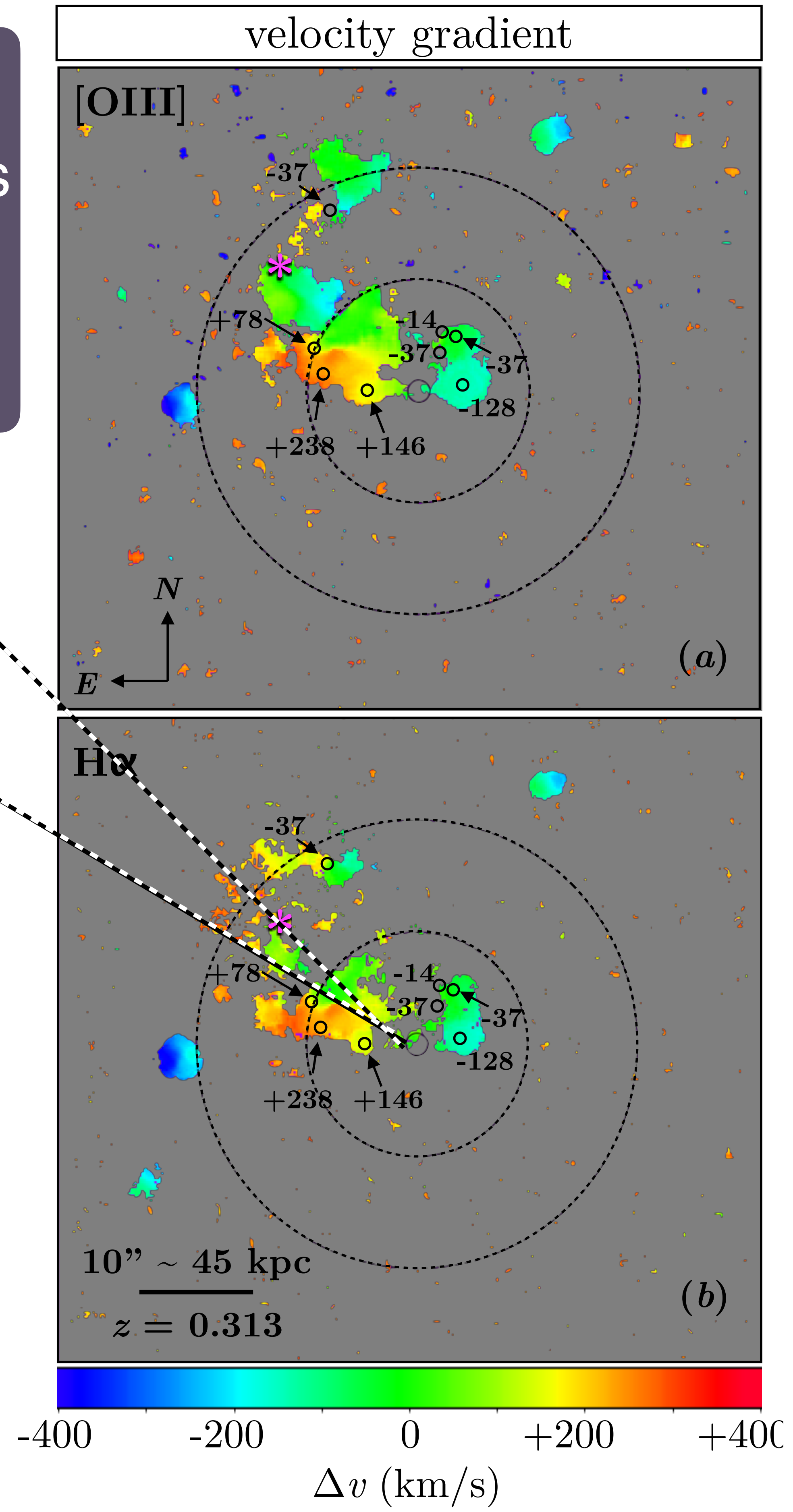

Mapping Cool Intragroup Gas in Emission

Chen et al. (2019)

strong line ratios indicate that shocks and/or turbulent mixing layers contribute significantly to the ionization of the gas

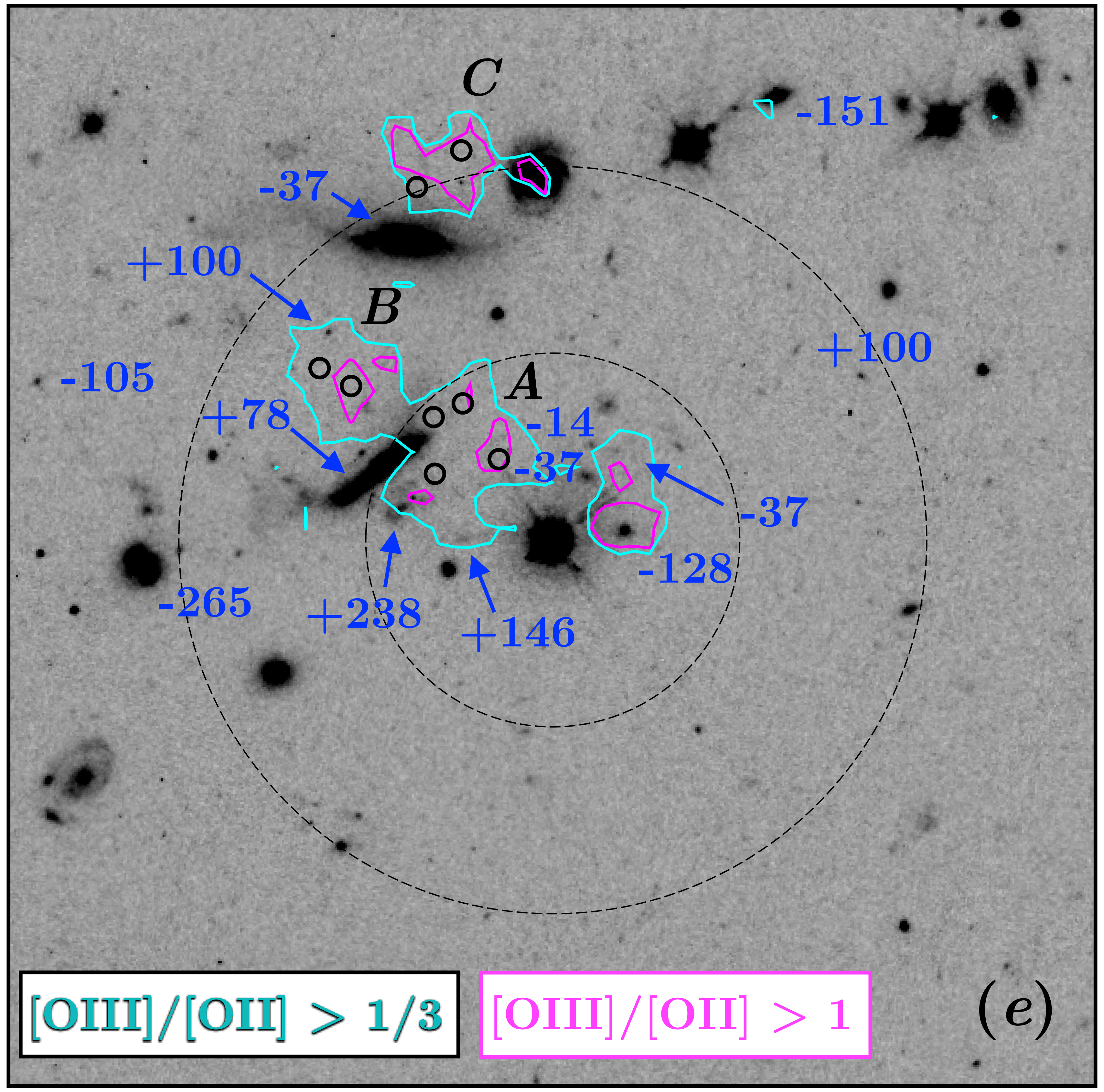

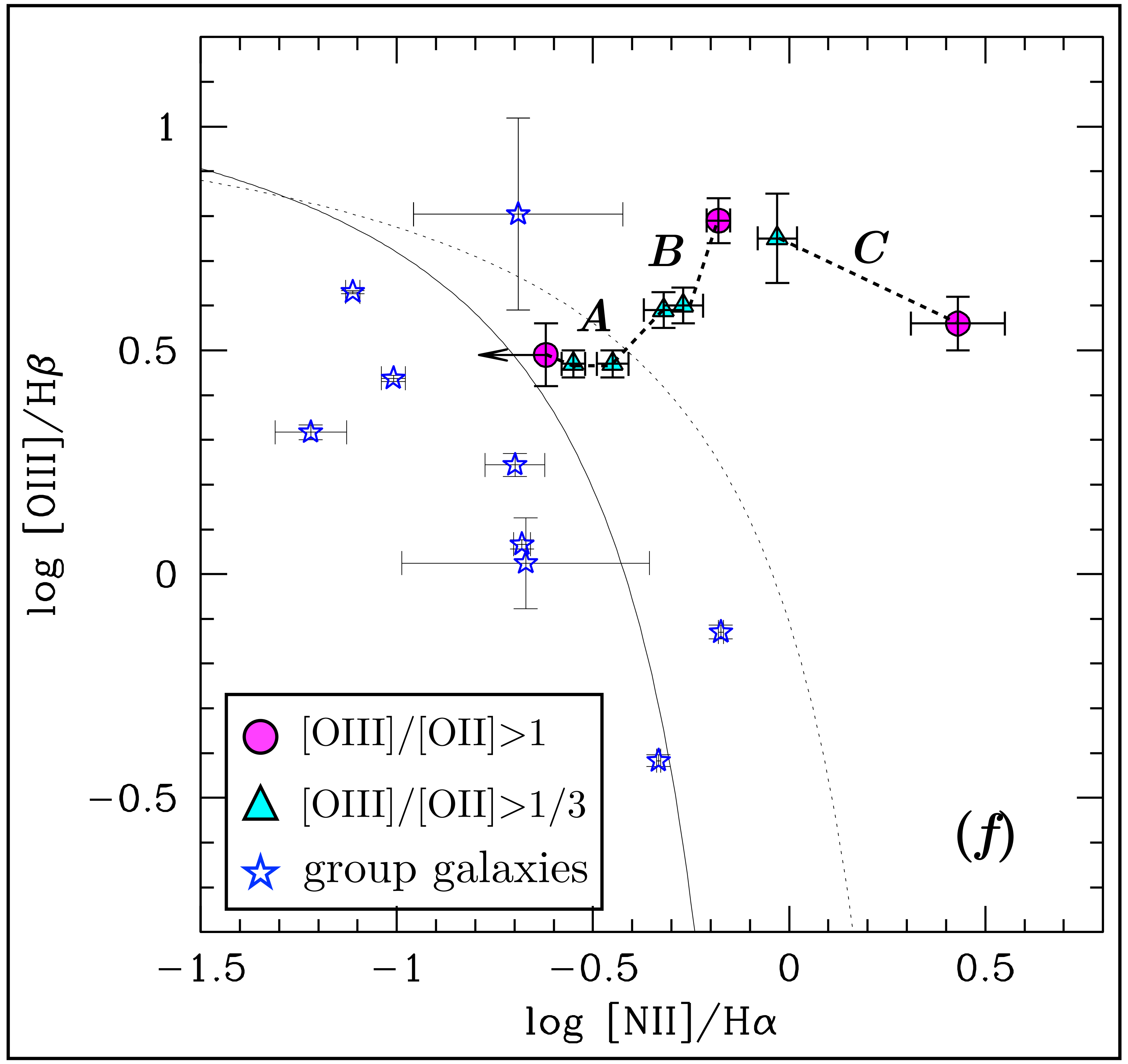

gas stripping in low-mass galaxy groups is effective in releasing metal-enriched gas from star-forming regions, producing absorption systems in QSO spectra;

Mapping Gas Flows in Halos around Star-forming Galaxies in the Early Epoch

Erb et al. (2018)

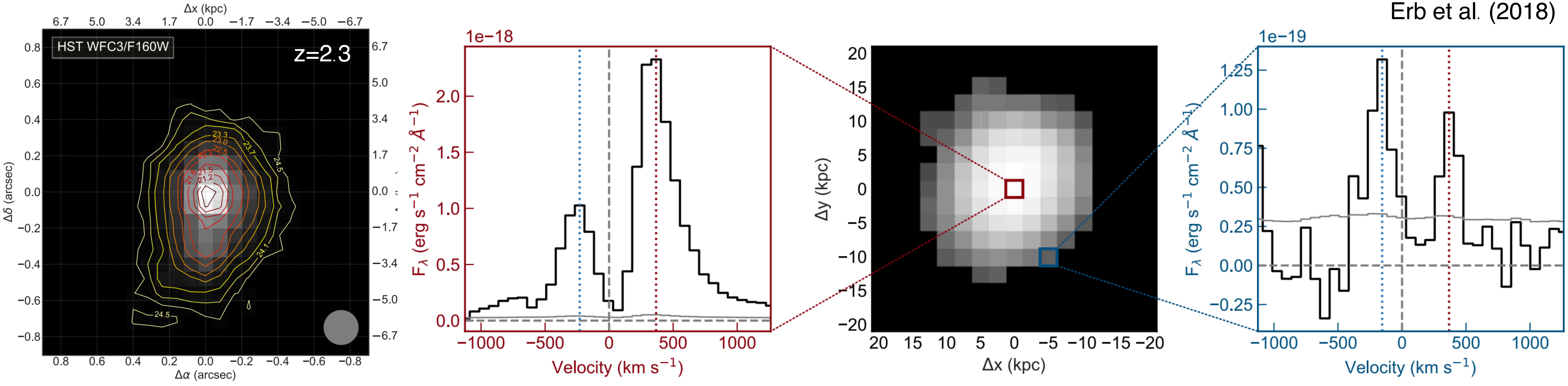

A low-mass ($M_{\rm star} = 5 \times 10^8\,M_\odot$) and low-metallicity (Z ≈ 0.25 Z⊙) star-forming galaxy with a half-light radius of 1.5 kpc at z = 2.3

Extended Lyα emission is detected out to ~ 25 kpc with a clear spatial variation in the observed double-peak profile, revealing a mixture of infall and outflows

Extracting kinematic properties requires a detailed Lyα radiative transfer model

Mapping Gas Flows in Halos around Star-forming Galaxies

M. Chen, HWC et al. (2021)

Cluster lensing to resolve star-forming regions on sub-kpc scales

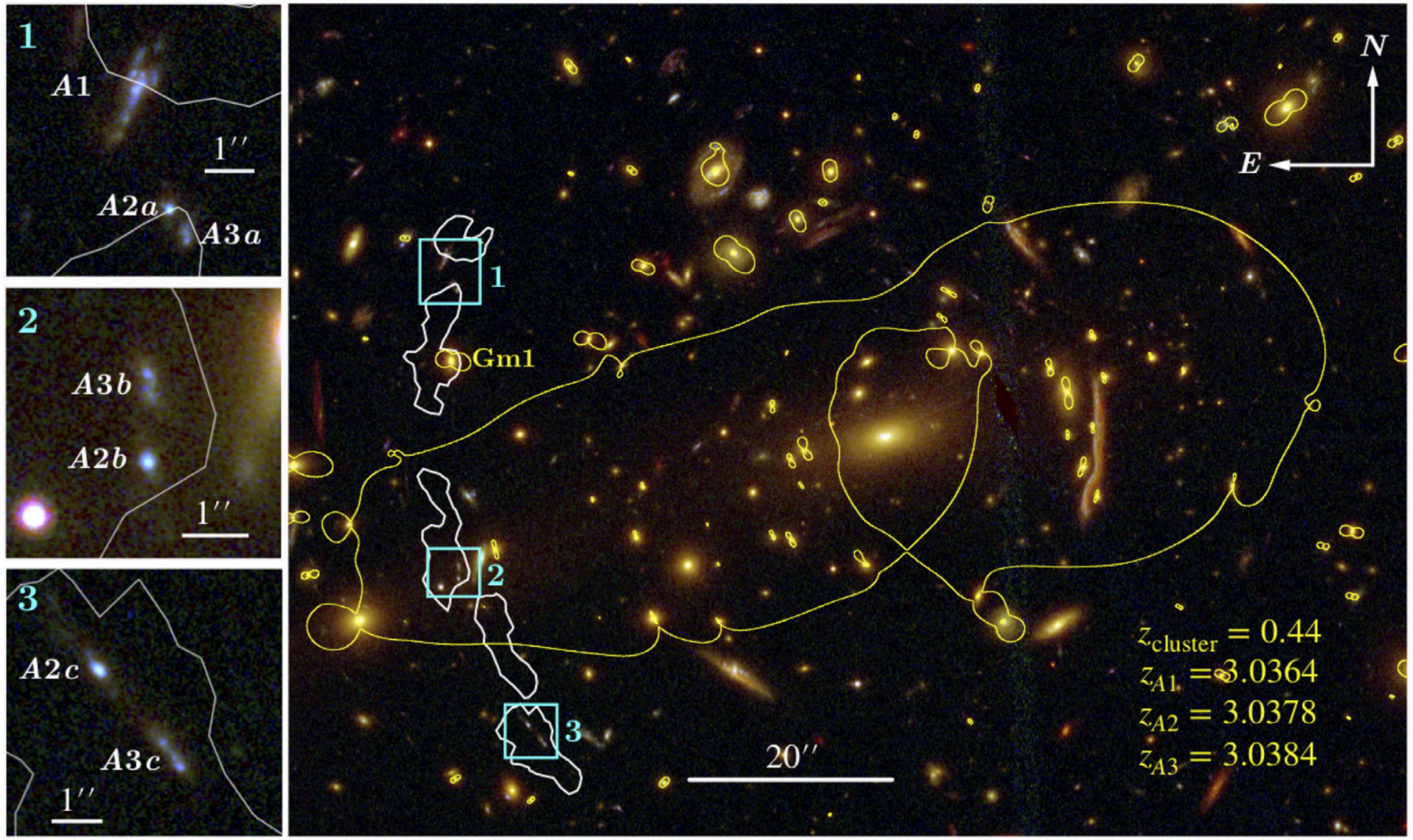

See Caminha et al. (2017)

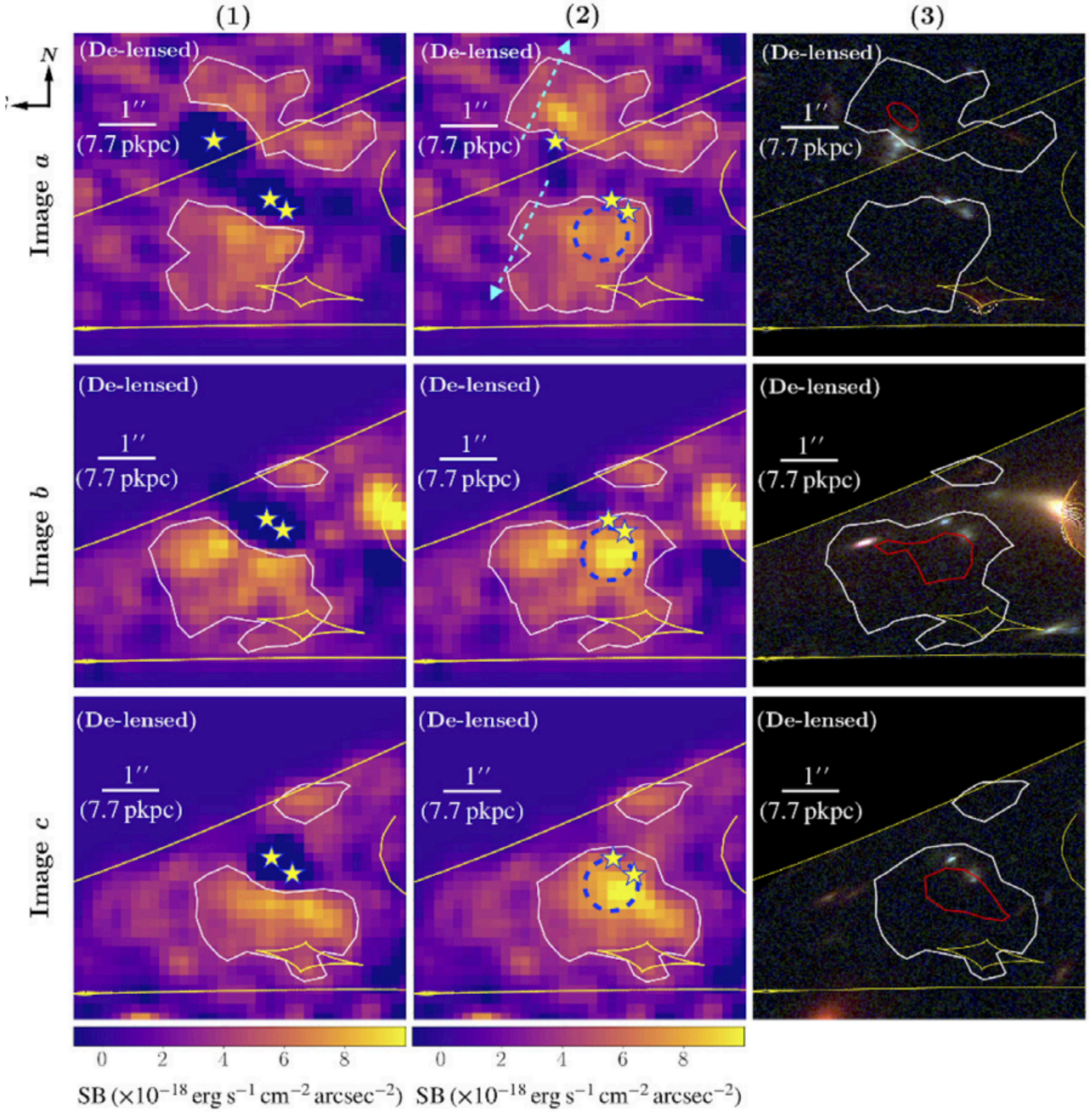

Mapping Gas Flows in Halos around Star-forming Galaxies

M. Chen, HWC et al. (2021)

Cluster lensing to resolve star-forming regions on sub-kpc scales

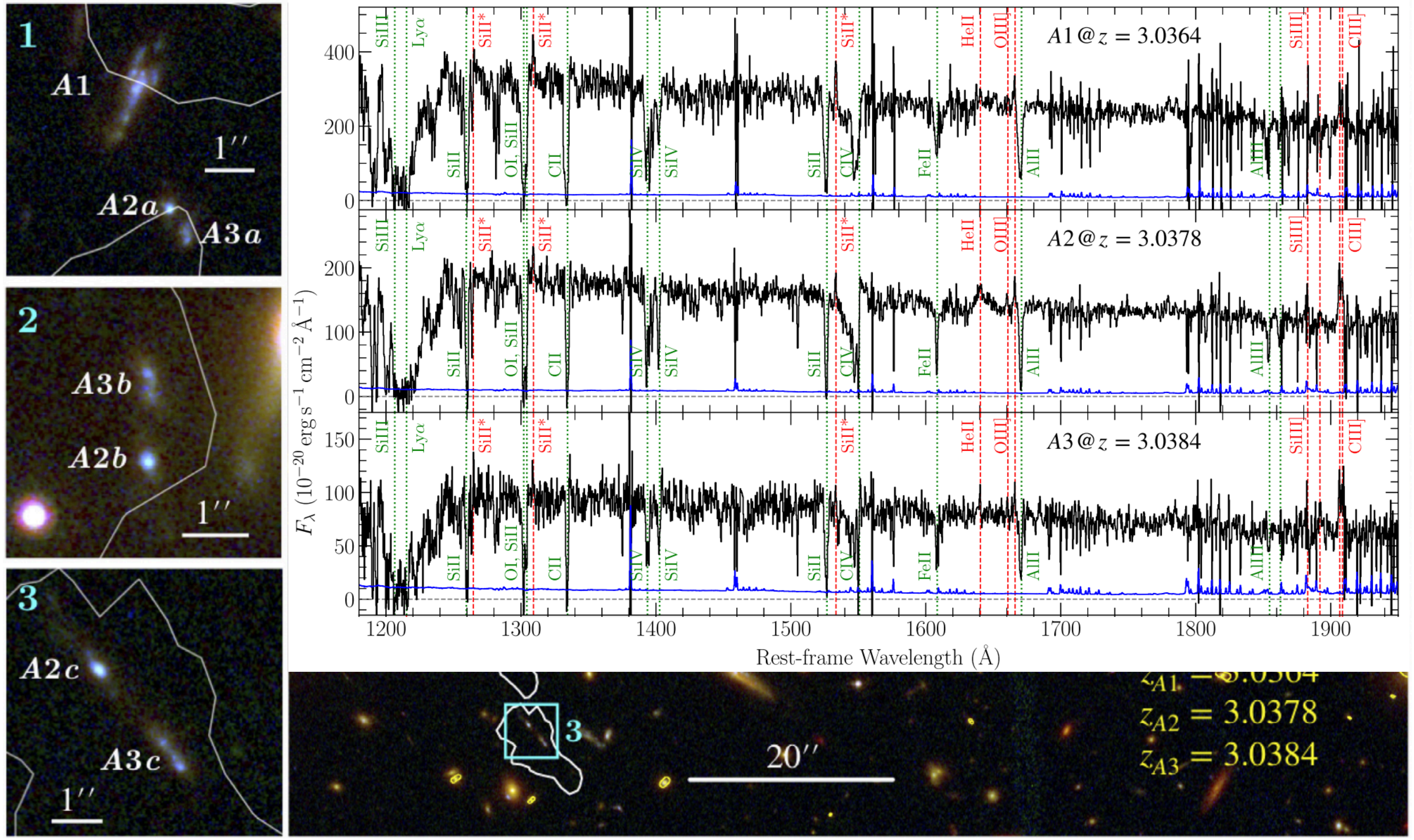

See Caminha et al. (2017)

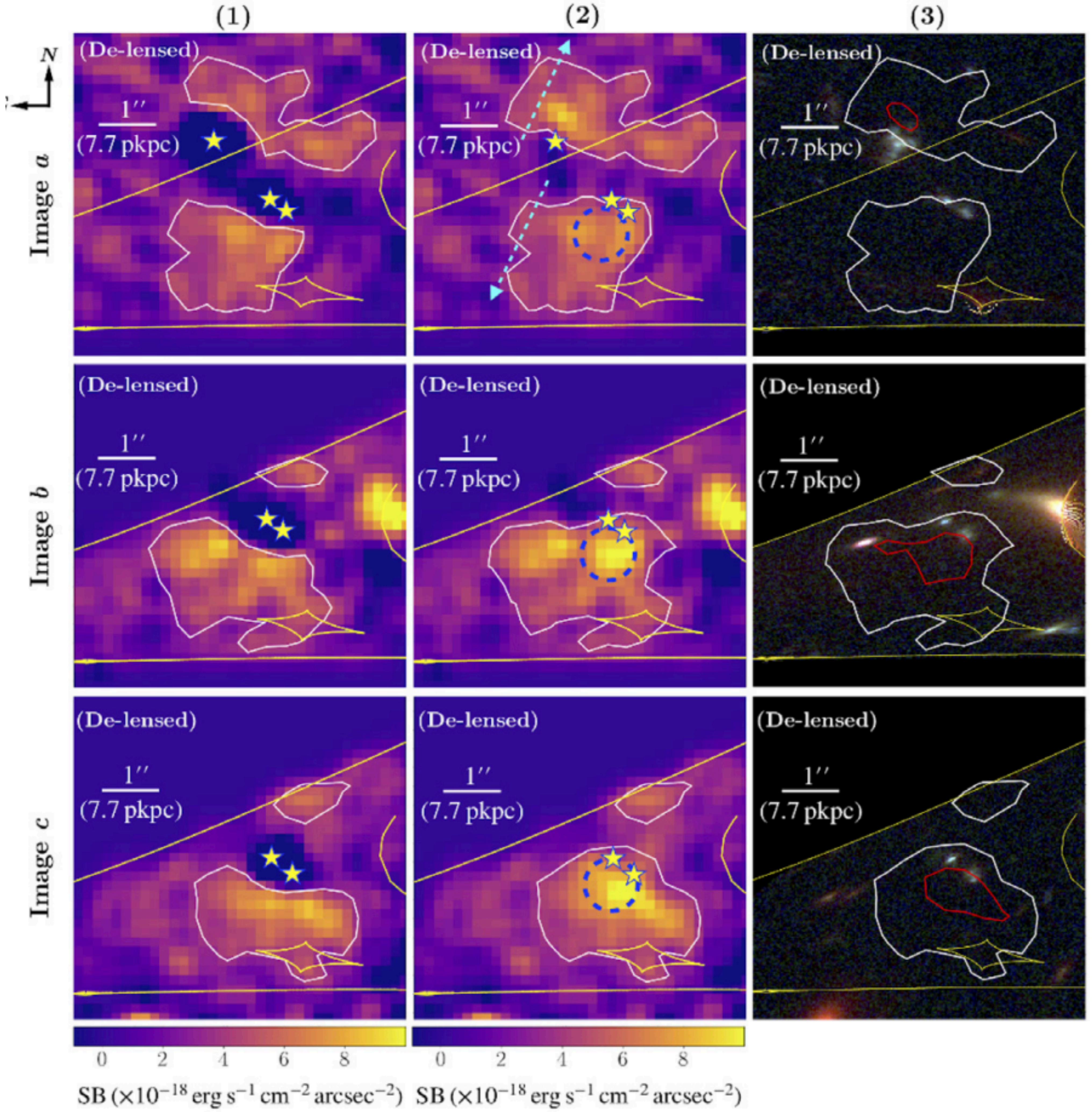

Mapping Gas Flows in Halos around Star-forming Galaxies

Spatial variations of Lyα profiles are apparent between northern and southern nebulae

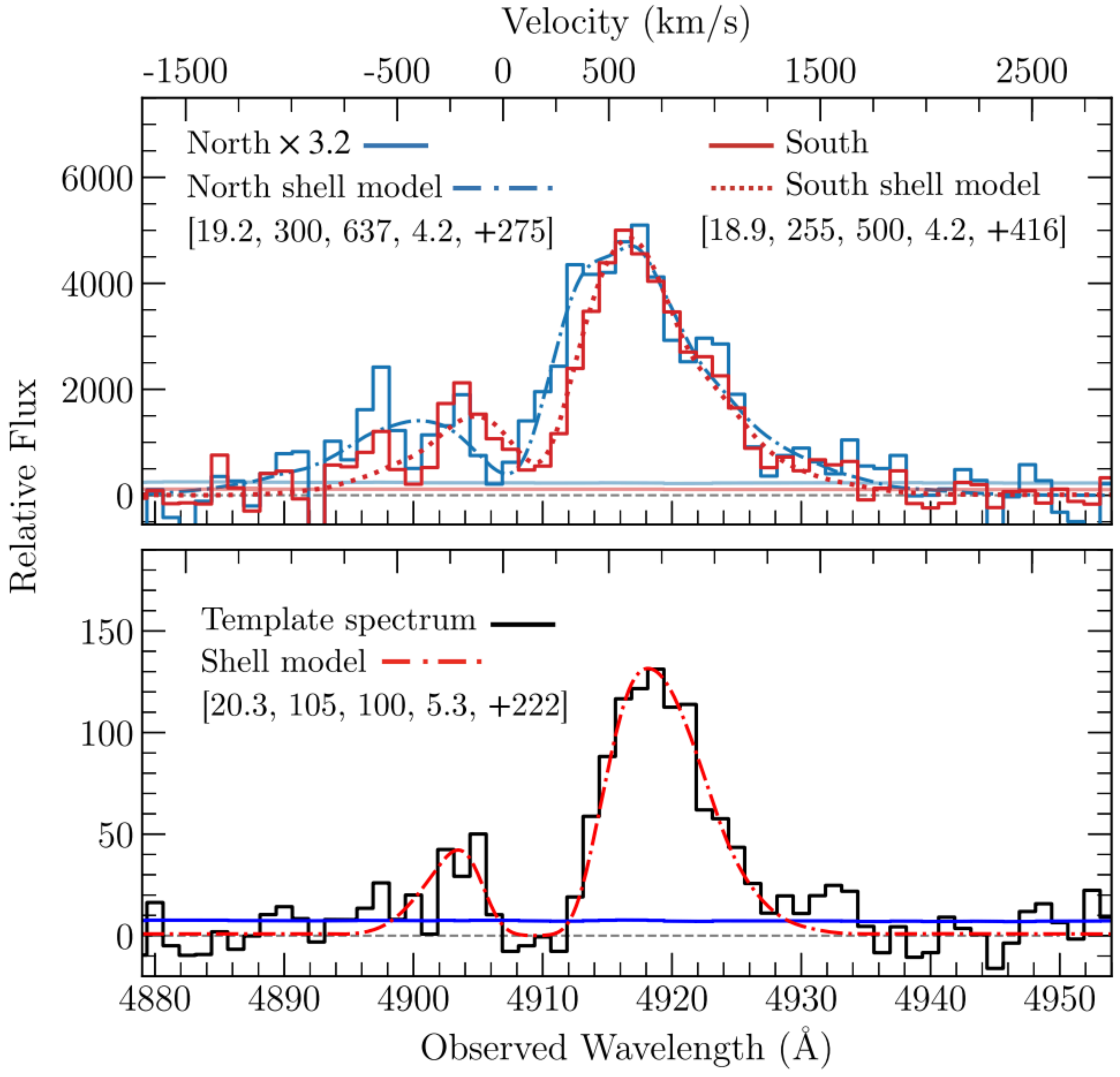

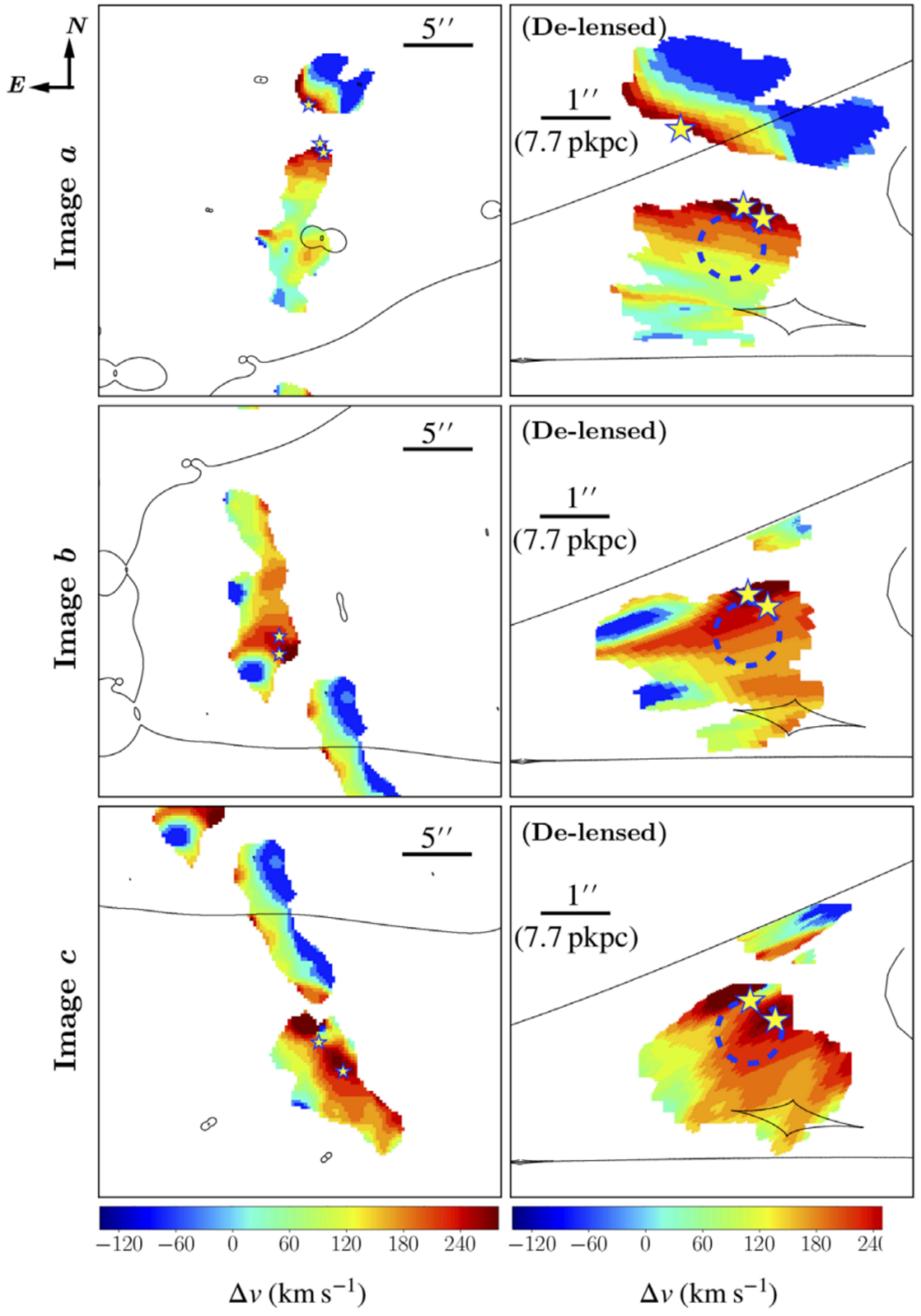

M. Chen, HWC et al. (2021)

the presence of a steep velocity gradient ($\Delta v/\Delta r_\perp \approx 25$ km/s/kpc) in a continuous flow of high column density gas from star-forming regions into a low-density halo environment.

Mapping Feeding and Feedback in Quasar Host Halos

Ubiquitous Lyα nebulae around z=3-4 quasars

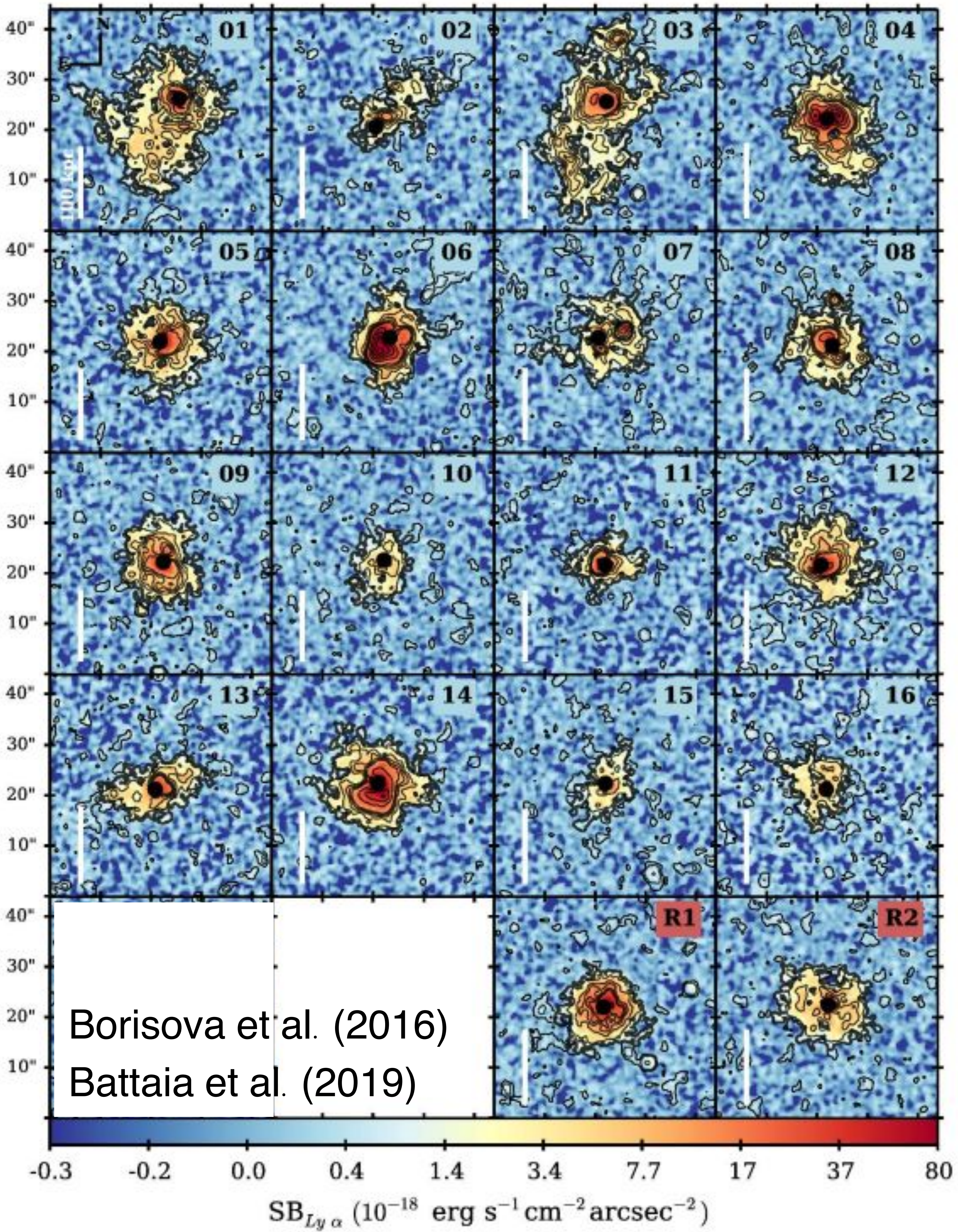

In contrast, roughly 1/3 of QSOs at z<1 have extended line-emitting nebulae detected in [OII] and/or [OIII]; evolution or ambiguities in the origin of Lya photons?

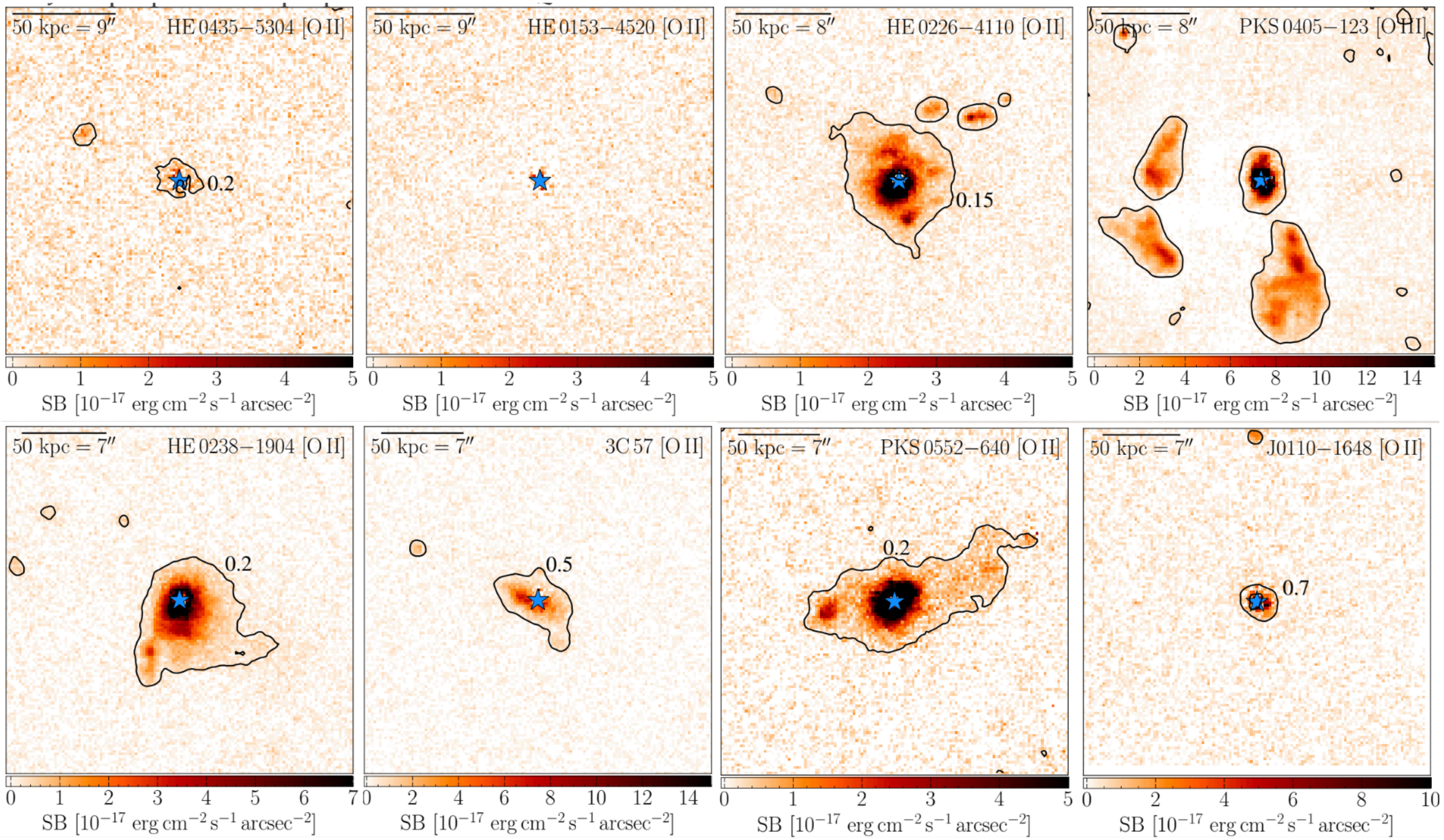

Johnson et al. (2023)

Mapping Feeding and Feedback in Quasar Host Halos

- Declining [OIII]/[OII] ratio with distance from the QSO supports the gas being photo ionized by the QSO
- Matching kinematics and morphologies to interacting galaxy pairs in the quasar host group support an origin in stripped ISM rather than large-scale quasar outflows

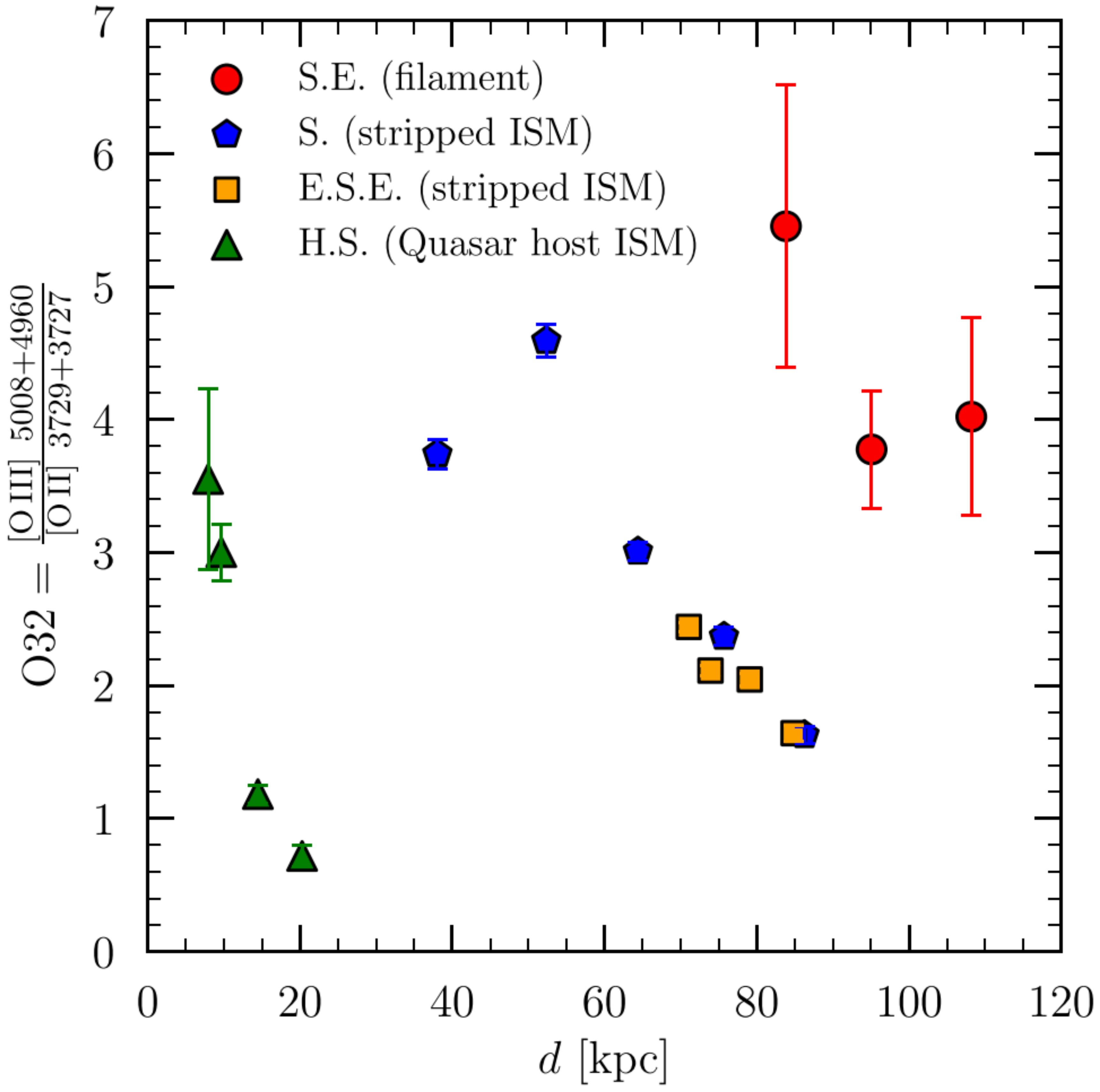

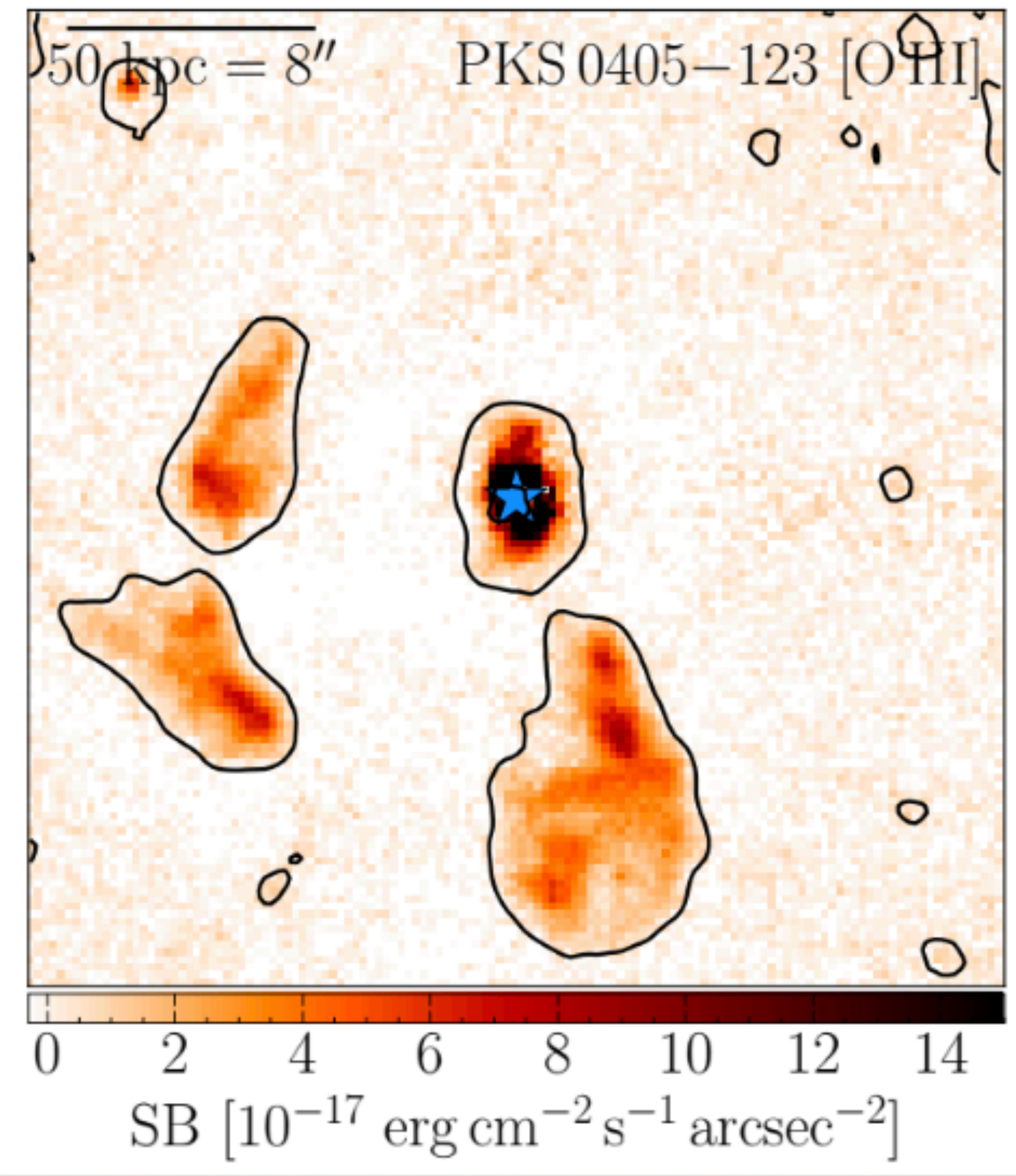

Johnson et al. (2018)

TURBULENT ENERGY CASCADE IN THE DIFFUSE CGM

- moments of the velocity structure functions (VSFs)

$$S_p(r) = \langle |v(\mathbf{x}) - v(\mathbf{x}+\mathbf{r})|^p \rangle \propto r^{\zeta(p)}$$

  The Kolmogorov theory predicts that ζ(p) = p/3 for homogeneous, isotropic, and incompressible fluids

- IFS observations of Hα filaments in intracluster medium enables turbulence measurements.

- The VSFs are found to be steeper than Kolmogorov.

- A number of factors complicates the interpretation of these measurements, including PSF smoothing, low volume filling, large-scale bulk flows (see e.g., Zhang et al. 2022)

Li et al. (2020)

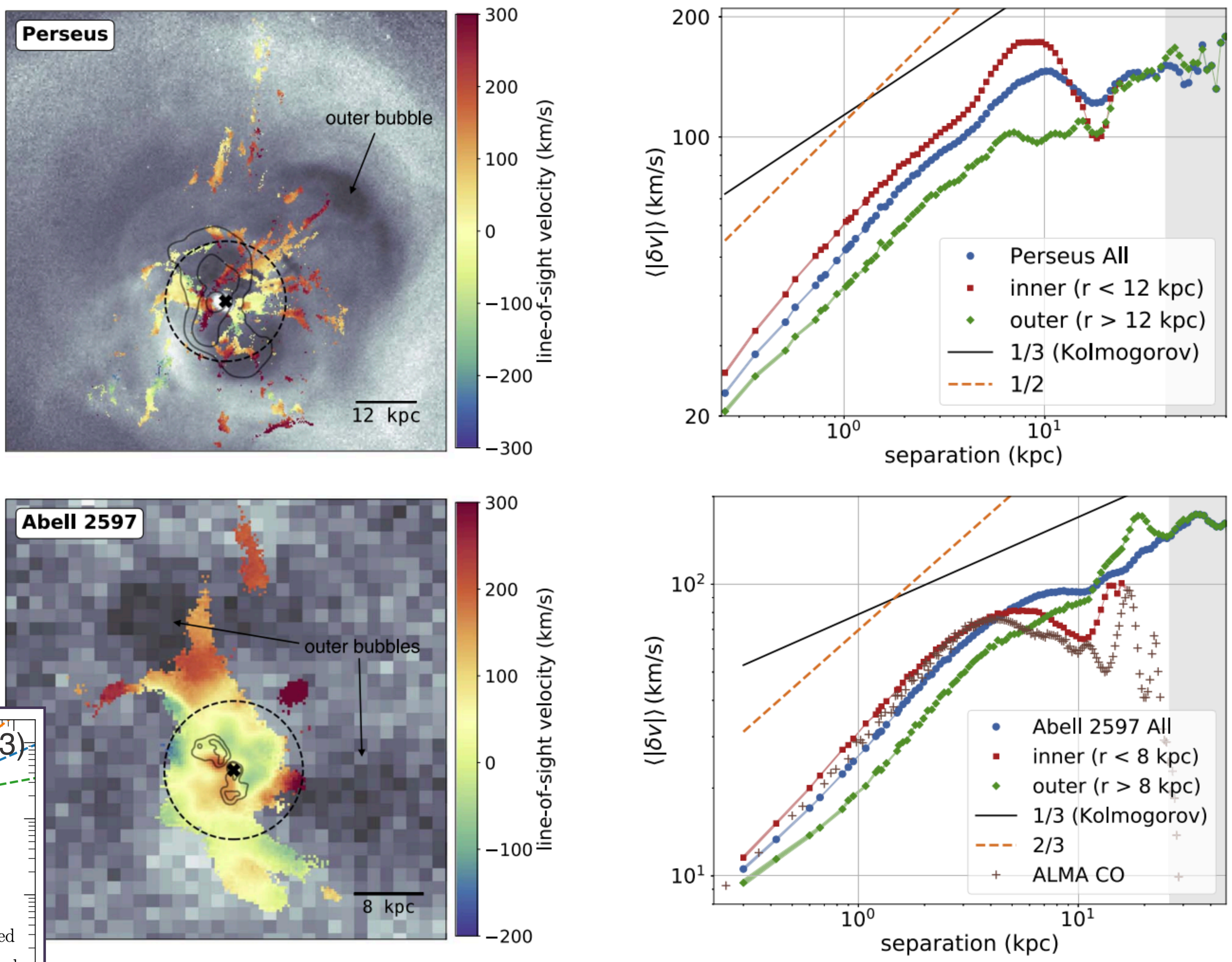

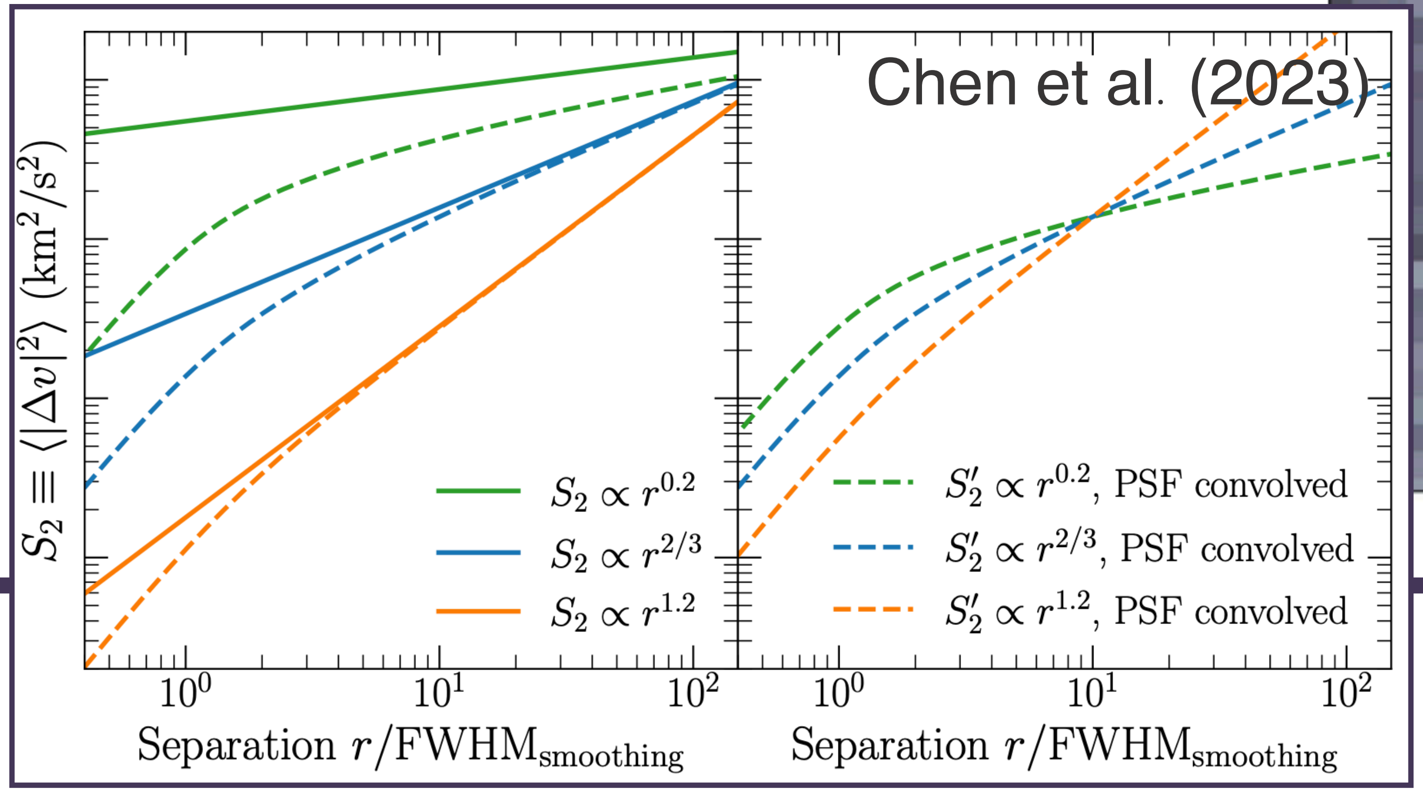

Mapping the Multiphase CGM with Absorption Spectroscopy

Mapping the Multiphase CGM with Absorption Spectroscopy

Tracers of multiphase CGM

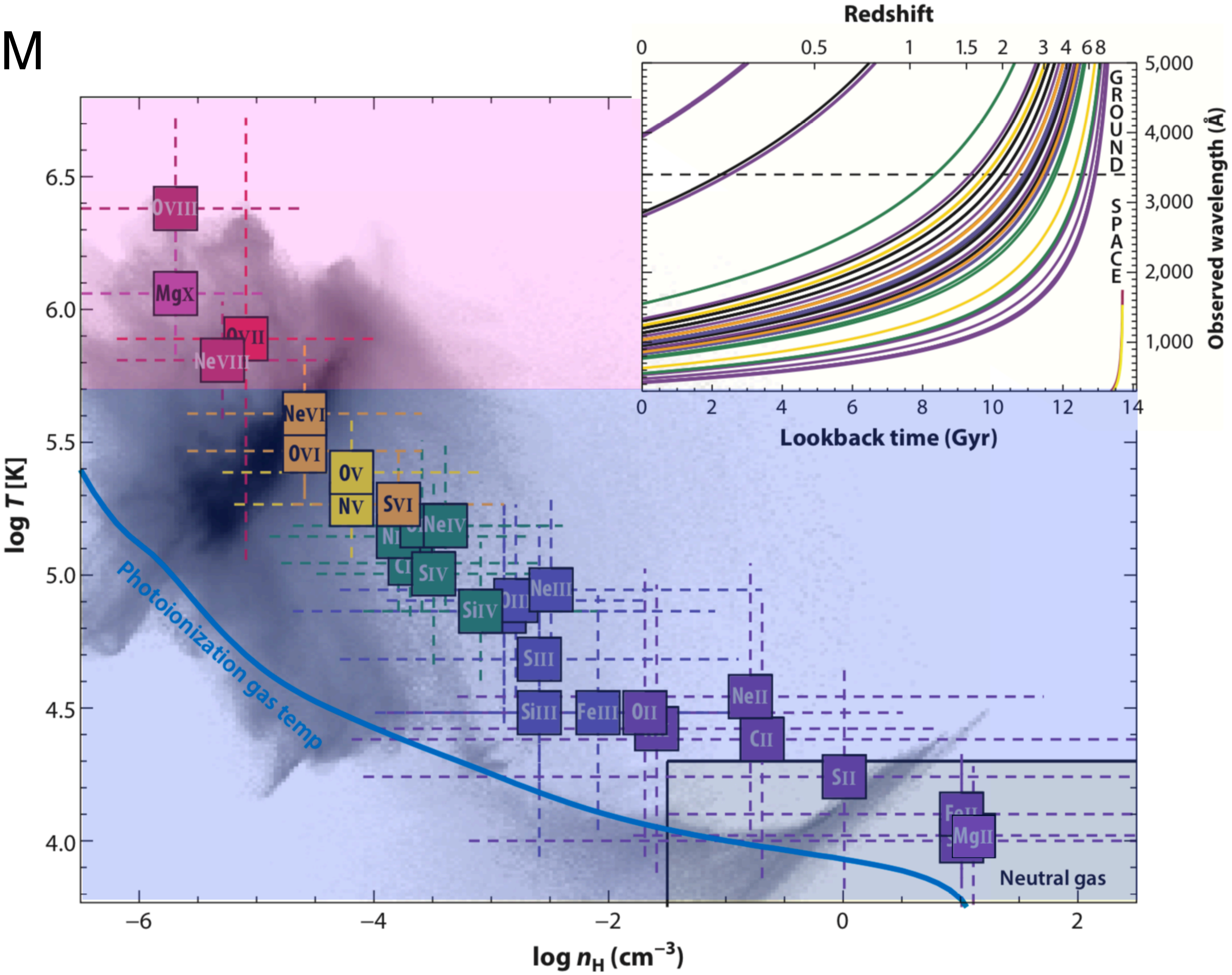

Tumlinson, Peeples, Werk (2017)

Mapping the Multiphase CGM with Absorption Spectroscopy

Cross-section characterization of different ions in galactic halos

Liang & Chen (2014)

Ensemble average

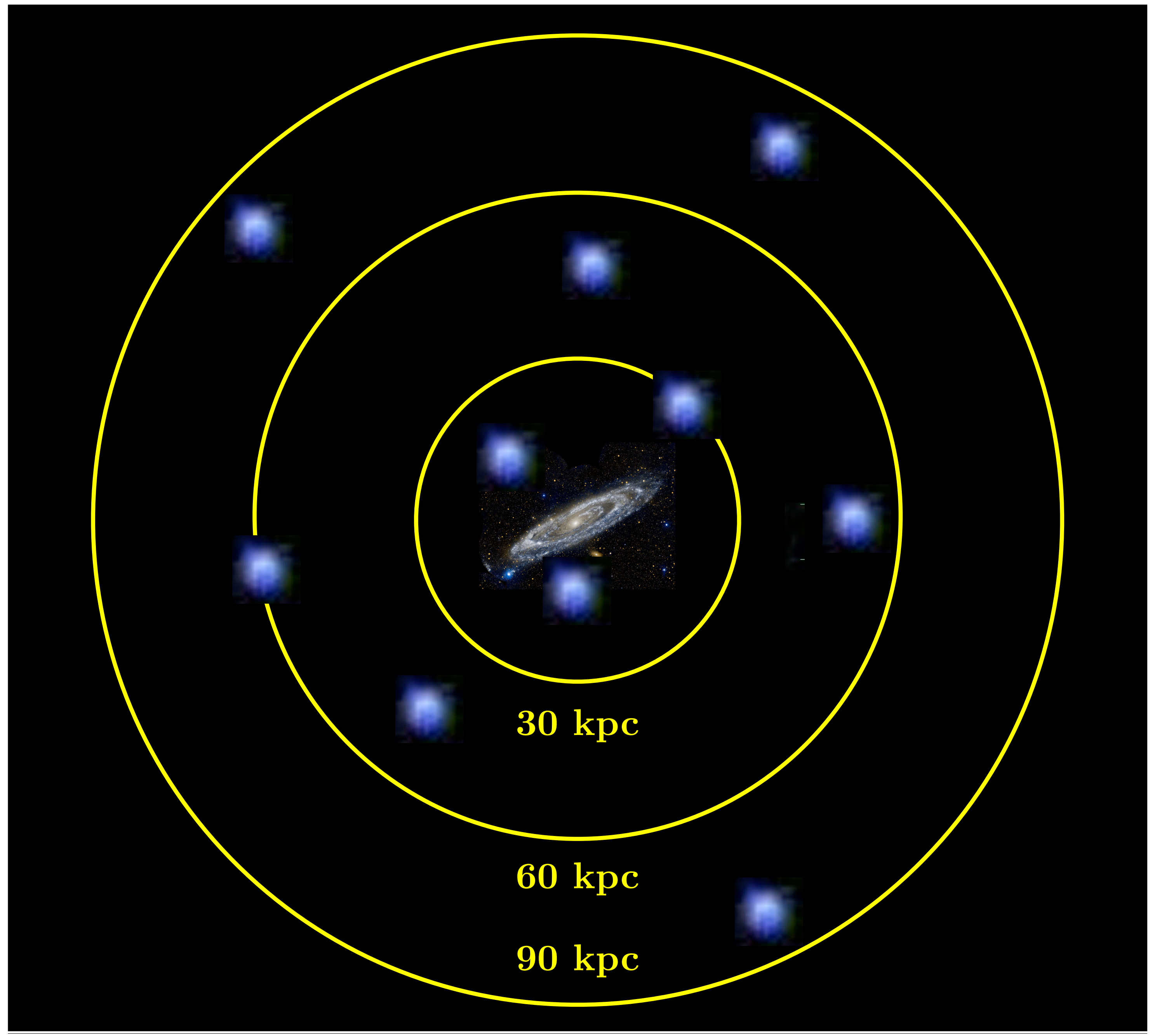

Boksenberg & Sargent '78; Boksenberg+'80; Bergeron '86; Cristiani '87; Lanzetta & Bowen '90,'92; Steidel '93; Steidel+'94; Lanzetta+'95; Bowen+'95; Steidel+'97; Guillemin & Bergeron '97; Le Brun+'97; Chen+'98,01a; Tripp+'98; Chen+01b; Churchill '01; Steidel+'02; Bowen+'02; Rao+'03; Churchill+'03; Adelberger+'03,'05; Stocke+'06; Kacprzak+'07,'10; Nestor+'07; Chen & Tinker '08; Barton & Cooke '09; Chen & Mulchaey '09; Chen+'10a,b; Gauthier+'09,'10; Gauthier & Chen '11,'12; Lovegrove & Simcoe '11; Rao+'11; Nestor+'11; Borthakur+'11; Tripp+'11; Prochaska+'11; Ménard+'11; Tumlinson+'11; Thom+'12; Rakic+'12,'13; Rudie+'13; Stocke+'13; Werk+'13; Borthakur+'13; Liang & Chen '14 …..

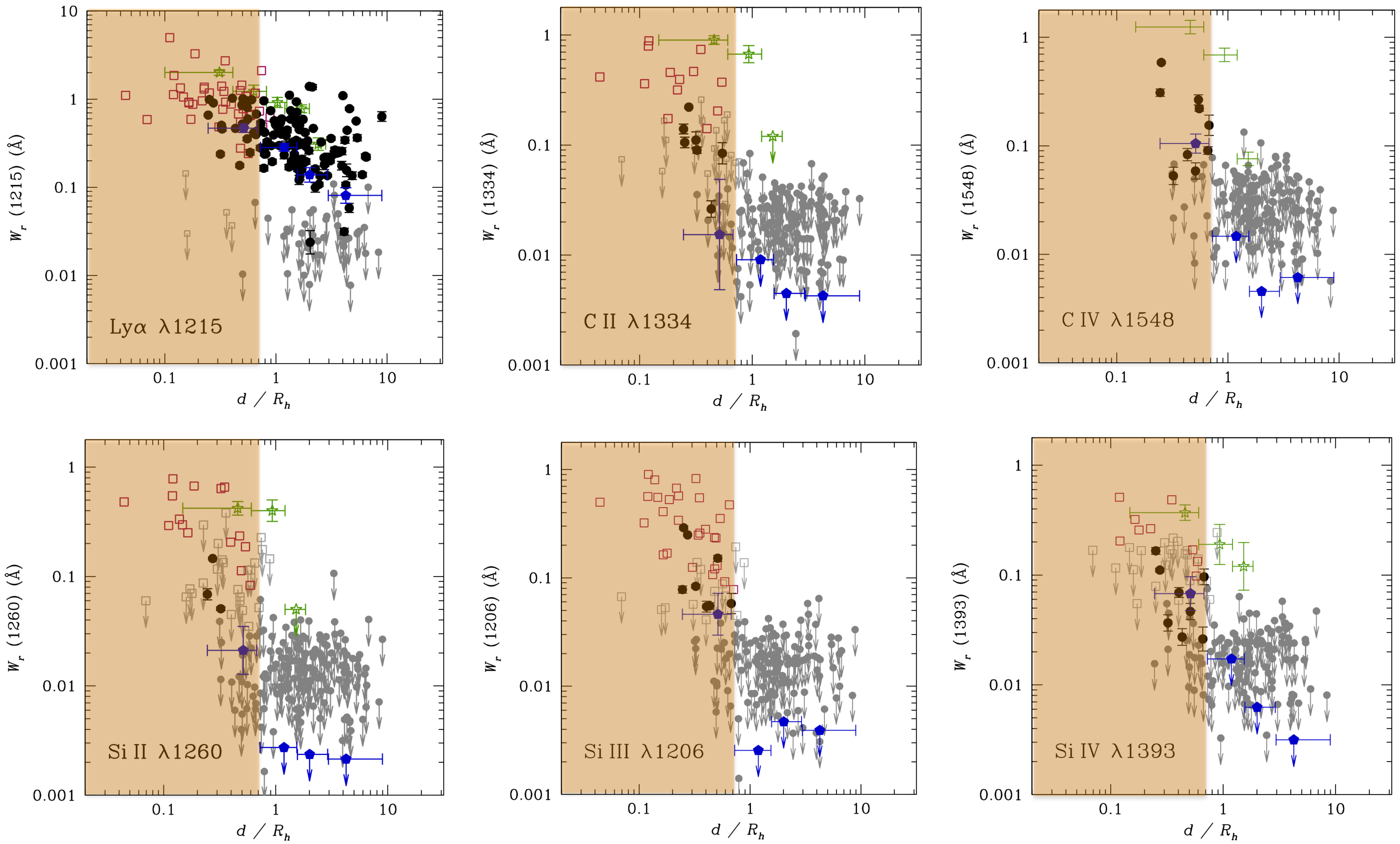

CONNECTING THE MULTIPHASE CGM WITH GALAXY PROPERTIES

bluer galaxies are found in more gas-rich halos: feeding or feedback?

increasing gas covering fraction

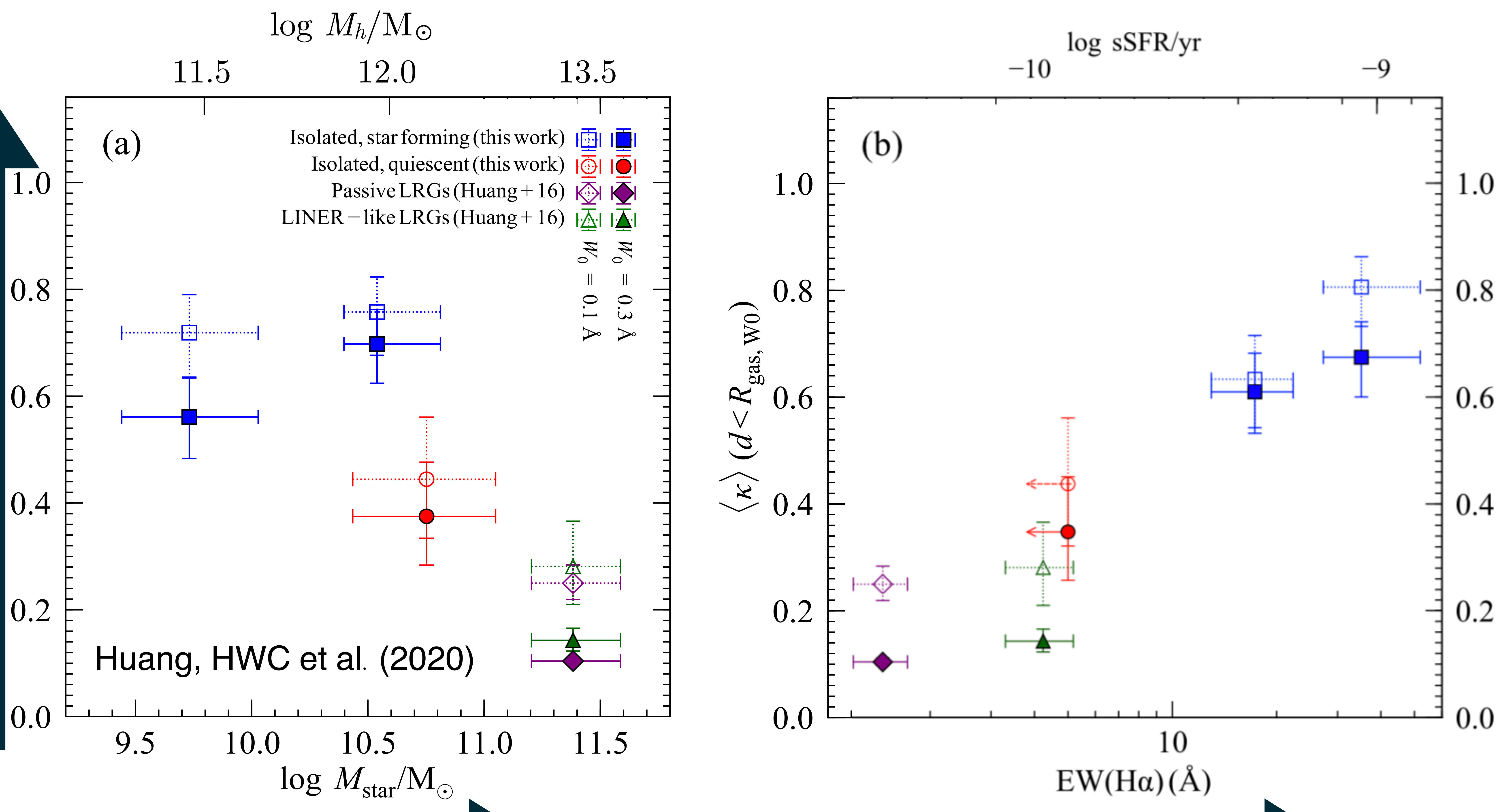

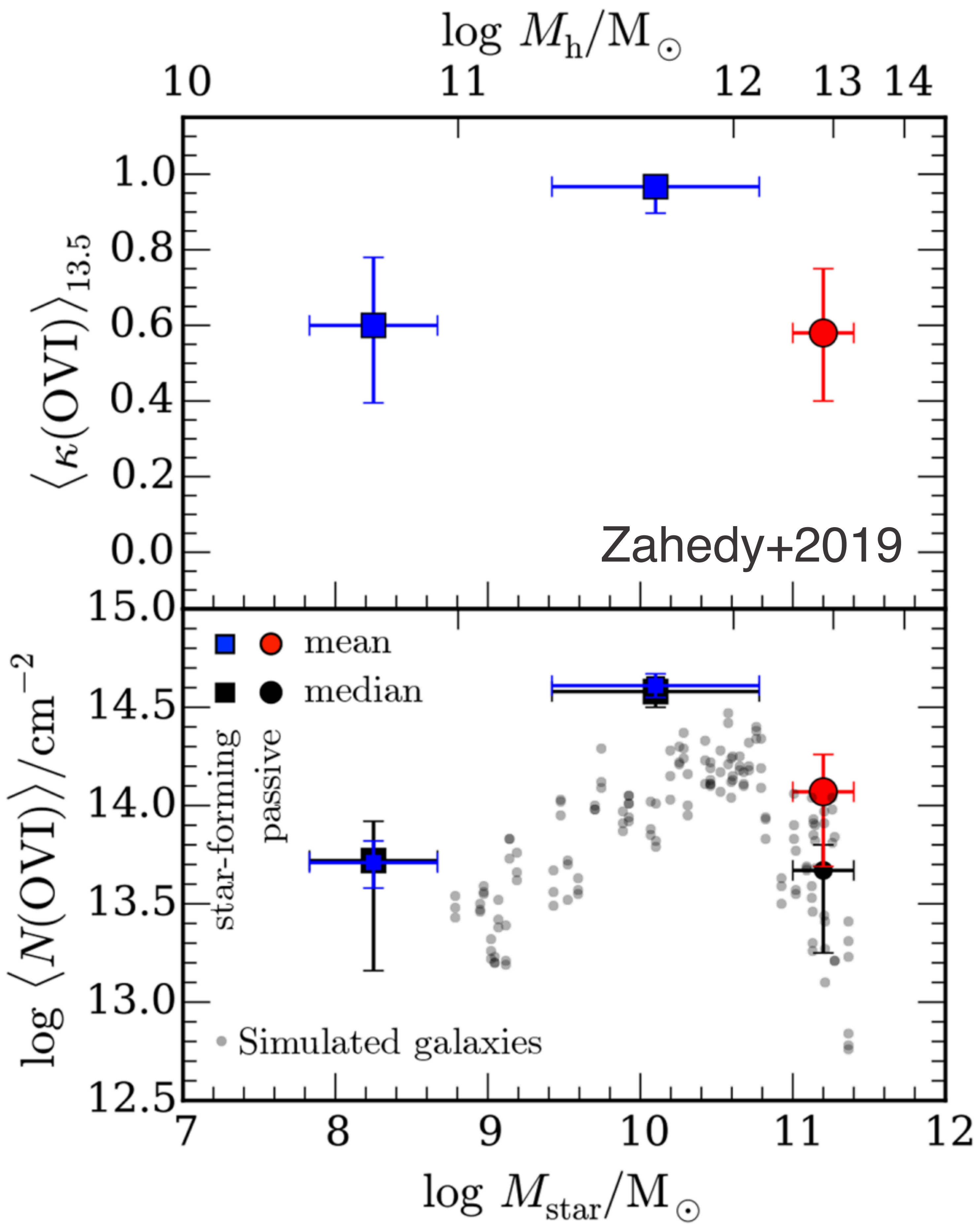

increasing mass

increasing SFR/mass

Cf. Kirill Tchernyshyov et al. (2023)

Pushing to the low mass regime at $M_{star} < 10^9\ M_\odot$

$M_{star} \sim 8e7\ M_\odot$ at d = 16 kpc

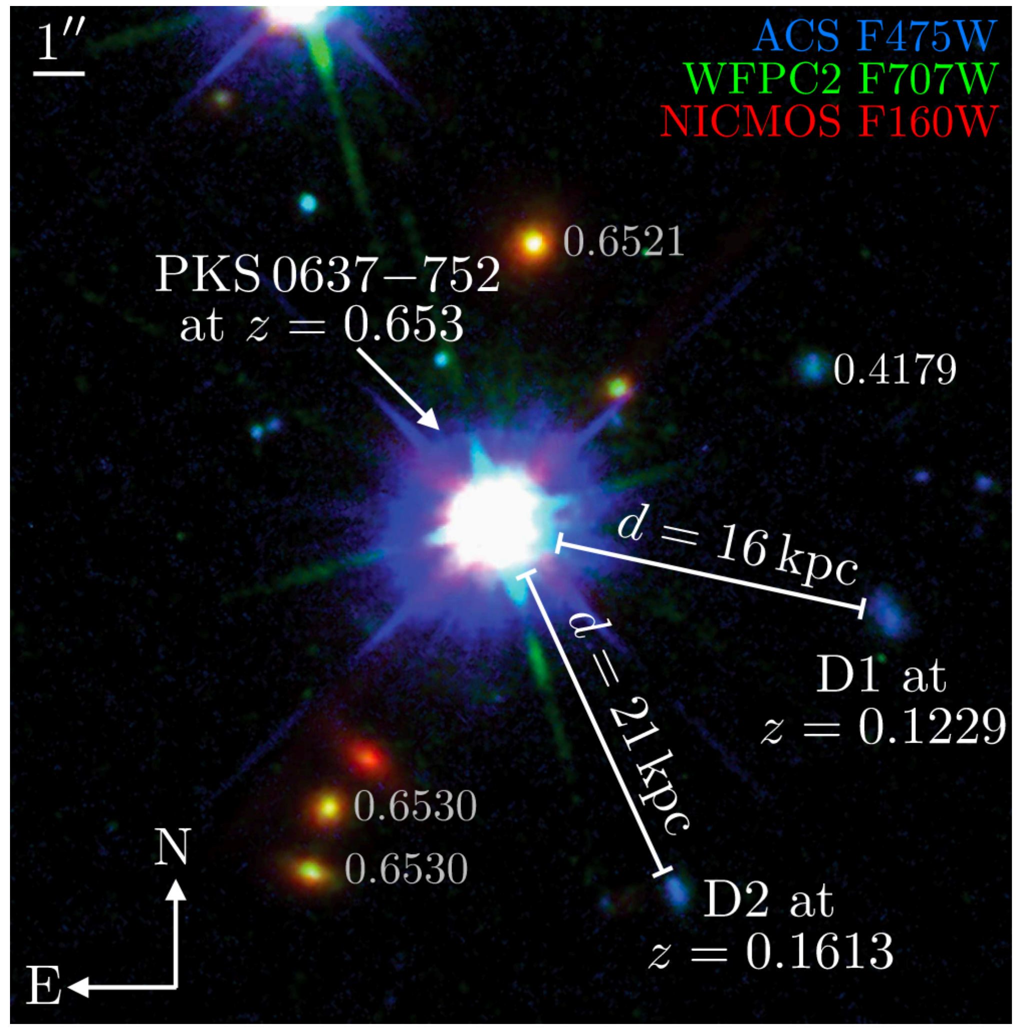

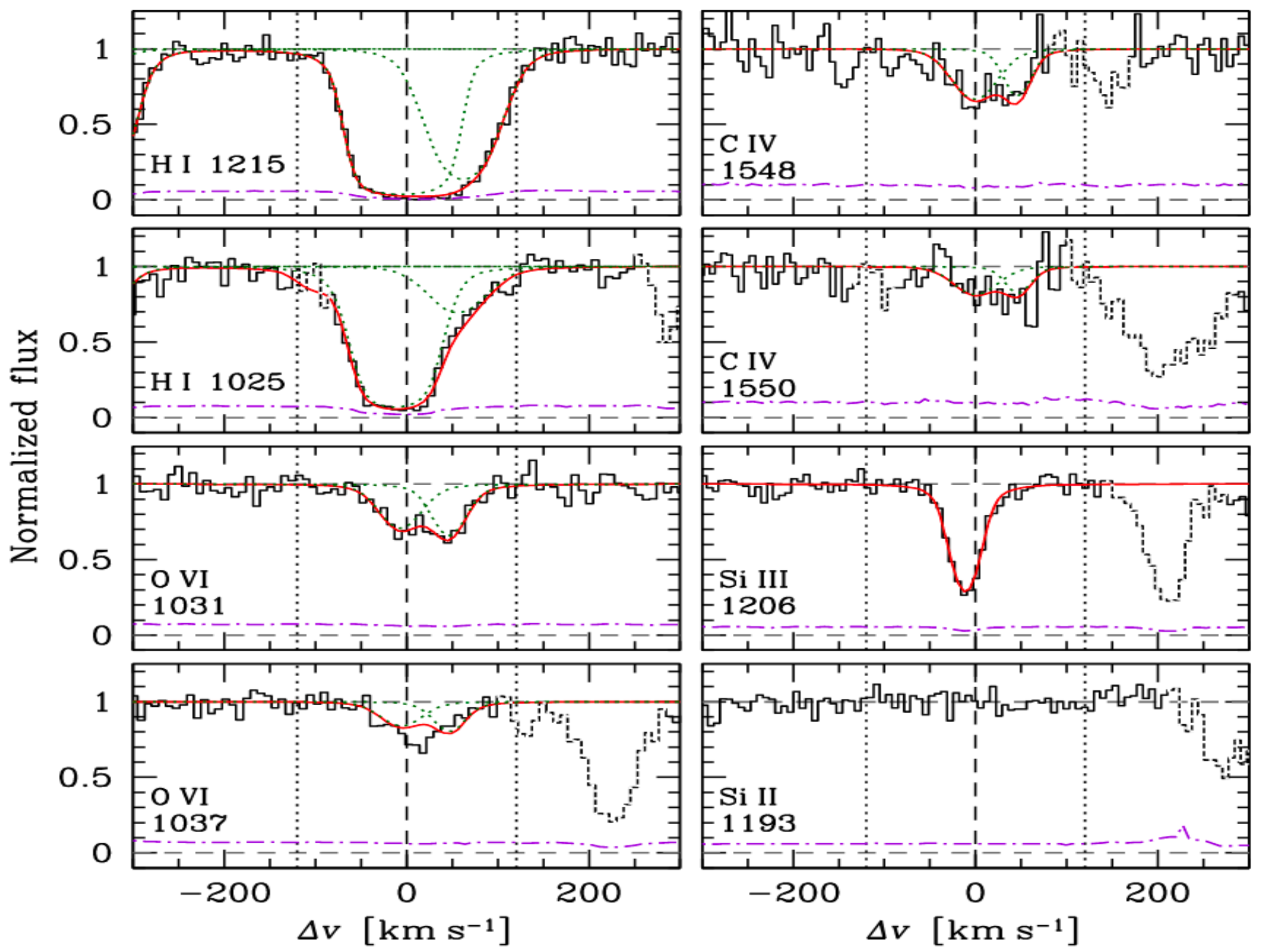

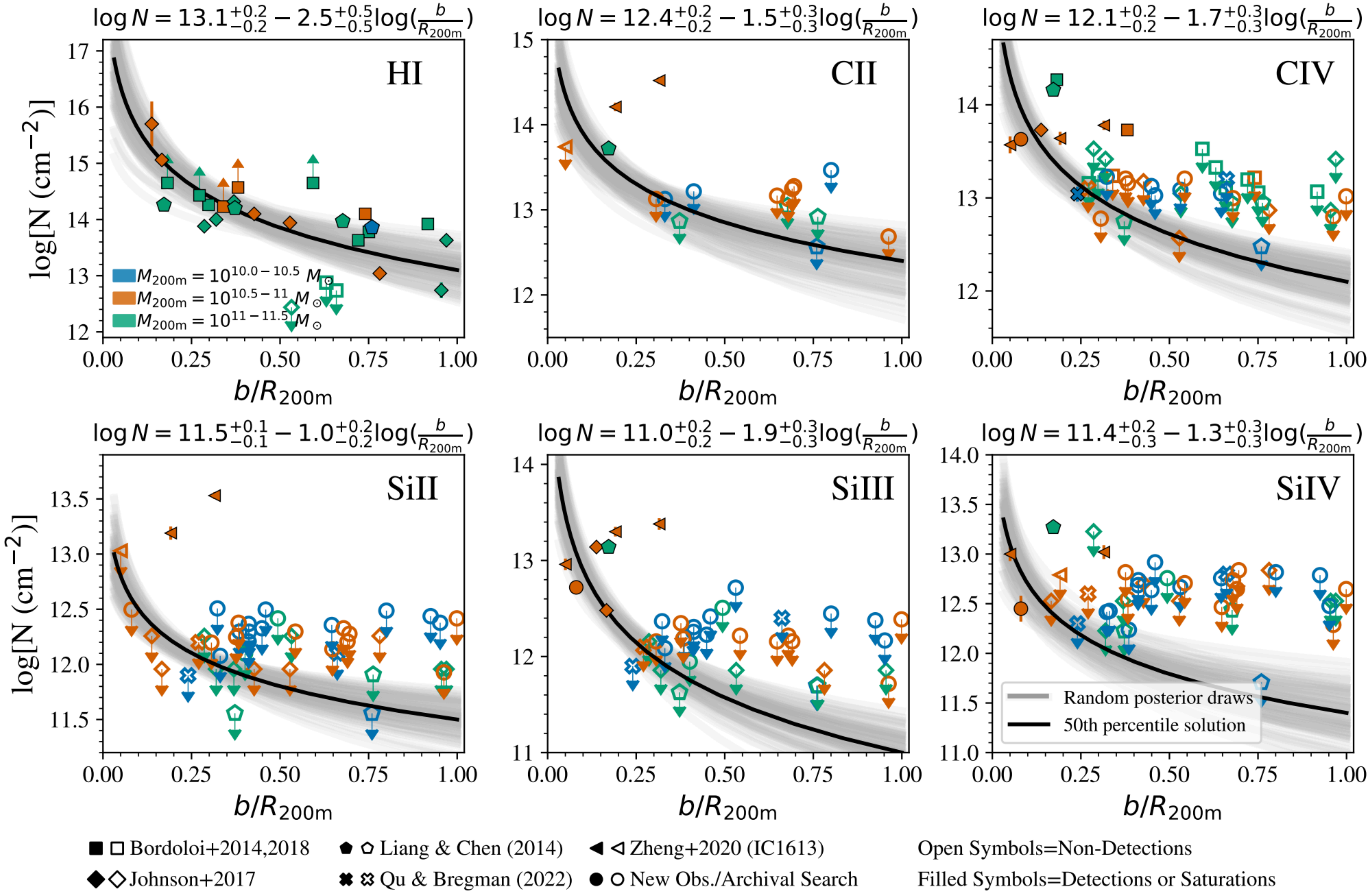

Johnson+2017

Zheng+2023

Pushing to the low mass regime at $M_{star} < 10^9\ M_\odot$

How do the clumps form and evolve in low-mass halos?

$M_{star} \sim 8e7\ M_\odot$ at d = 16 kpc

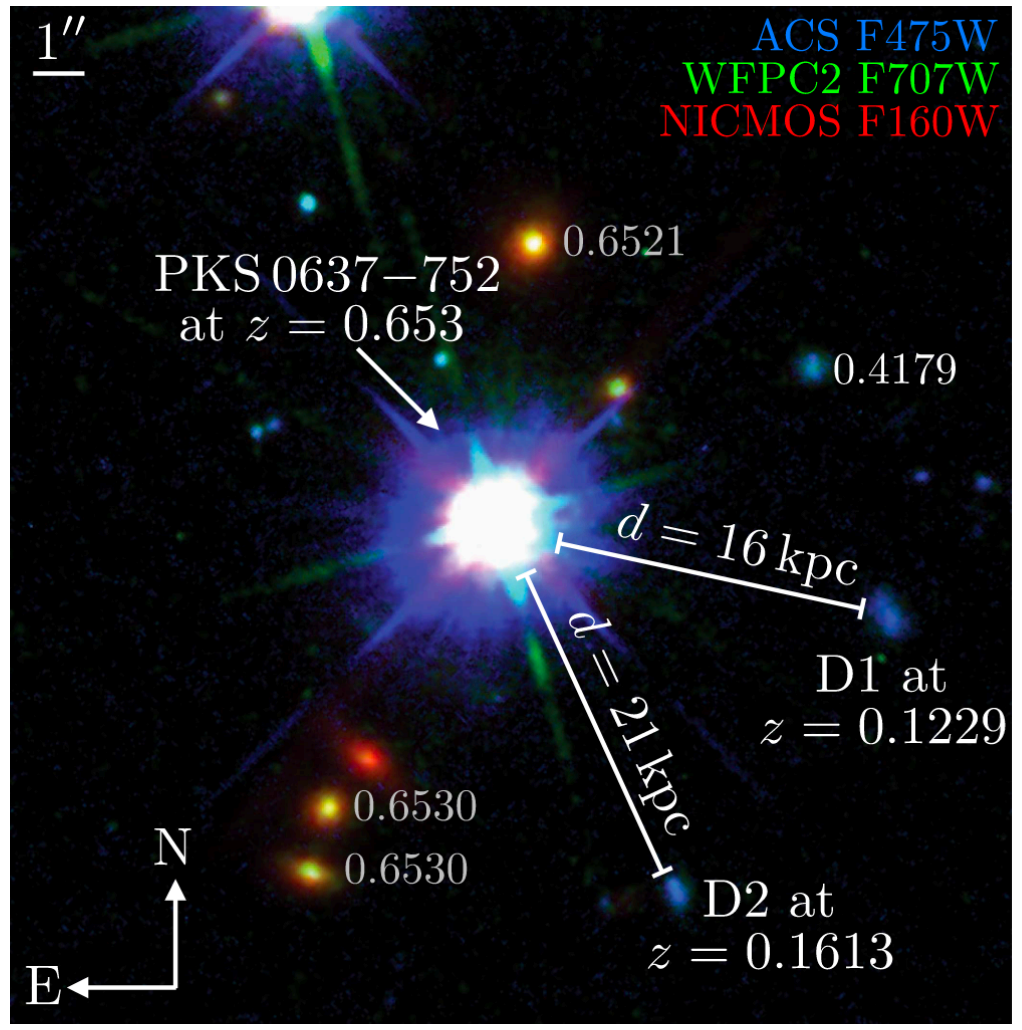

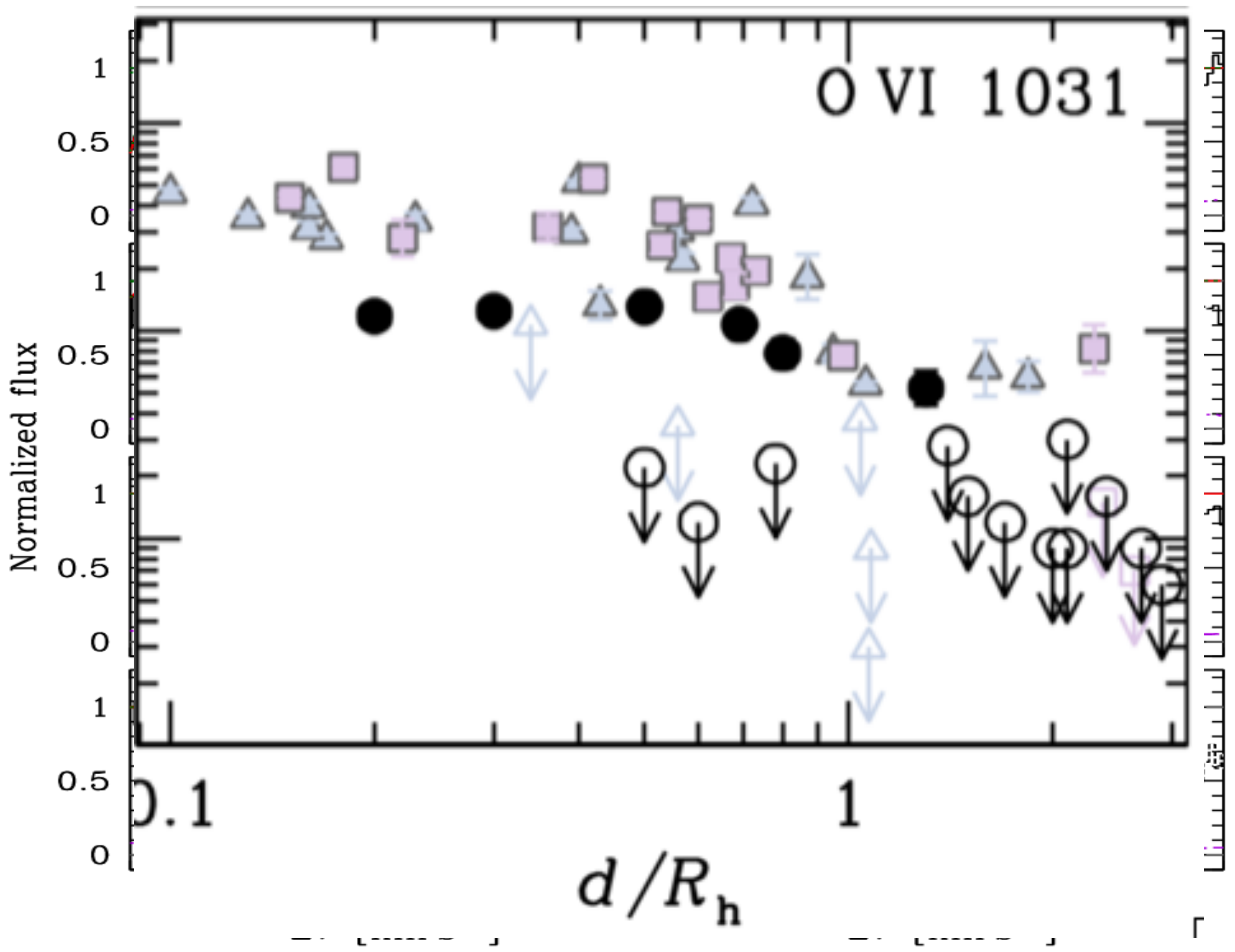

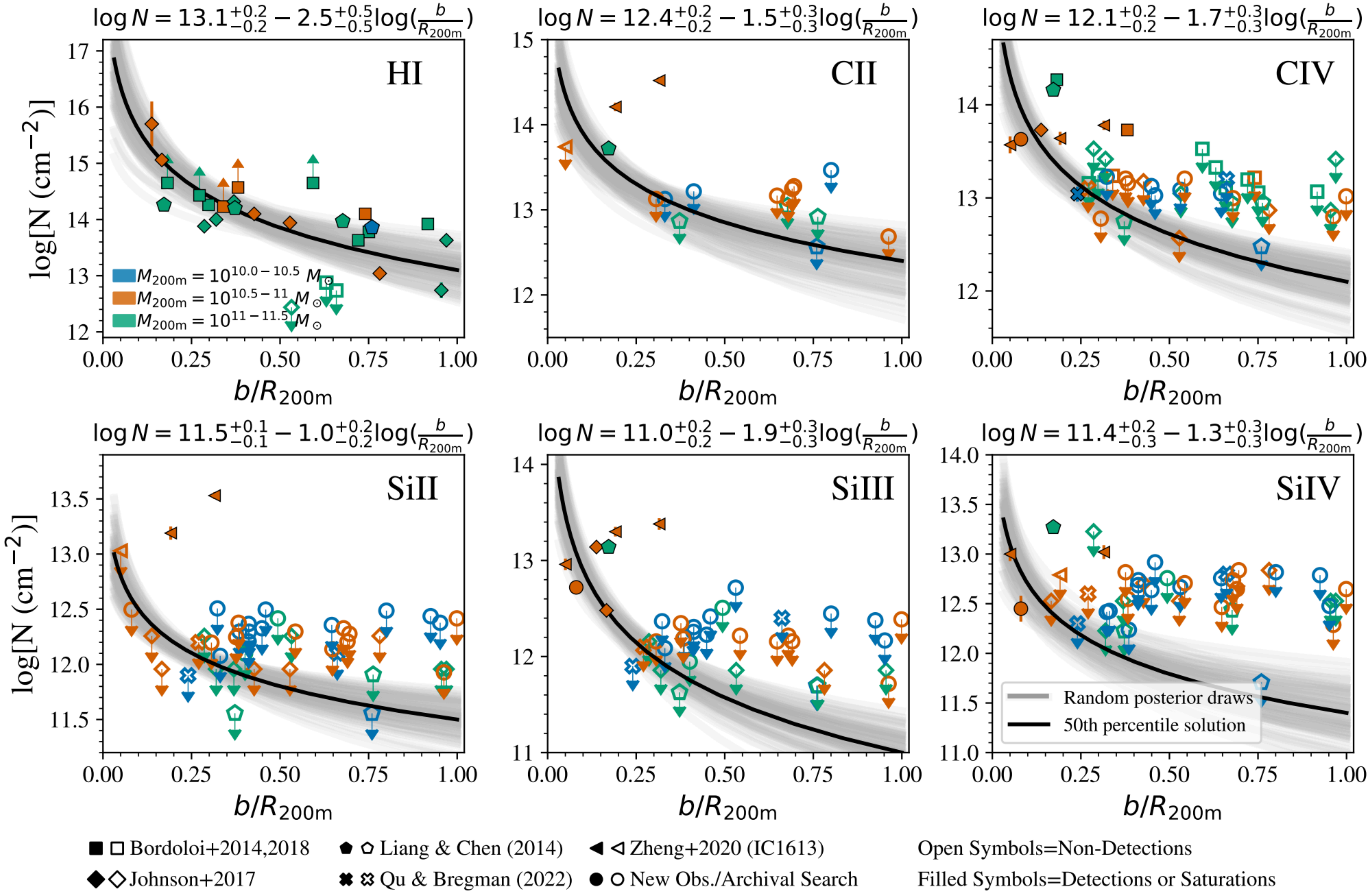

Johnson+2017

Zheng+2023

Resolving the physical properties (n_H, T, Z) from observed relative abundance ratios between different ions

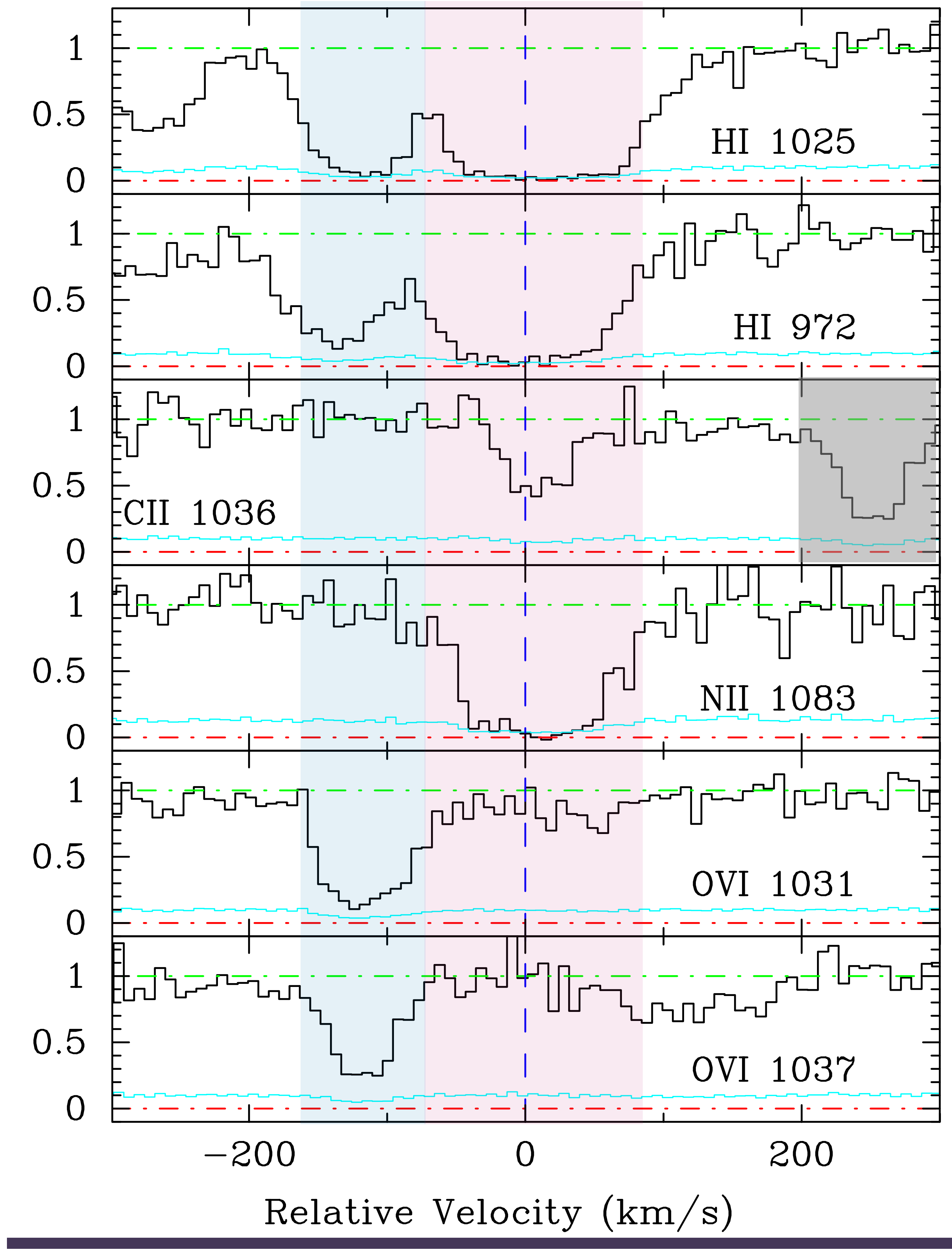

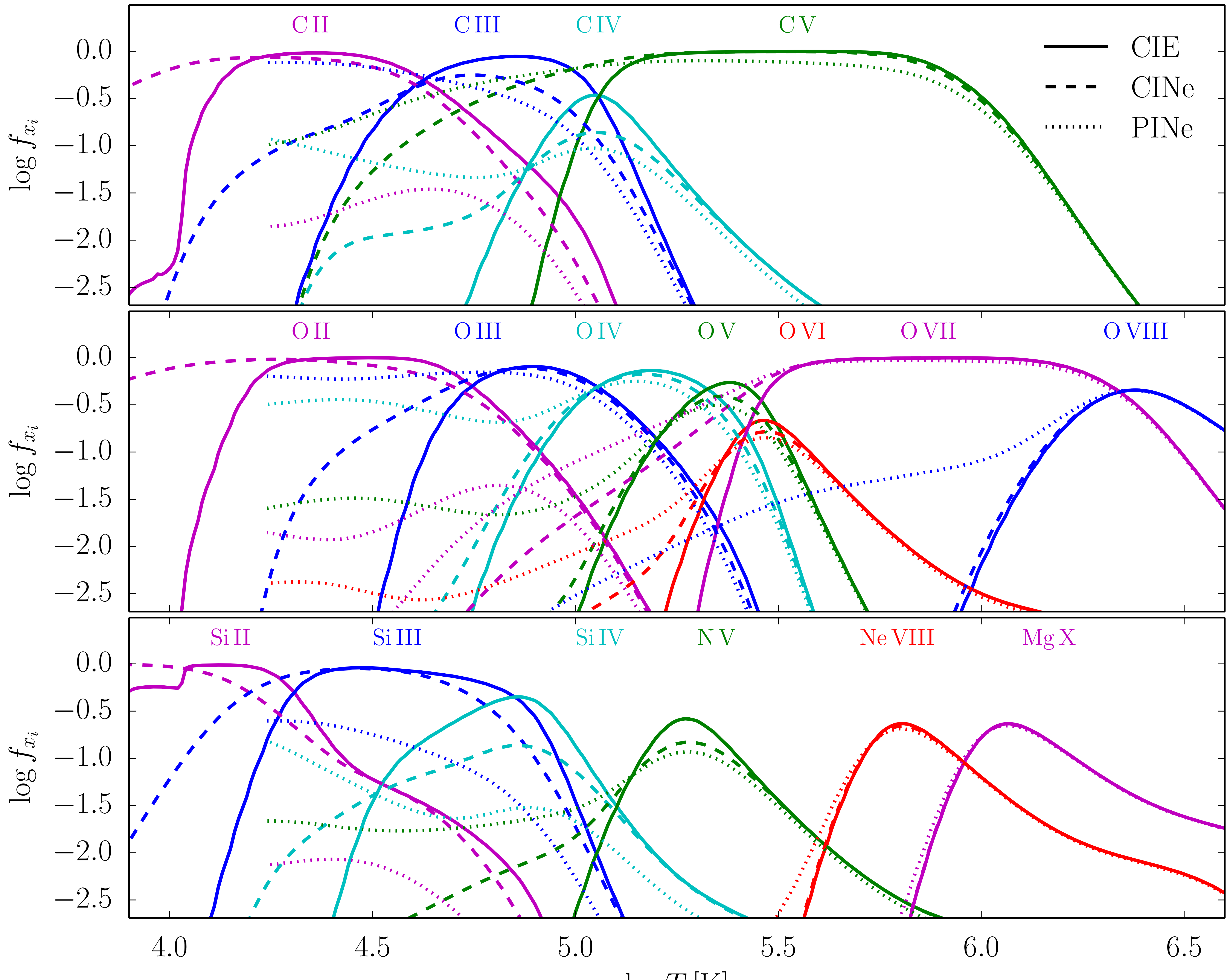

Oppenheimer et al. (2013)

NECESSARY INGREDIENTS FOR ACCURATE IONIZATION MODELS

- broad spectral coverage of multiple ionization states

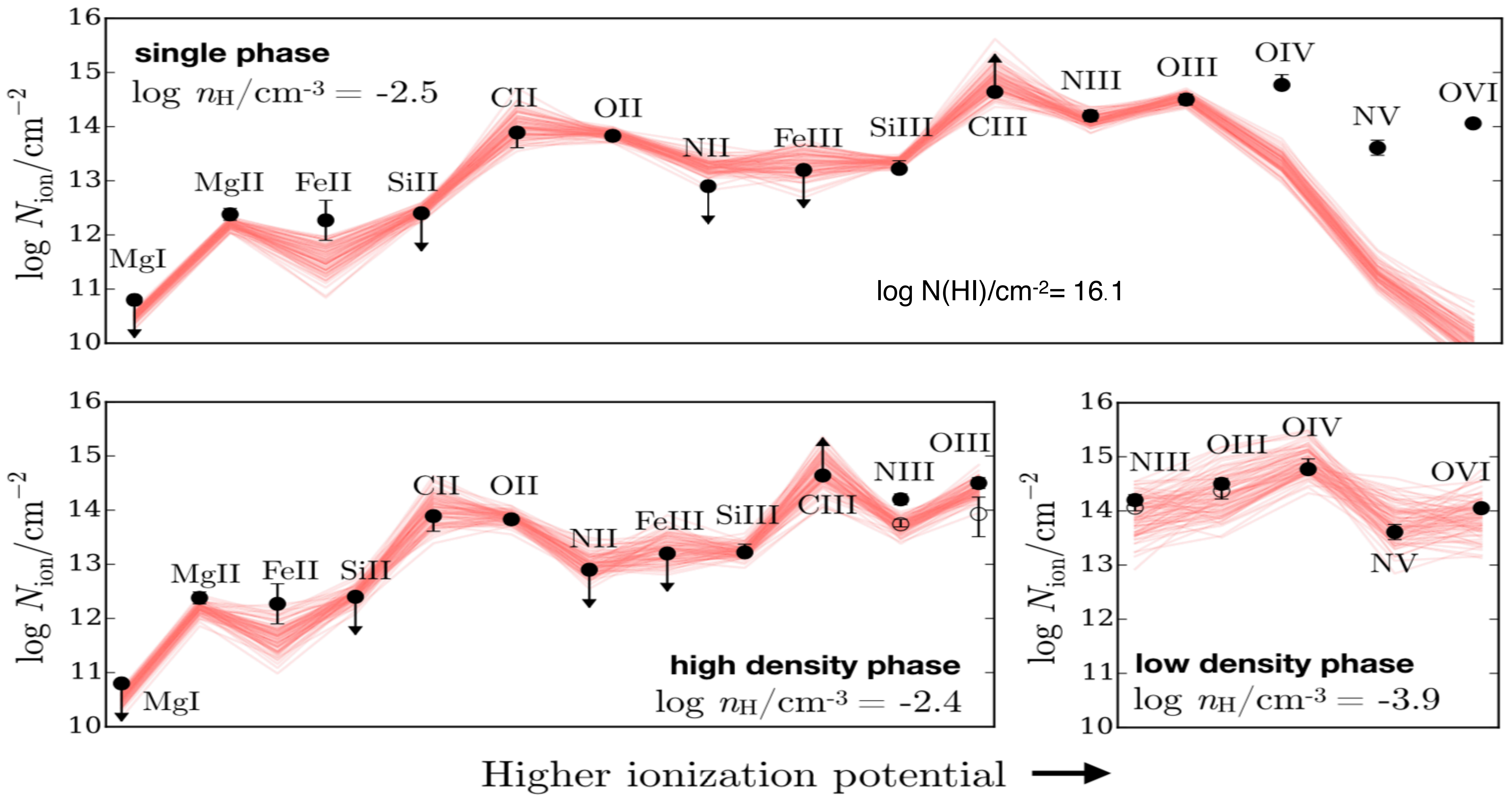

Zahedy+2021; Cooper+2021; Qu+2022; see also Sameer+2021

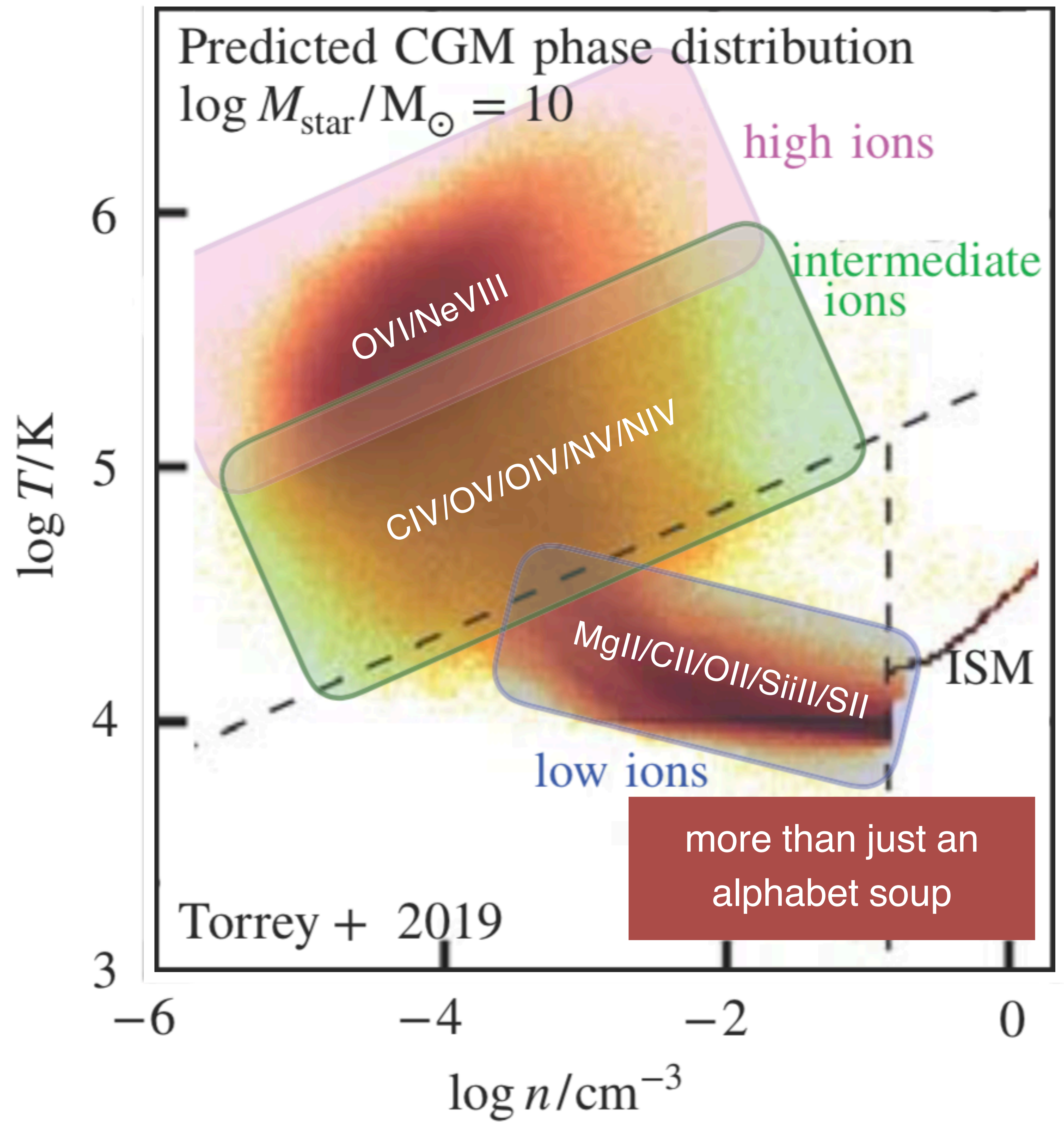

NECESSARY INGREDIENTS FOR ACCURATE IONIZATION MODELS

- broad spectral coverage of multiple ionization states
- high spectral resolution to <u>differentiate gas kinematics</u> and resolve the multiphase structure

$$b_I^2 = \frac{2k_B T}{m_I} + b_{non-thermal}^2$$

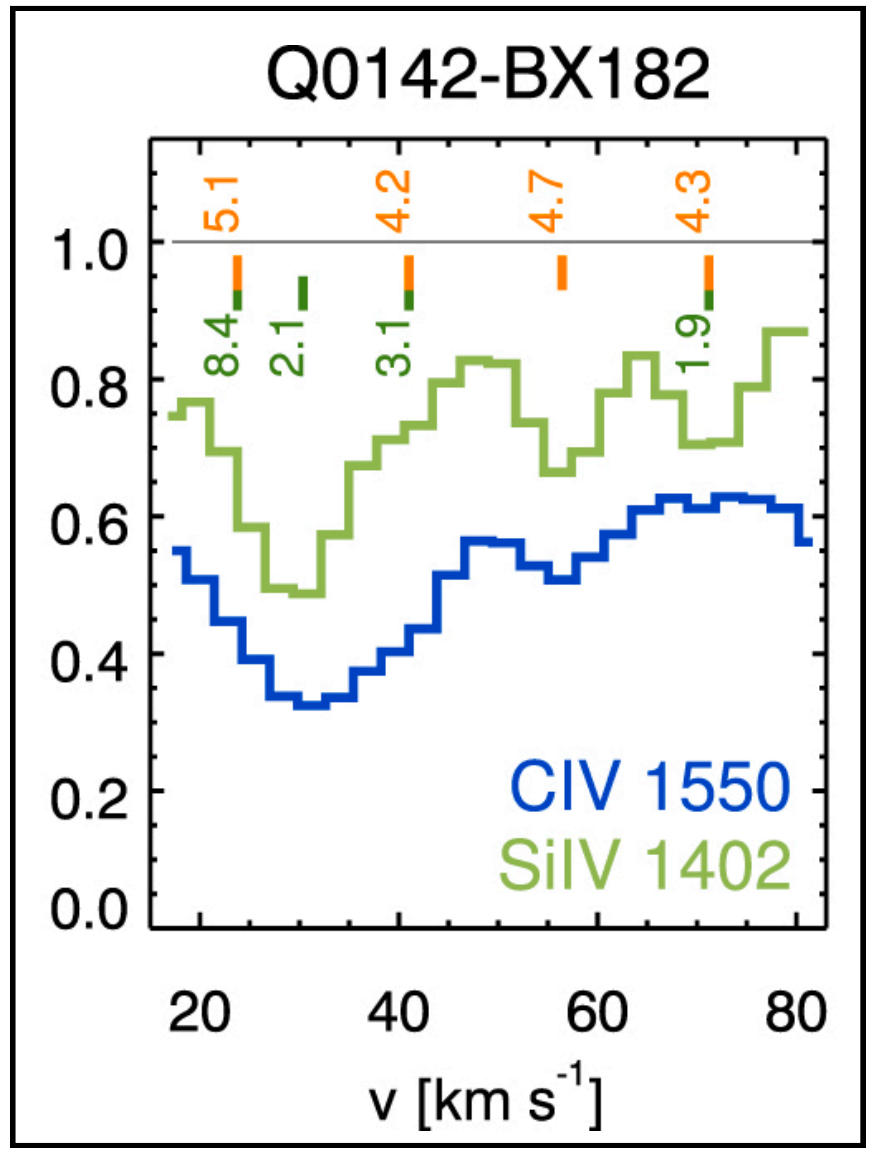

thermal driven

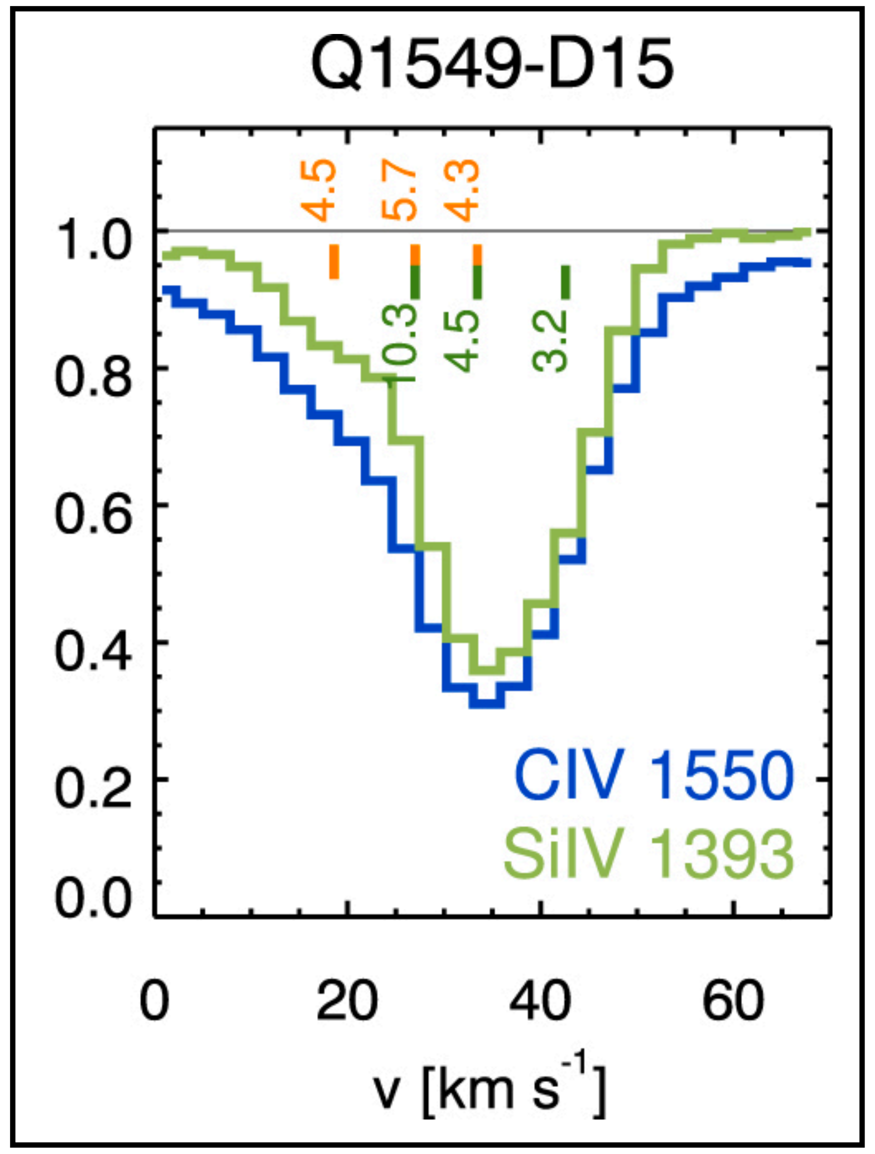

turbulent

Rudie+2019

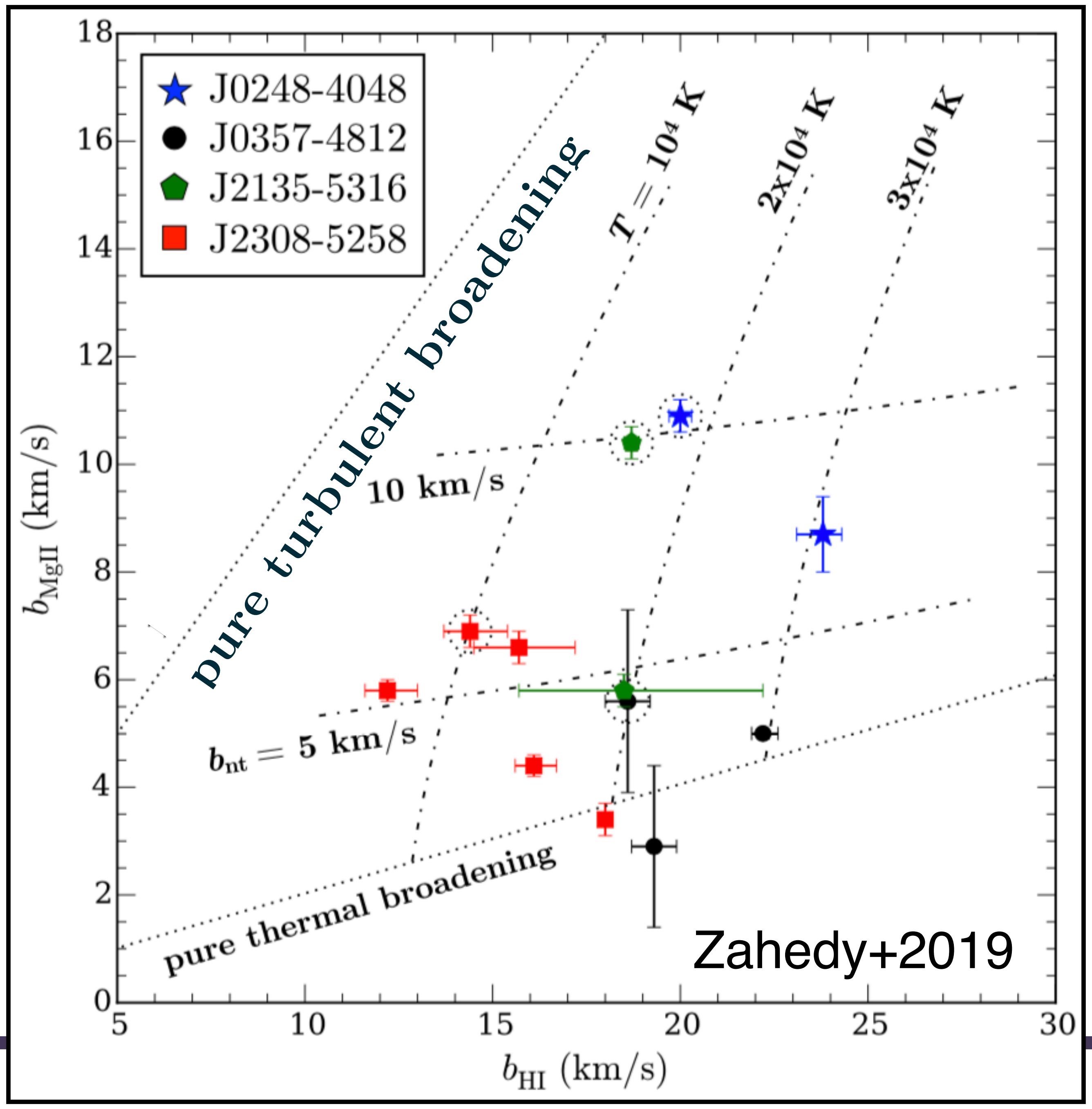

n_H-T distribution is consistent with PIE

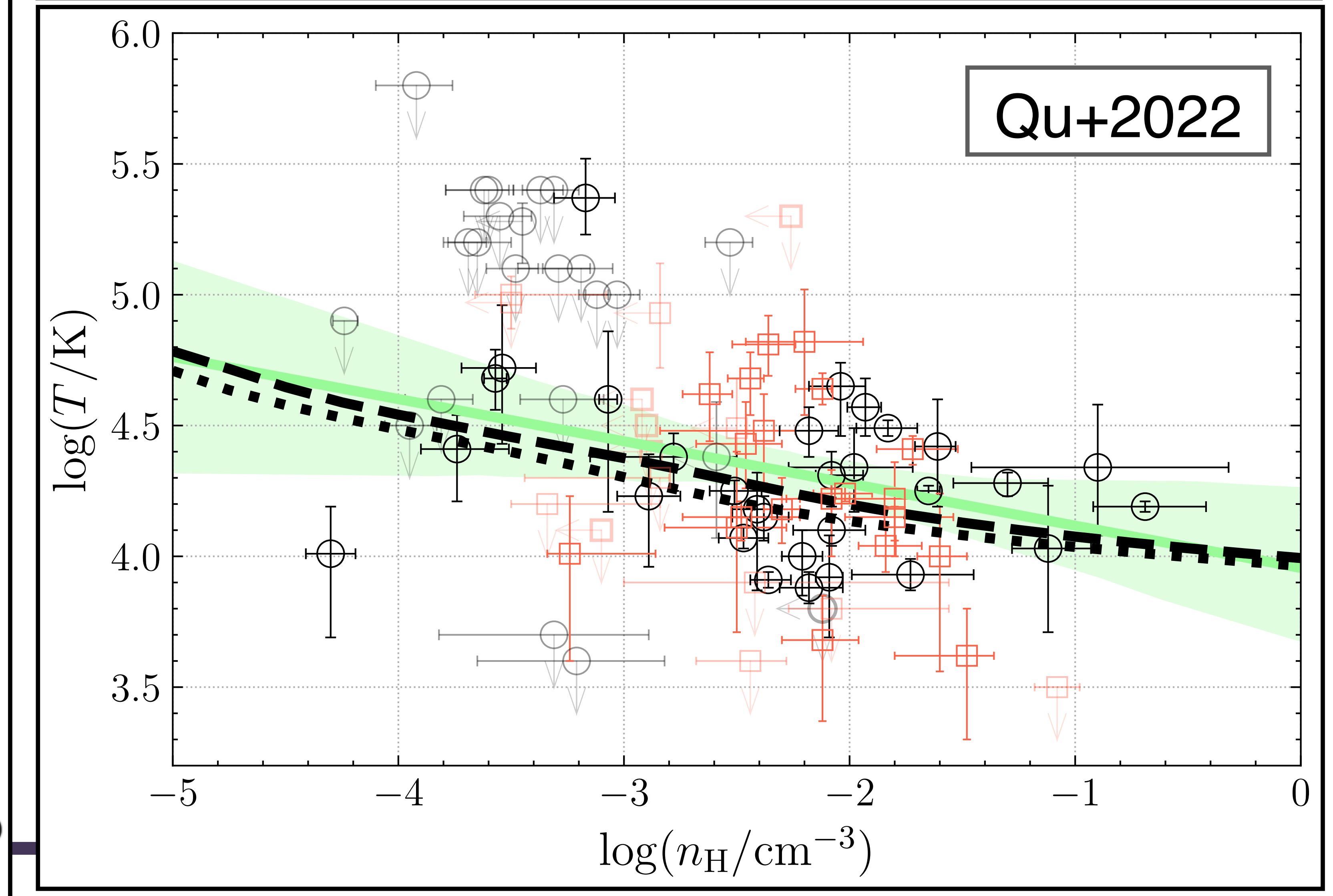

NECESSARY INGREDIENTS FOR ACCURATE IONIZATION MODELS

- broad spectral coverage of multiple ionization states
- high spectral resolution to differentiate gas kinematics and <u>resolve the multiphase structure</u>

increasing b with increasing I.P.

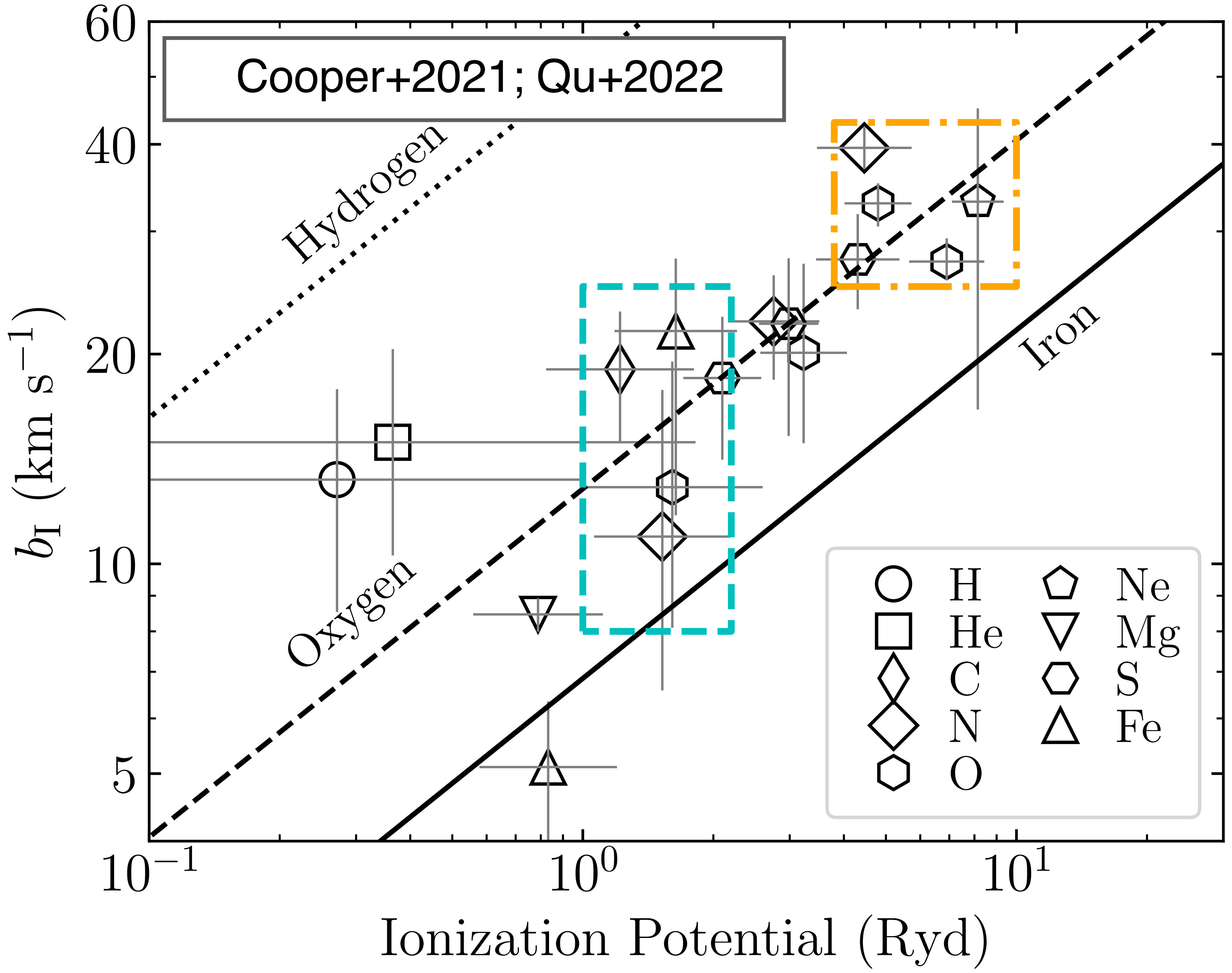

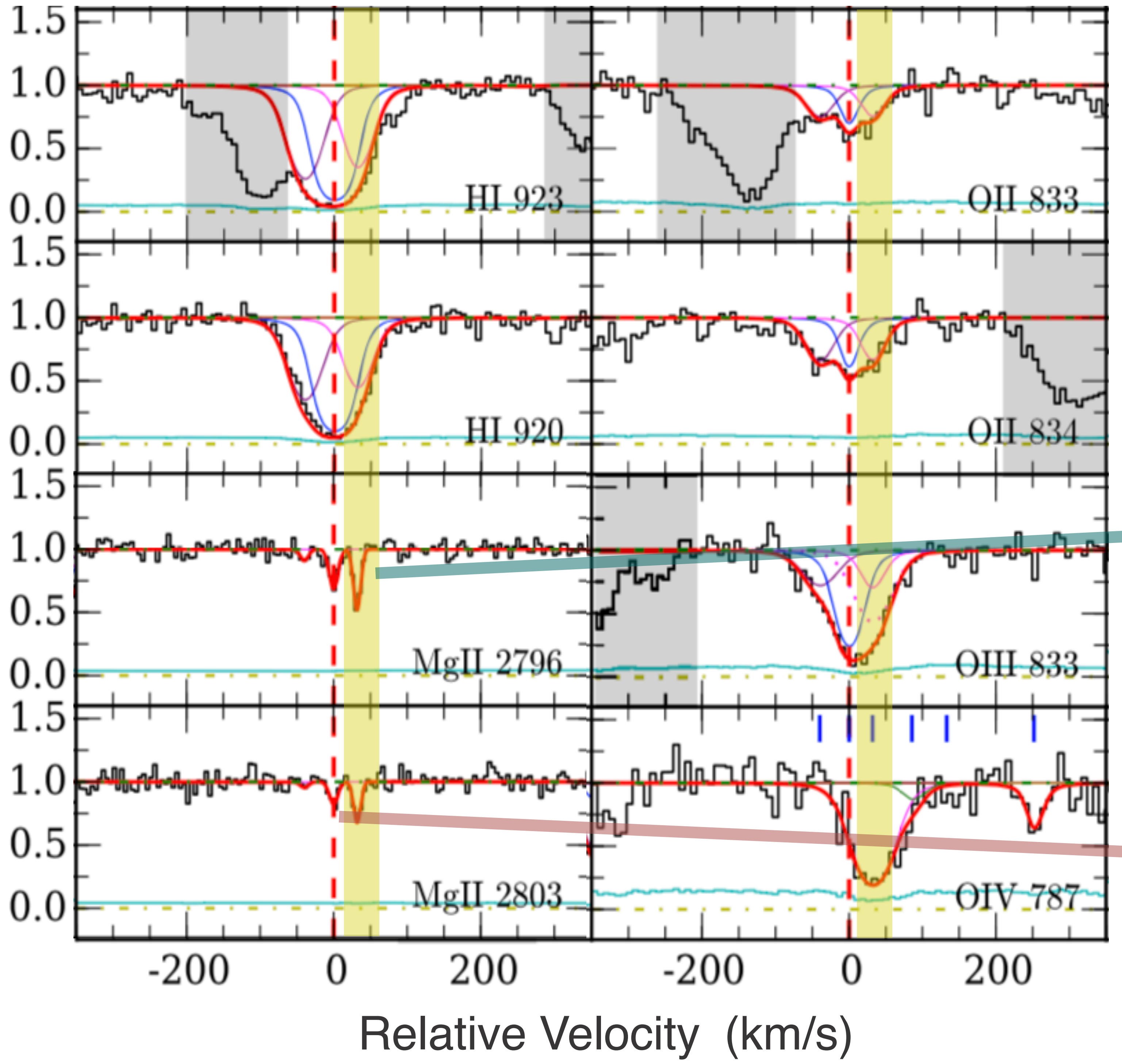

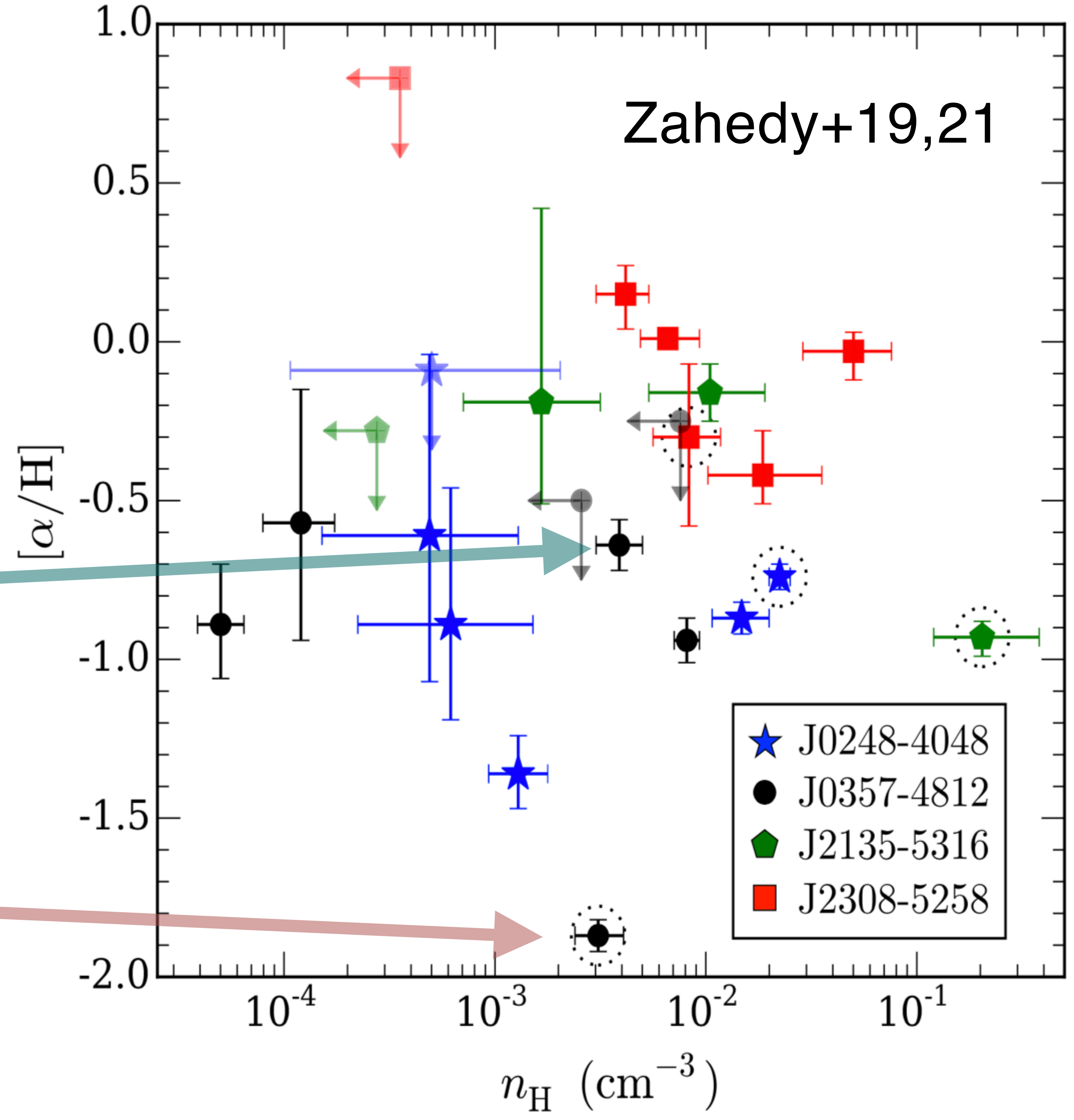

NECESSARY INGREDIENTS FOR ACCURATE IONIZATION MODELS

- broad spectral coverage of multiple ionization states
- high spectral resolution to differentiate gas kinematics and <u>resolve the multiphase structure</u>

large scatter in n_H between individual clumps in pressure equilibrium with the hot halo

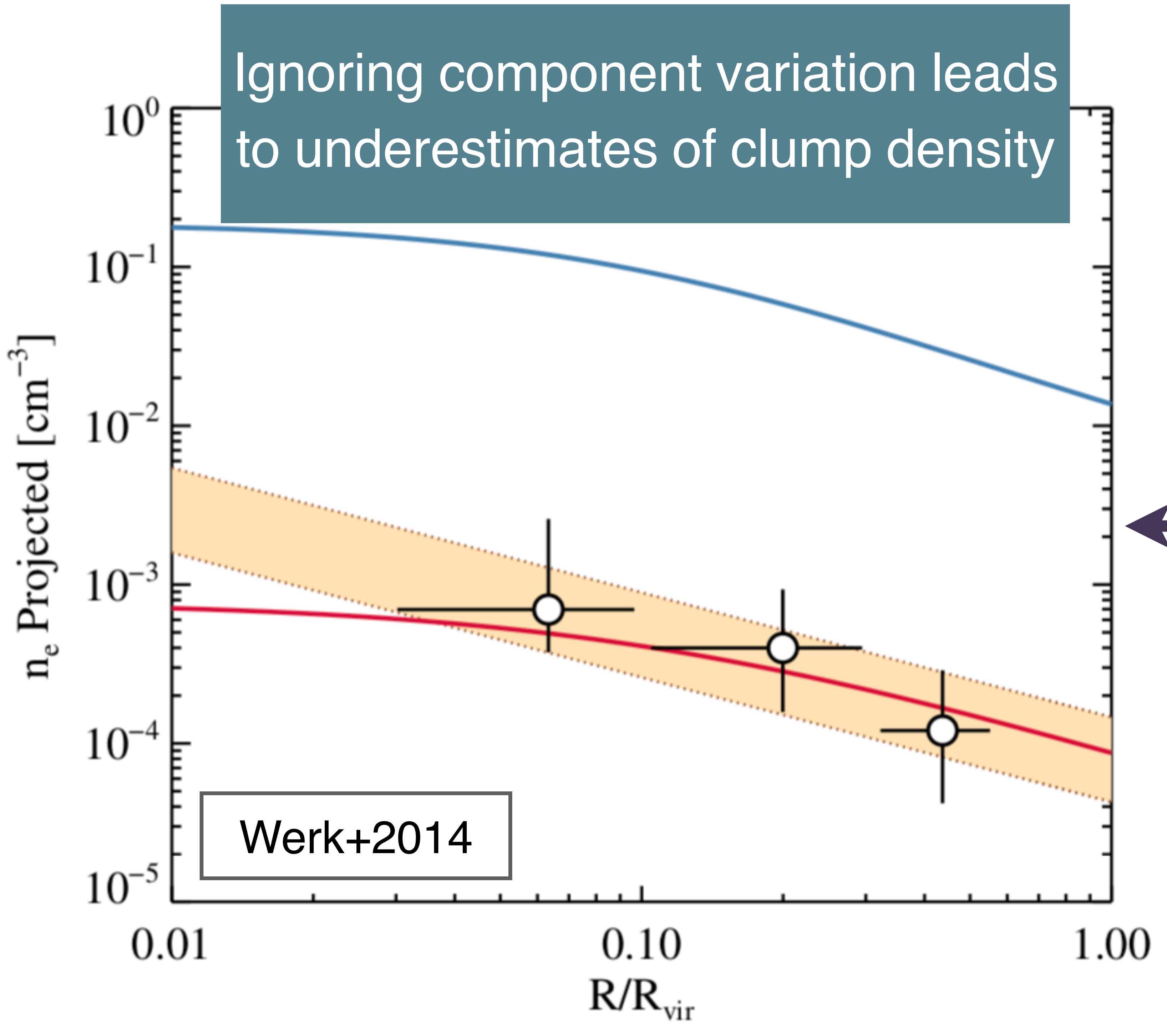

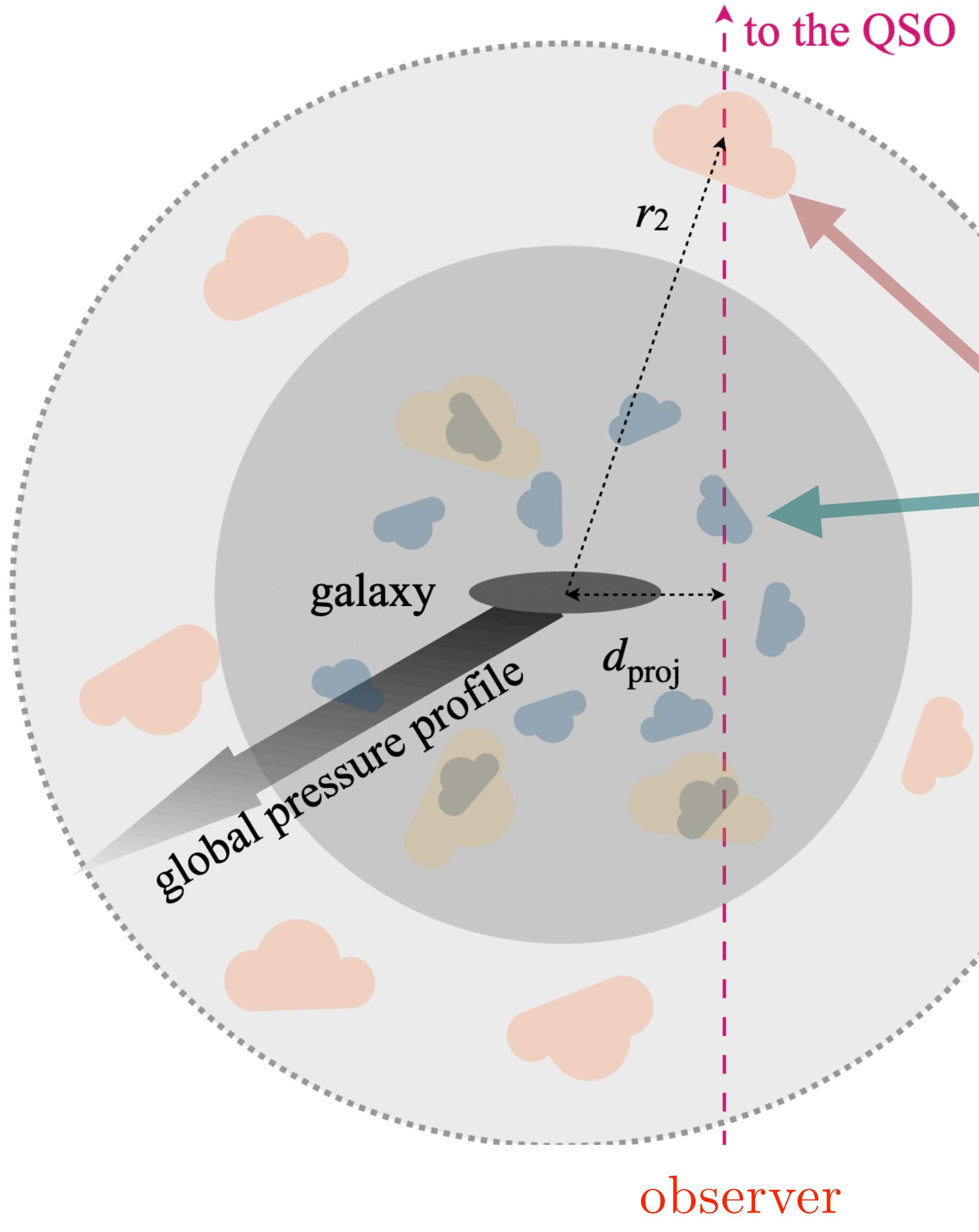

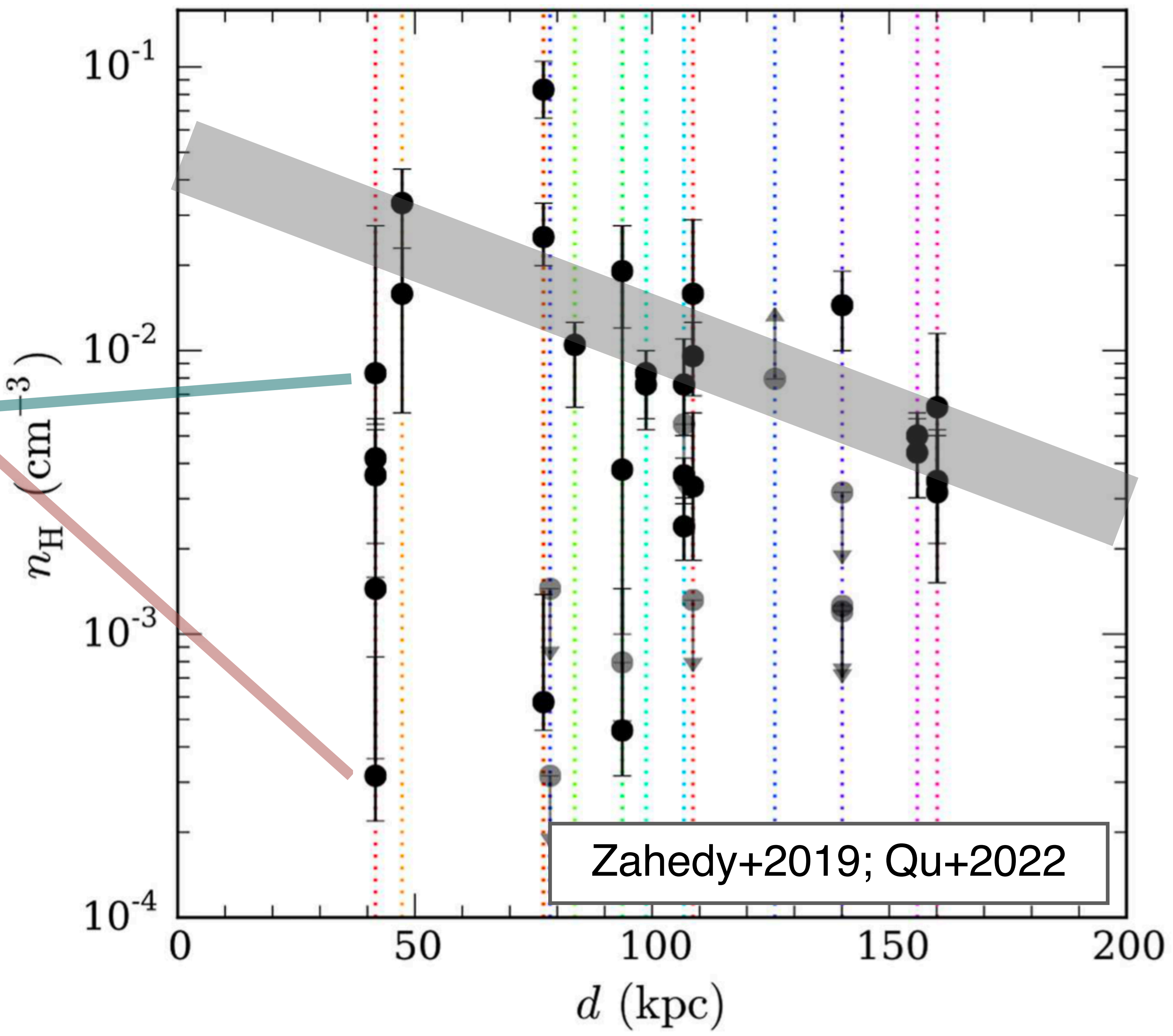

NECESSARY INGREDIENTS FOR ACCURATE IONIZATION MODELS

- broad spectral coverage of multiple ionization states
- high spectral resolution to differentiate gas kinematics and resolve the multiphase structure
- Uncertainties in the ionizing radiation field, global & local

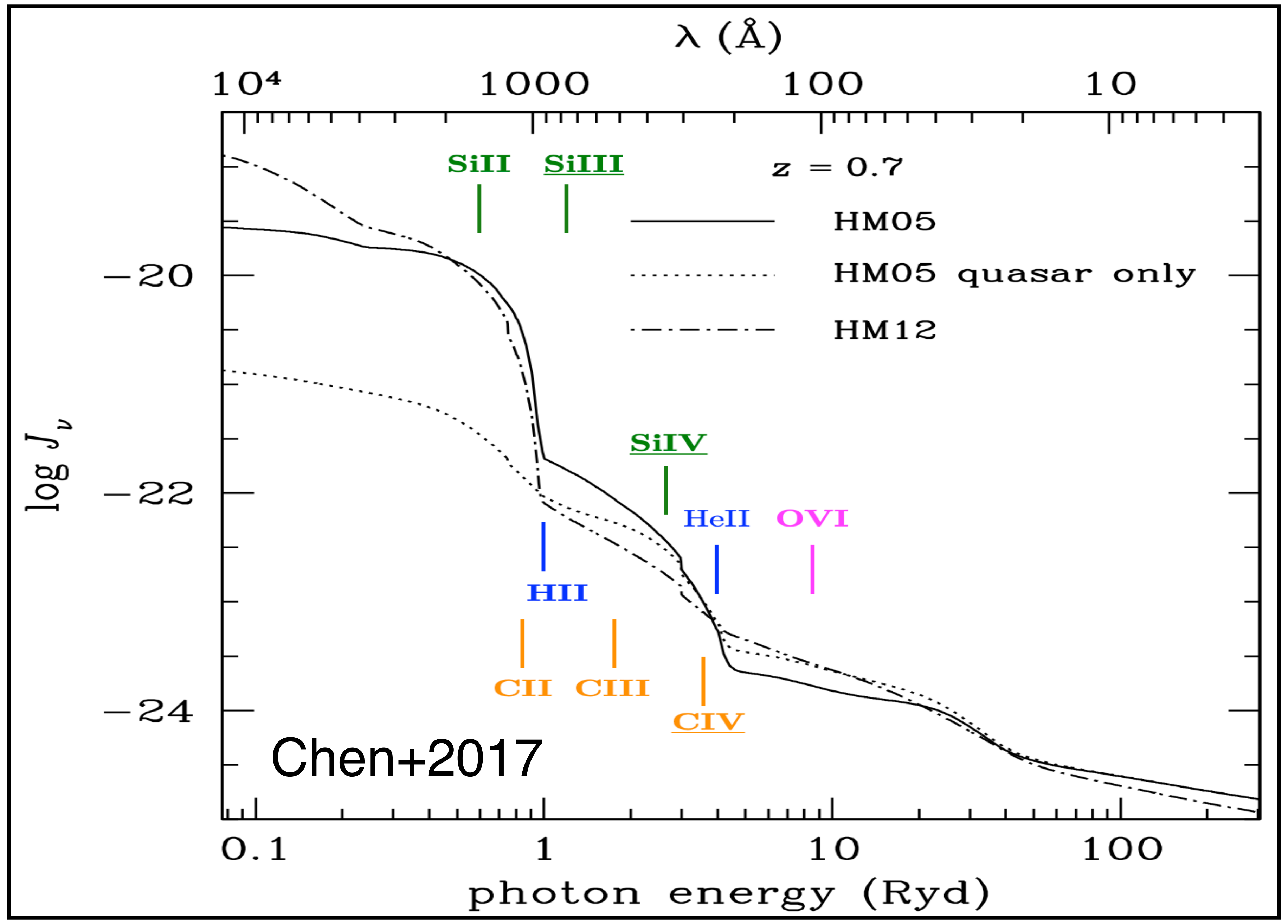

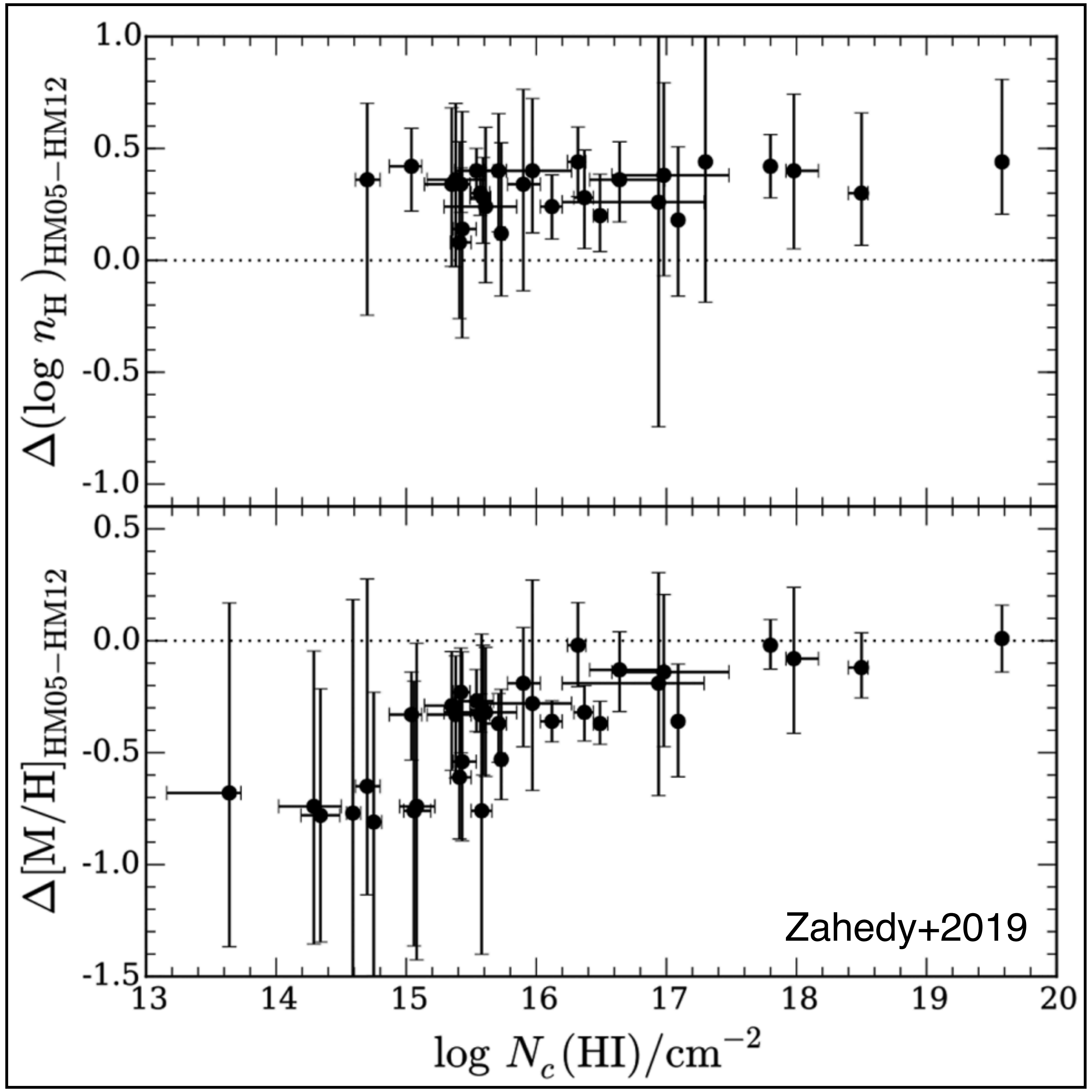

NECESSARY INGREDIENTS FOR ACCURATE IONIZATION MODELS

- broad spectral coverage of multiple ionization states
- high spectral resolution to differentiate gas kinematics and resolve the multiphase structure
- Uncertainties in the ionizing radiation field, global & local

photoionization by a standard UVB can explain all low ions but HeI

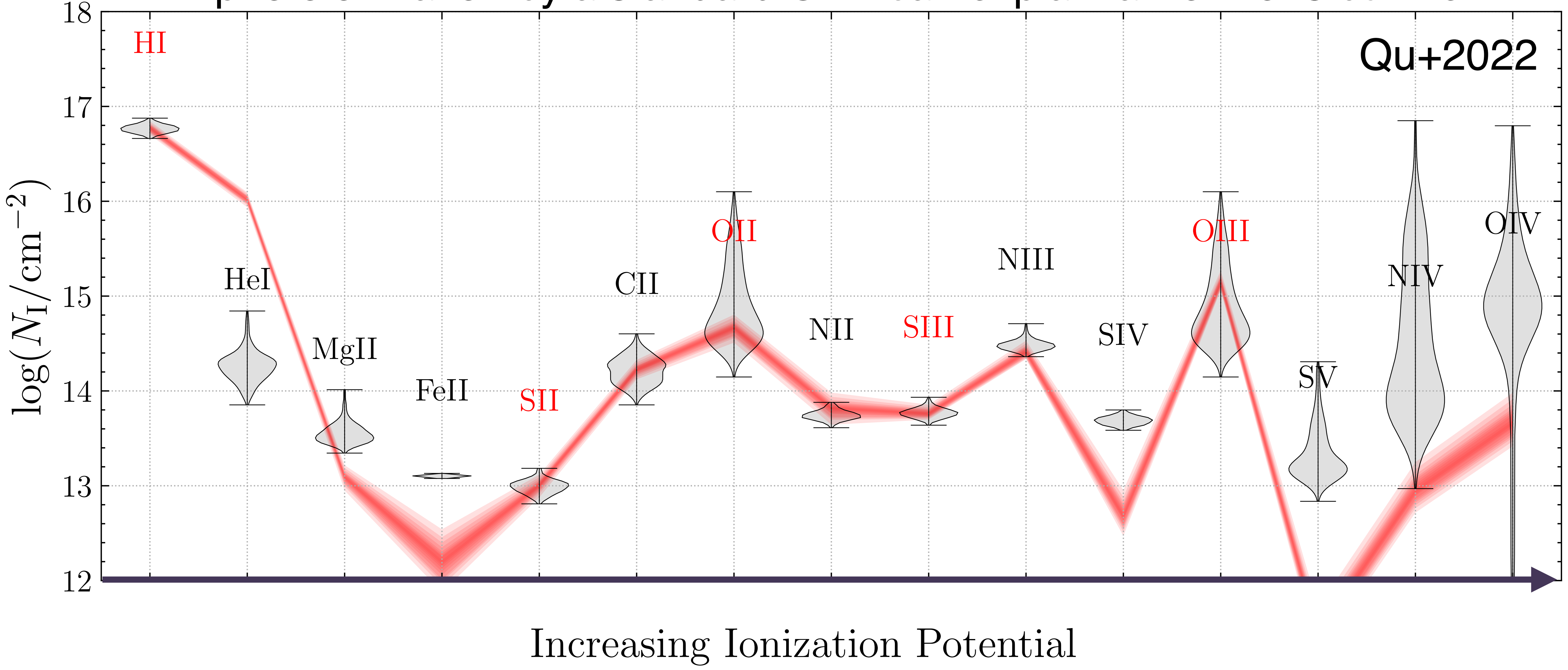

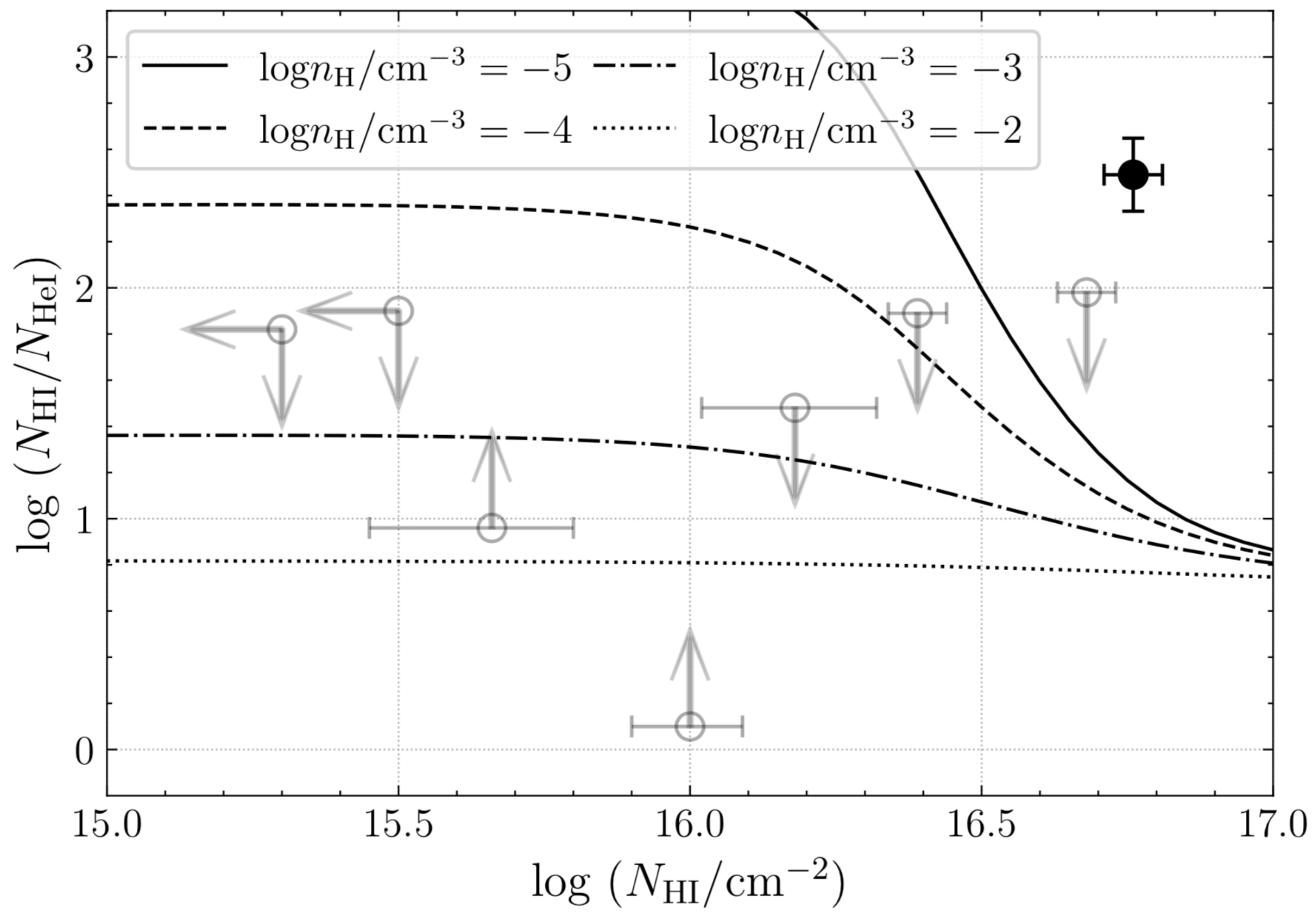

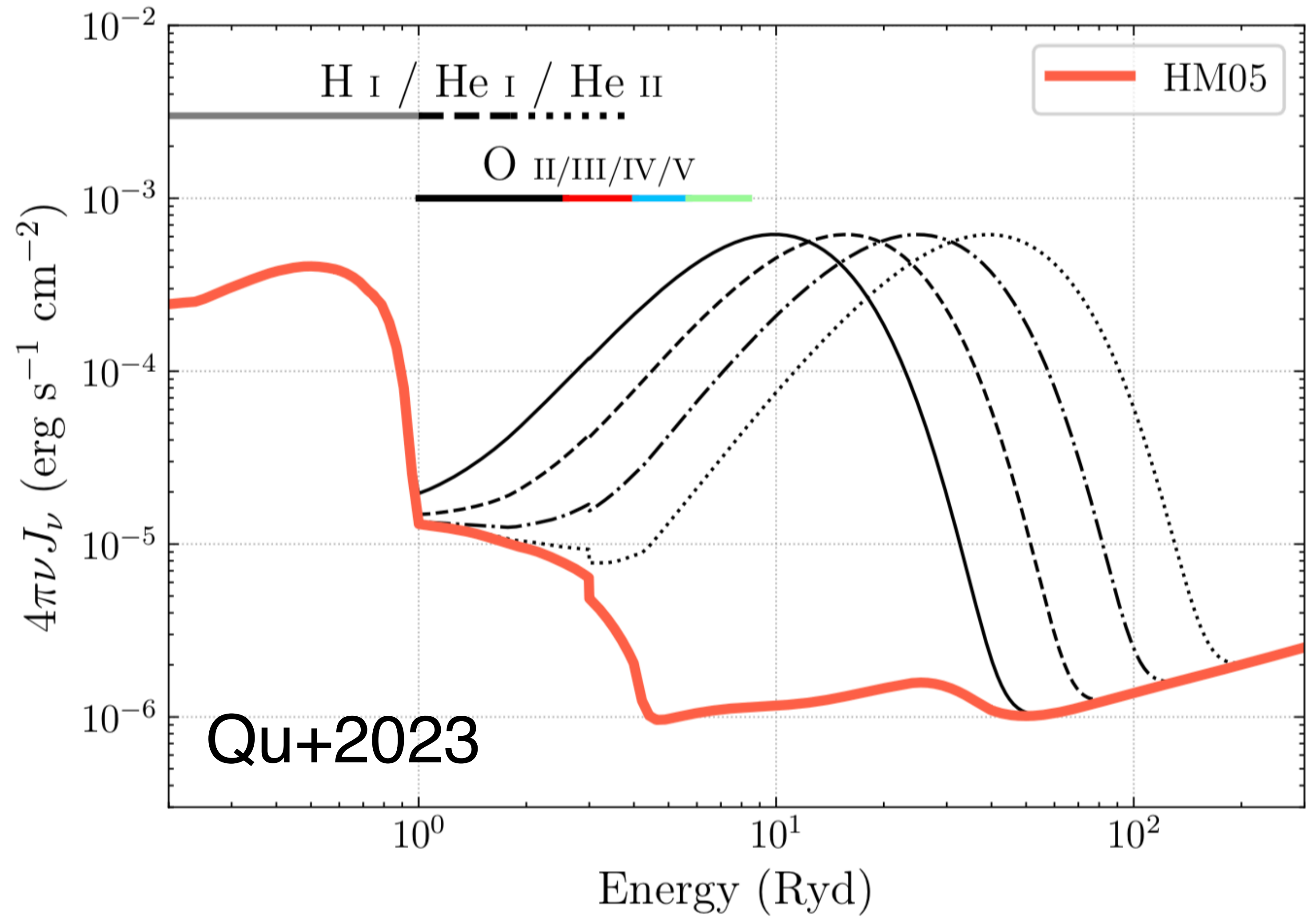

NECESSARY INGREDIENTS FOR ACCURATE IONIZATION MODELS

- broad spectral coverage of multiple ionization states
- high spectral resolution to differentiate gas kinematics and resolve the multiphase structure
- local fluctuations in the ionizing radiation field

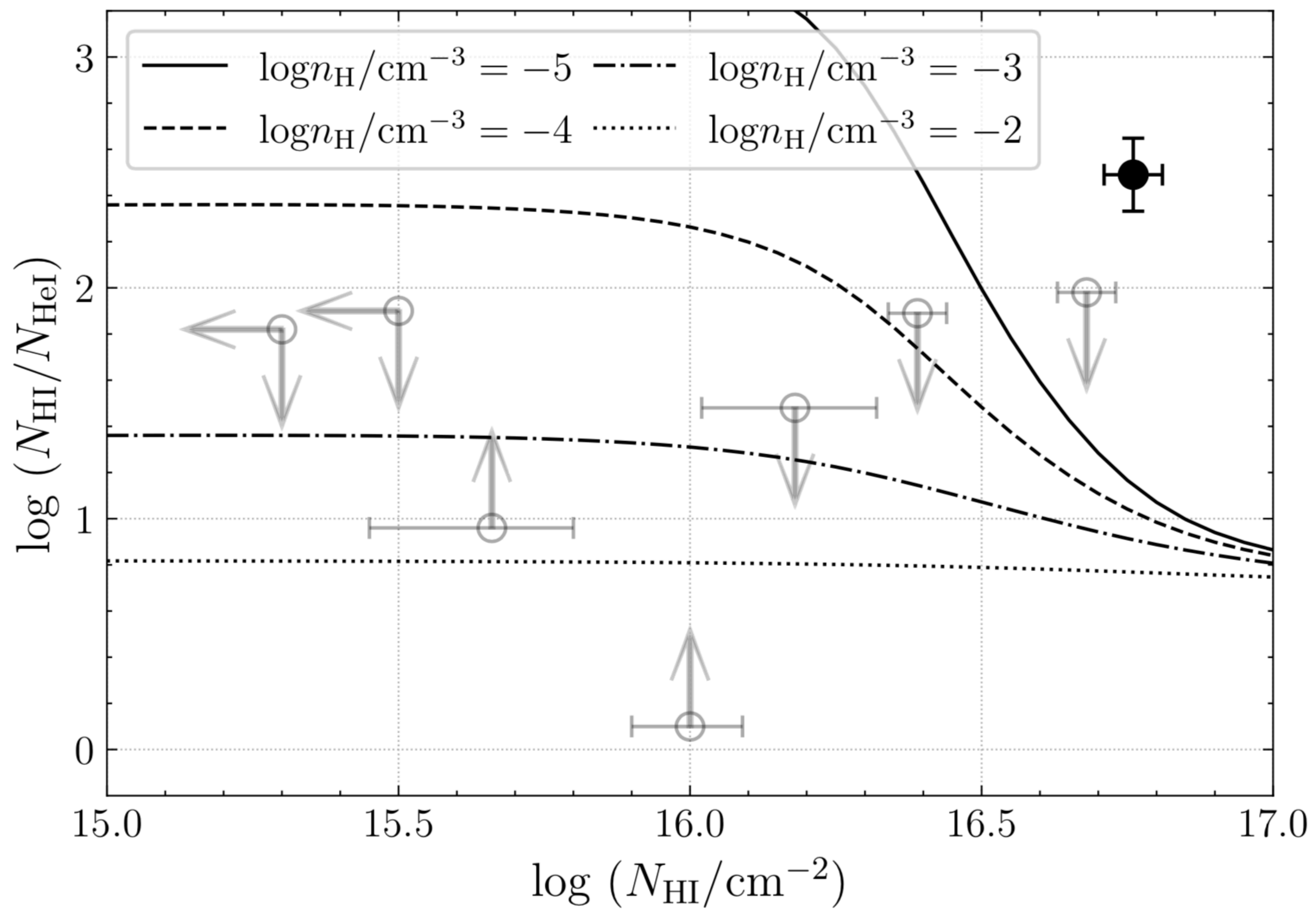

photoionization by a standard UVB + BB brings better agreement

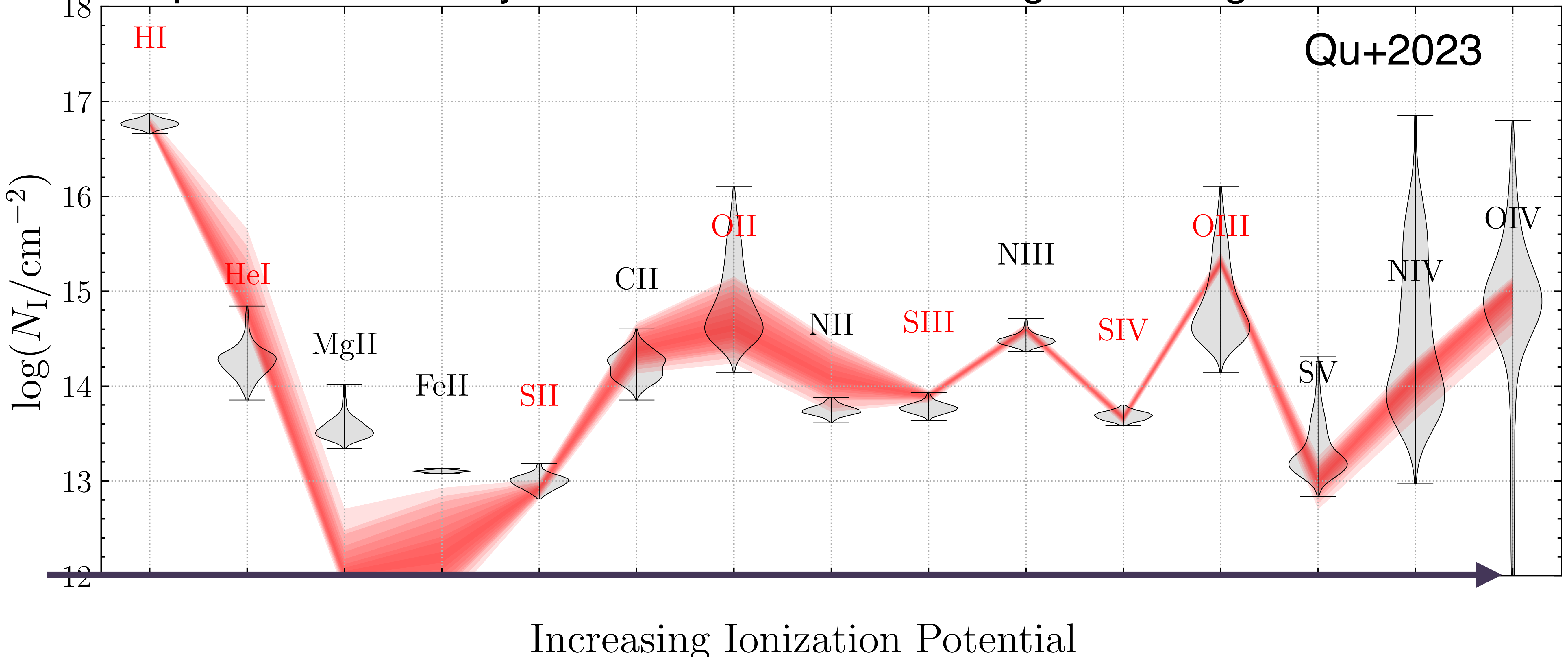

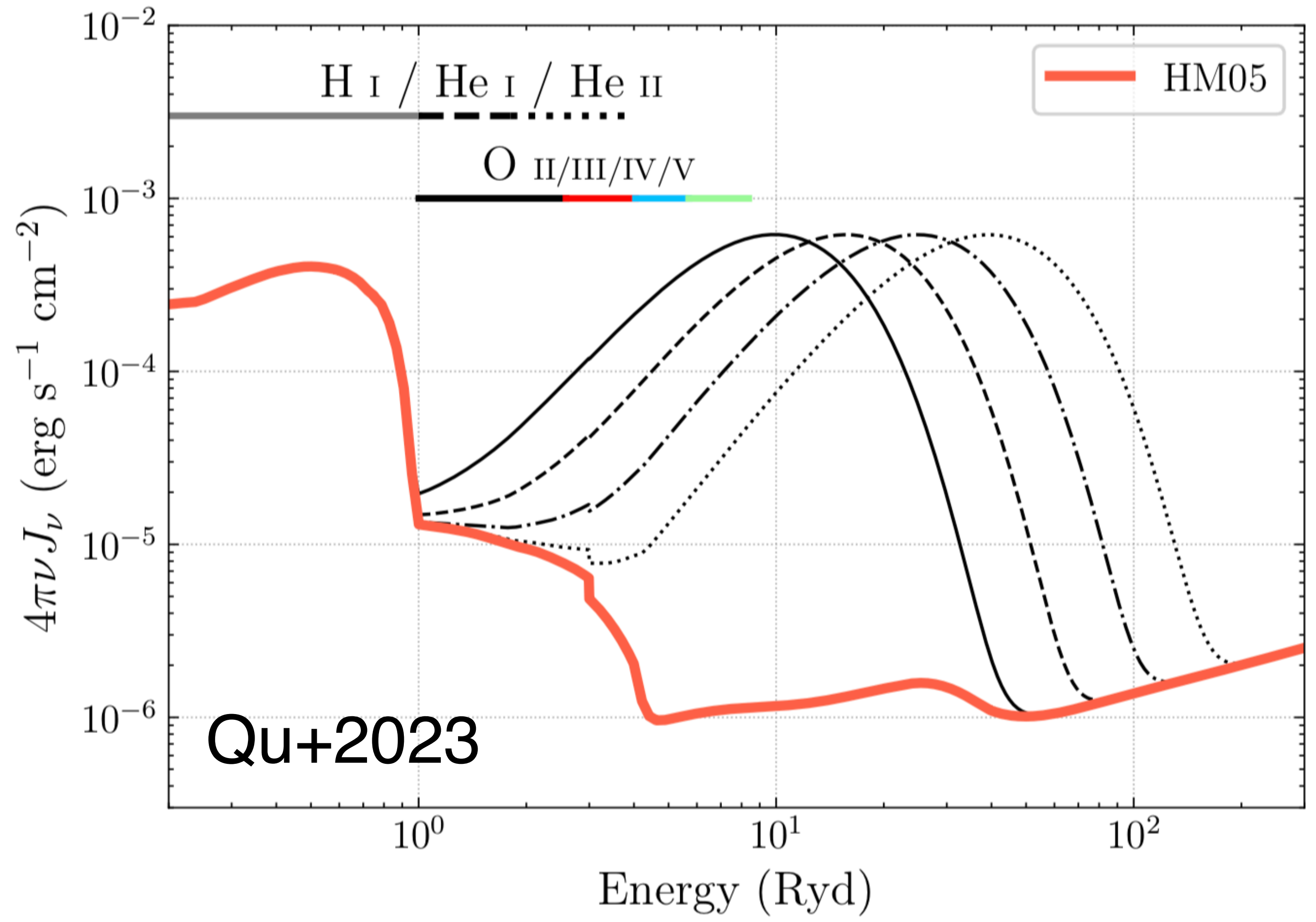

NECESSARY INGREDIENTS FOR ACCURATE IONIZATION MODELS

- broad spectral coverage of multiple ionization states
- high spectral resolution to differentiate gas kinematics and resolve the multiphase structure
- local fluctuations in the ionizing radiation field
- non-solar elemental abundance pattern

non-solar abundance pattern in the CGM

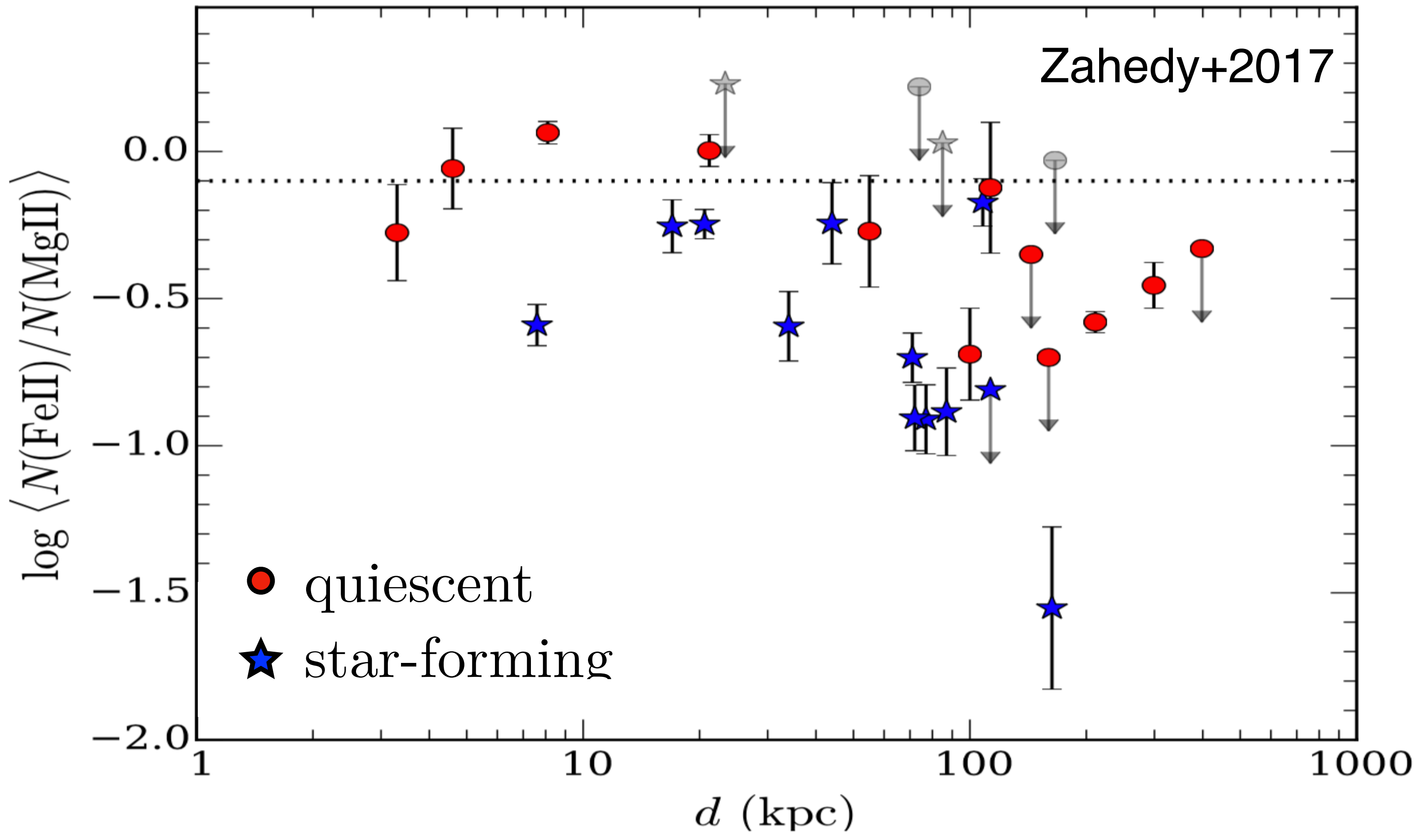

Elemental abundances of Milky Way stars

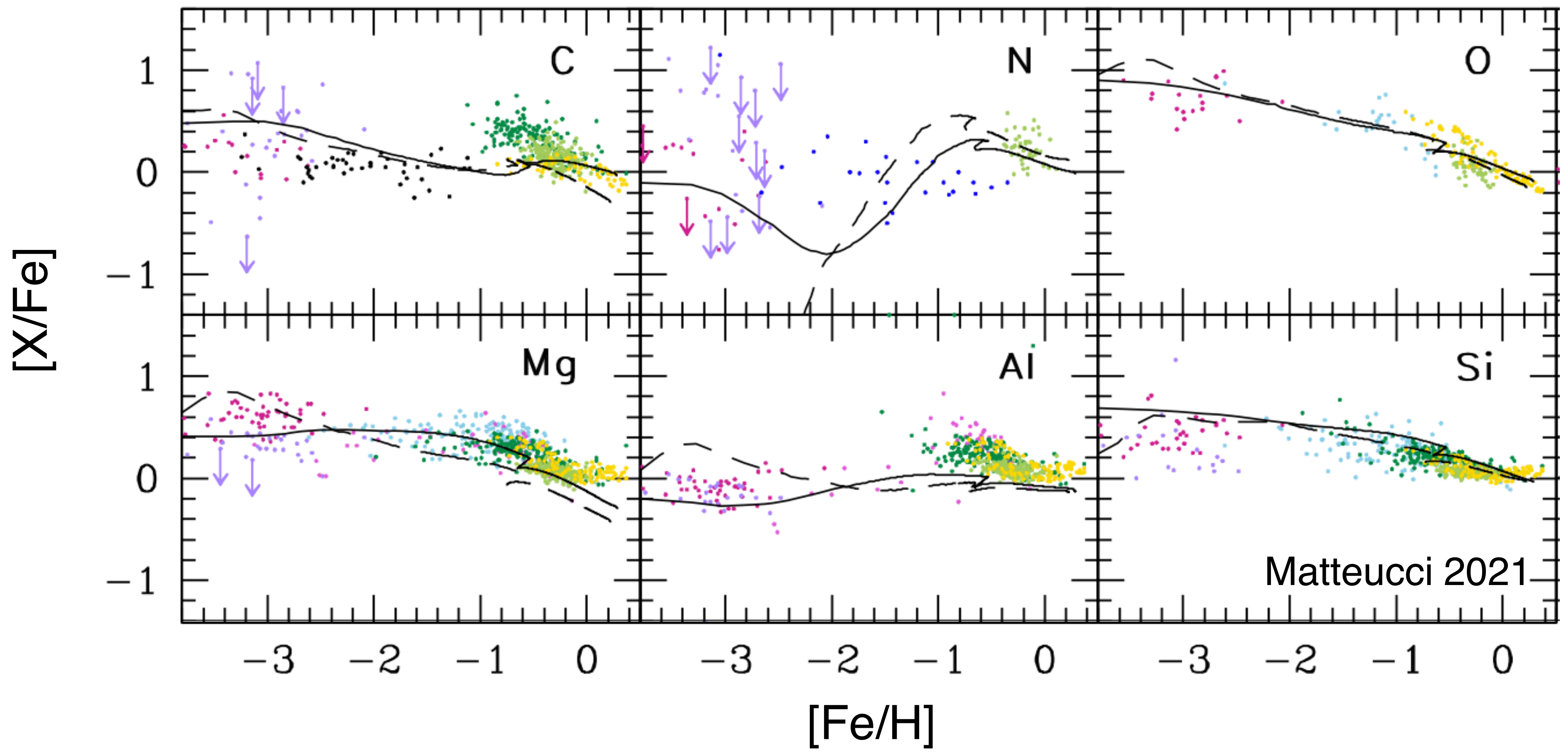

HII region gas-phase elemental abundances

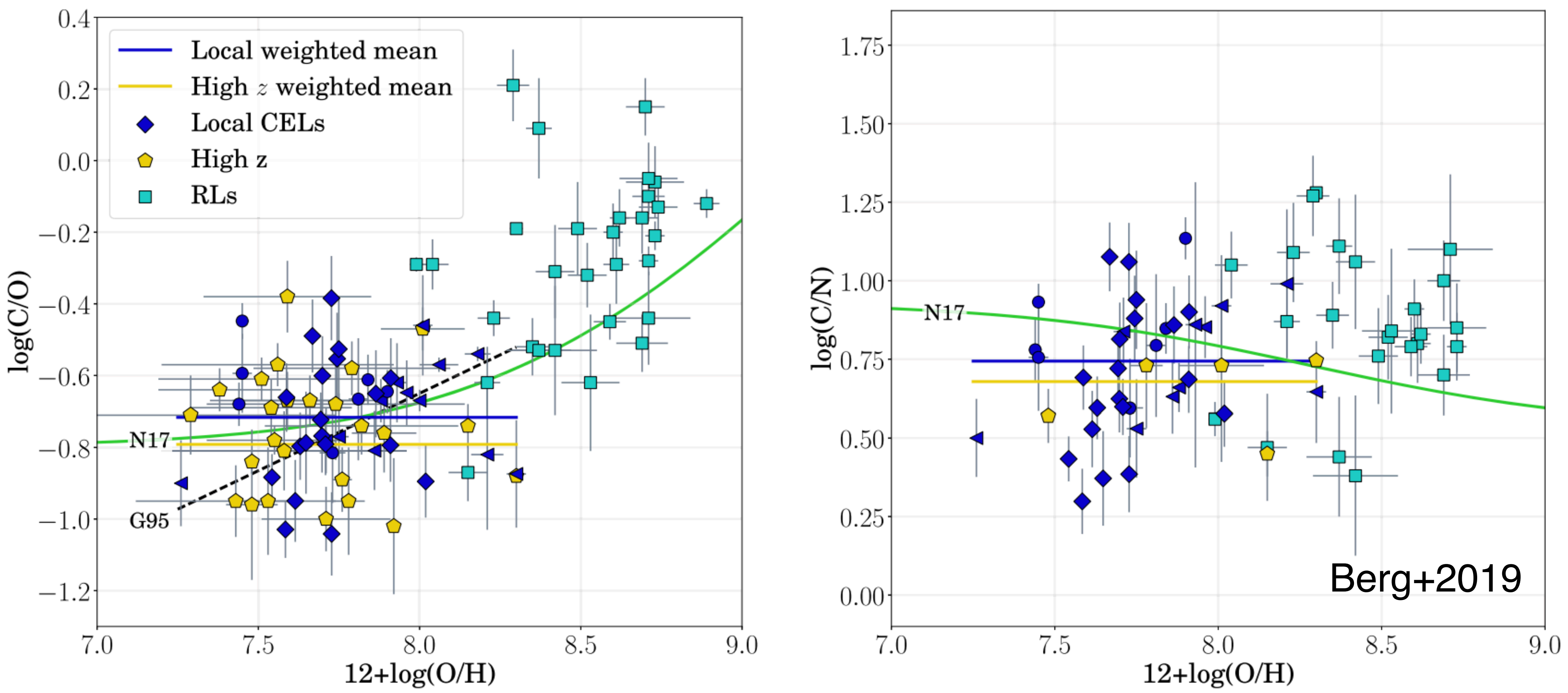

CONNECTING ENRICHMENT PATTERN FROM STARS/ISM TO THE CGM

The Cosmic Ultraviolet Baryon Survey (CUBS)

chemically evolved gas is seen in the low-metallicity CGM

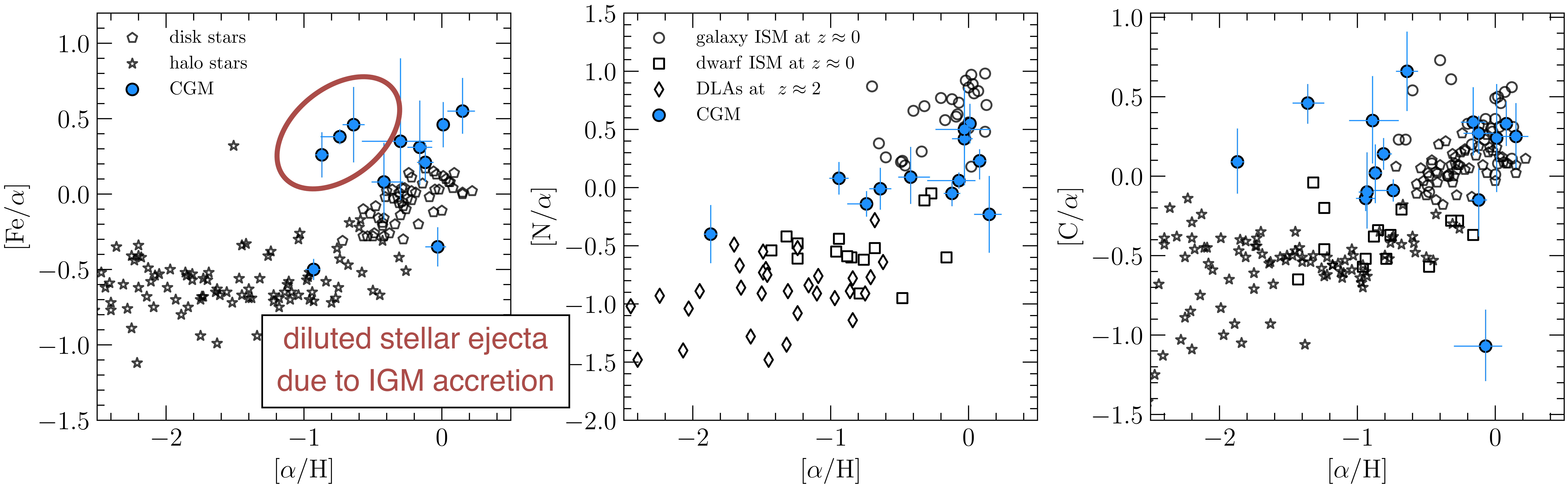

Zahedy+2021, Cooper+2021, Qu+2022

CONNECTING ENRICHMENT PATTERN FROM STARS/ISM TO THE CGM

complex mix of infall and outflows around a mature disk at z~0.4

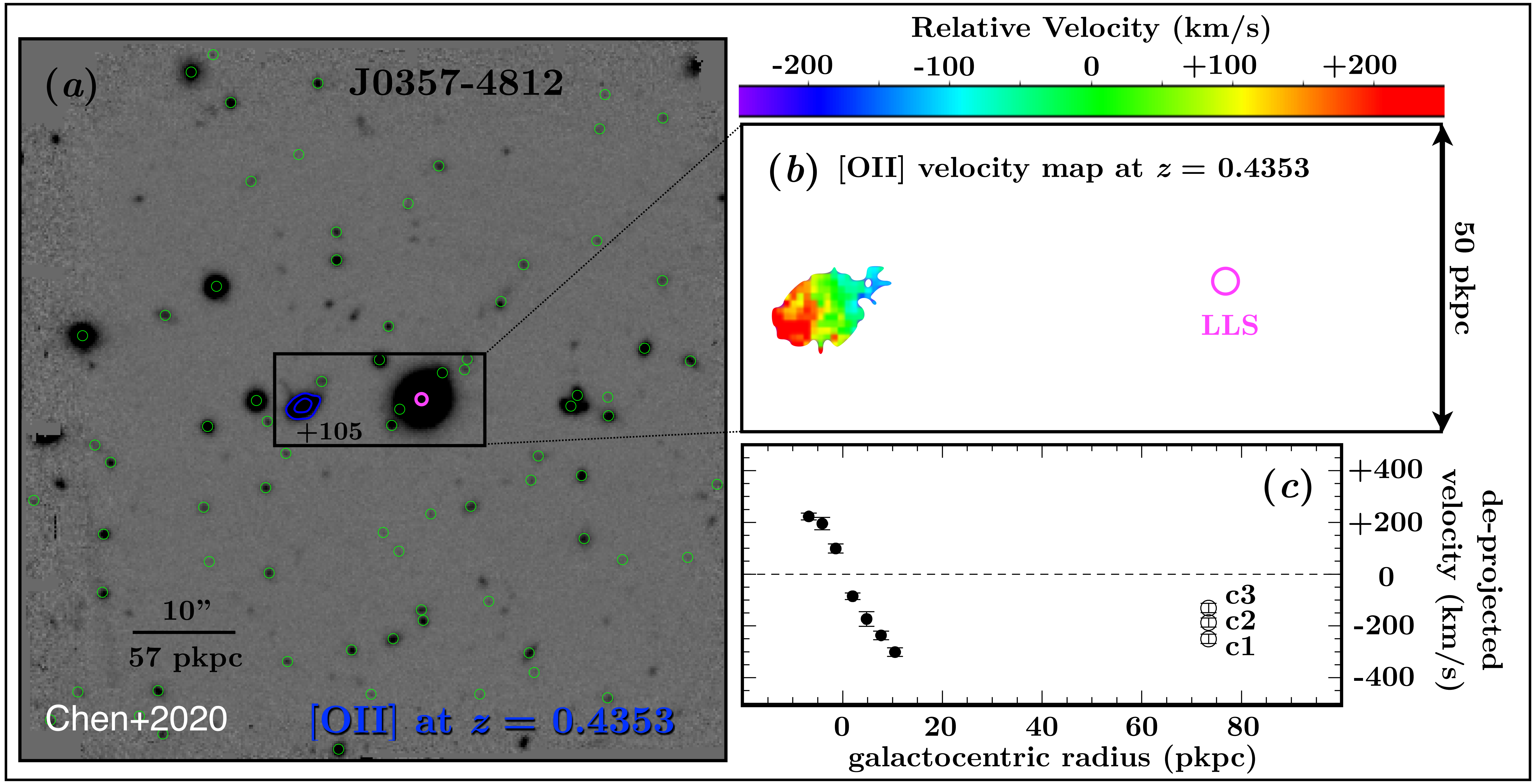

Zahedy+2021

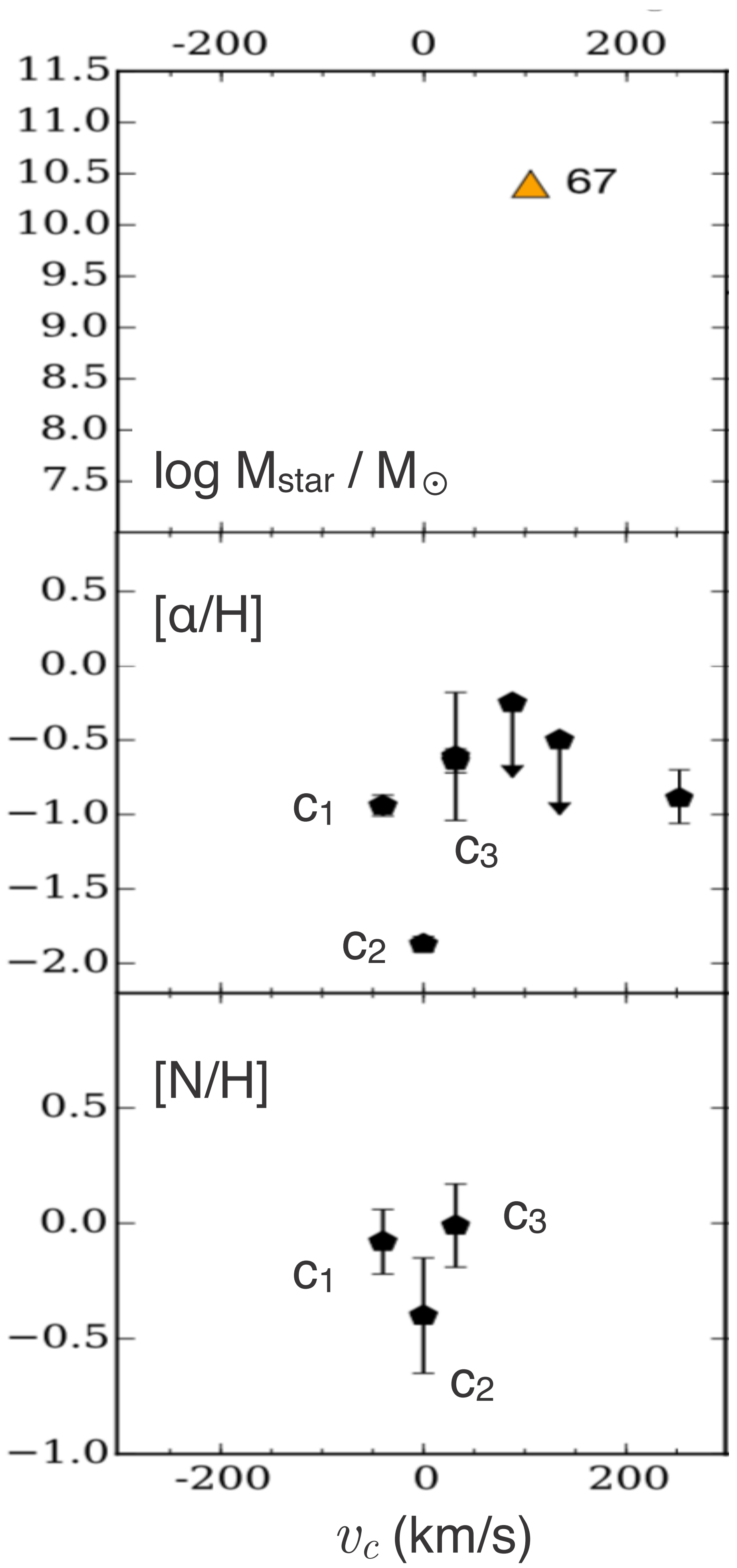

CONNECTING THE MULTIPHASE CGM WITH GALAXY PROPERTIES

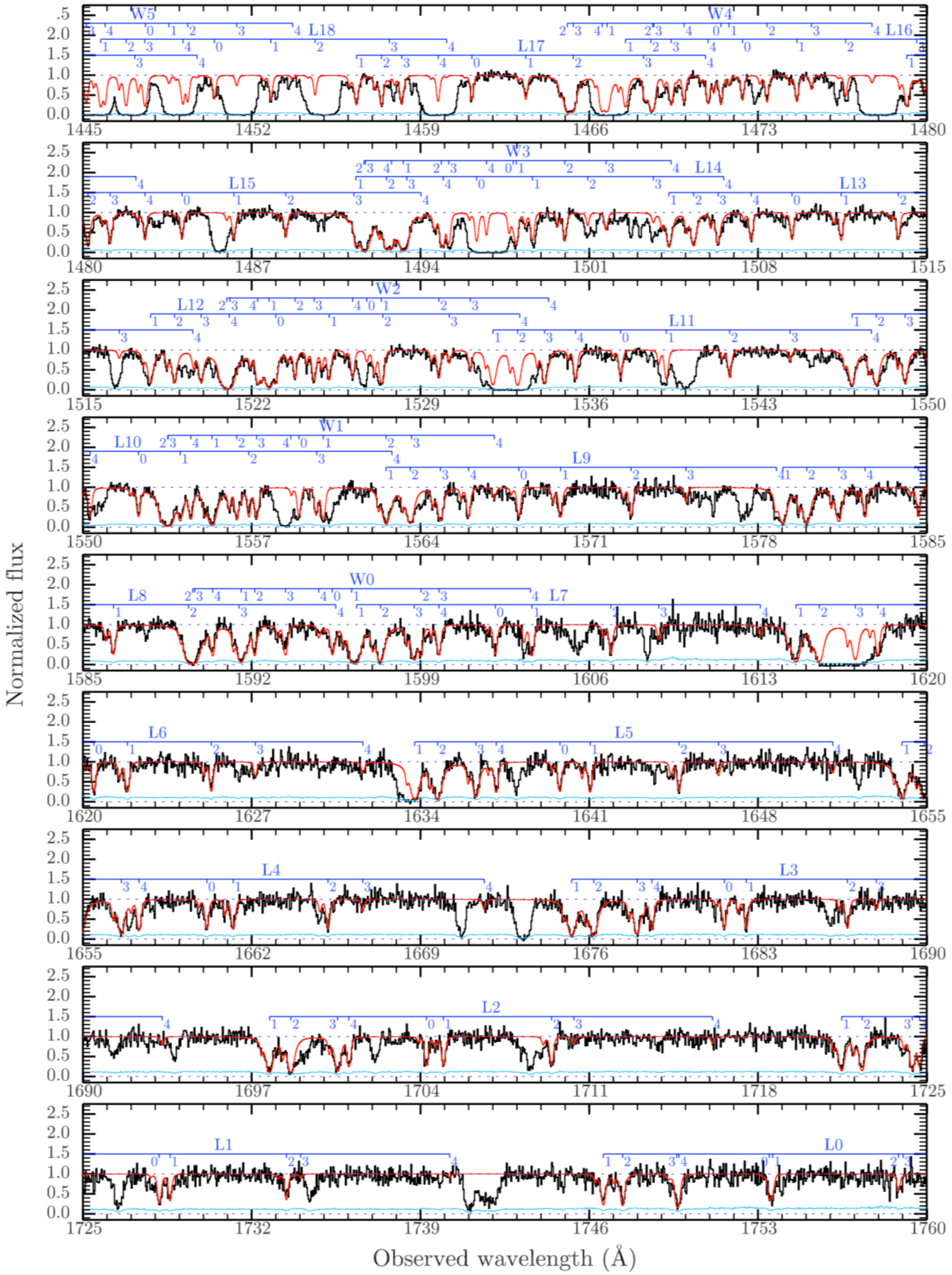

Discovery of circumgalactic molecules at ~40 kpc from an elliptical galaxy

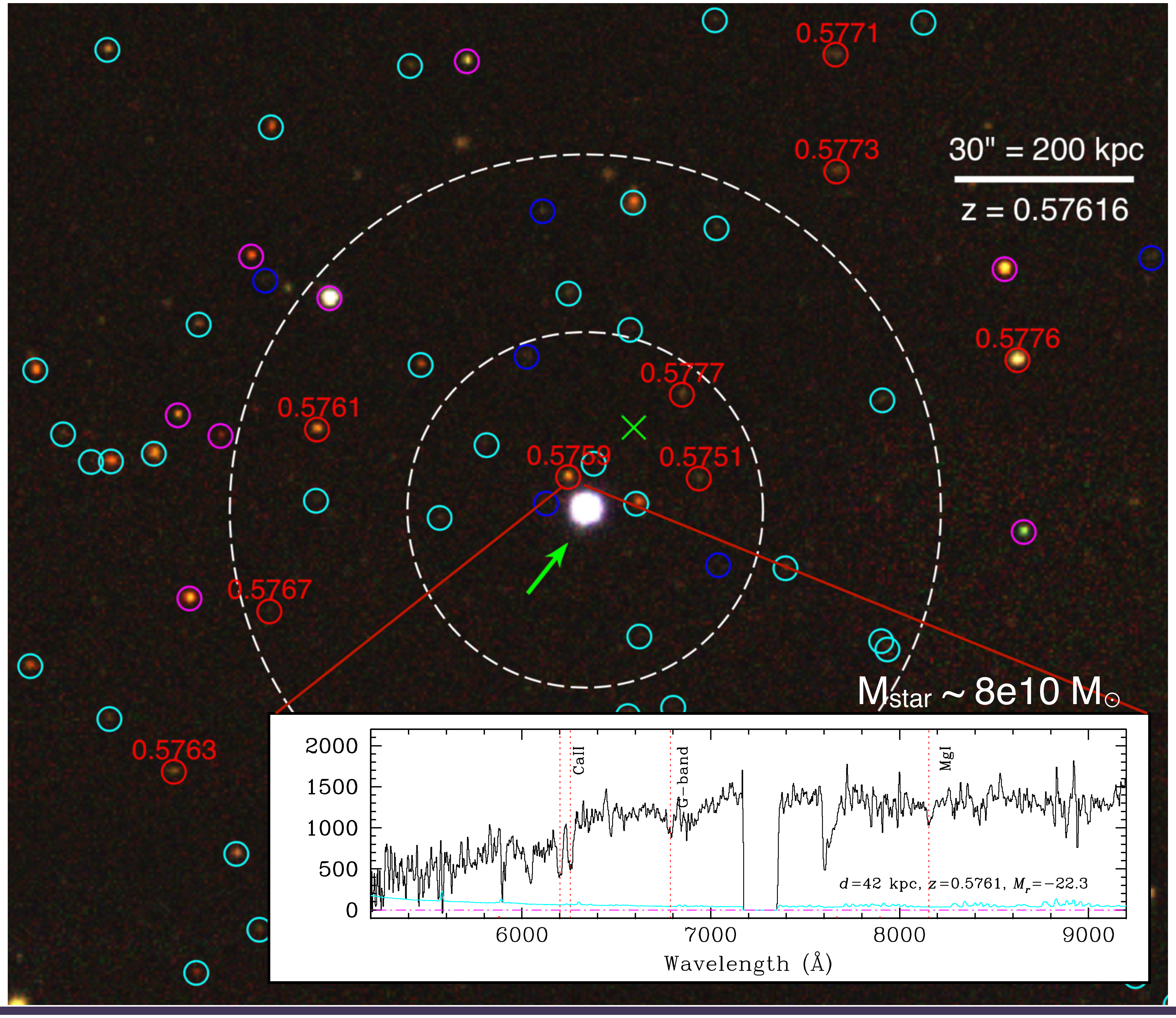

Boettcher+2021

CONNECTING THE MULTIPHASE CGM WITH GALAXY PROPERTIES

Dependence of Internal turbulent energy on star formation history

Thermal energy in individual clumps is $E_T = \frac{1}{\gamma - 1} kT$,

where $\gamma = 5/3$ for a monatomic gas

Turbulent energy is $E_{\rm turb} = \frac{1}{2} \mu m_{\rm H} v_{\rm turb}^2$

The sound speed is $c_s^2 = \frac{\gamma kT}{\mu m_{\rm H}}$

We have $\frac{E_T}{E_{\rm total}} = \frac{1}{1 + \frac{\gamma(\gamma-1)}{2}\mathscr{M}^2}$, where $\mathscr{M} = \frac{v_{\rm turb}}{c_s}$

massive, quenched halos exhibit a higher internal turbulent energy in the cool CGM than star-forming ones.

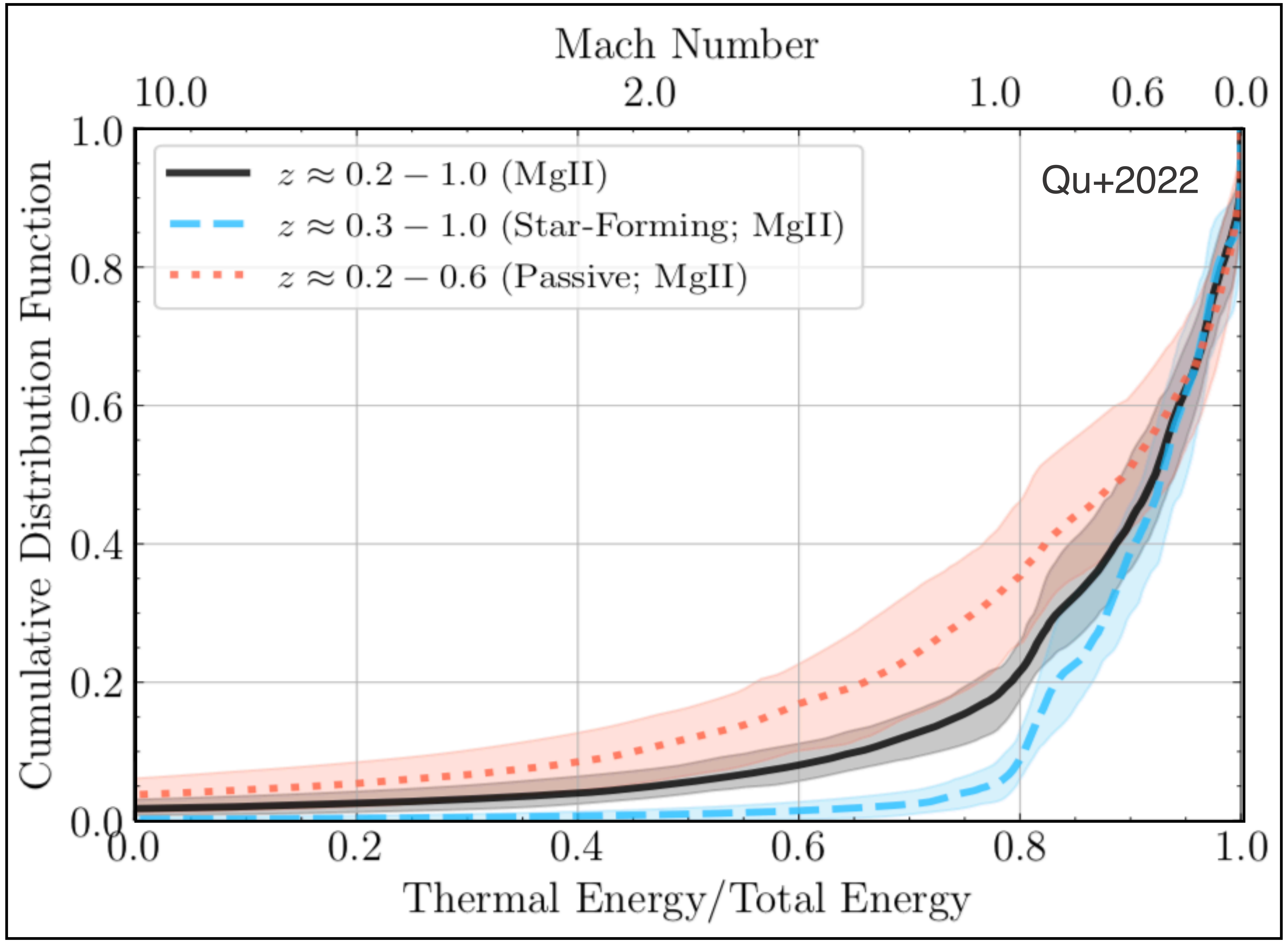

THE TURBULENT VELOCITY-SIZE CORRELATION

High-resolution absorption spectroscopy of a suite of ionic transitions enables identifications of clumps as small as $l_{cl} \approx 1$ pc and densities lower than $n_H \approx 10^{-3}\ cm^{-3}$

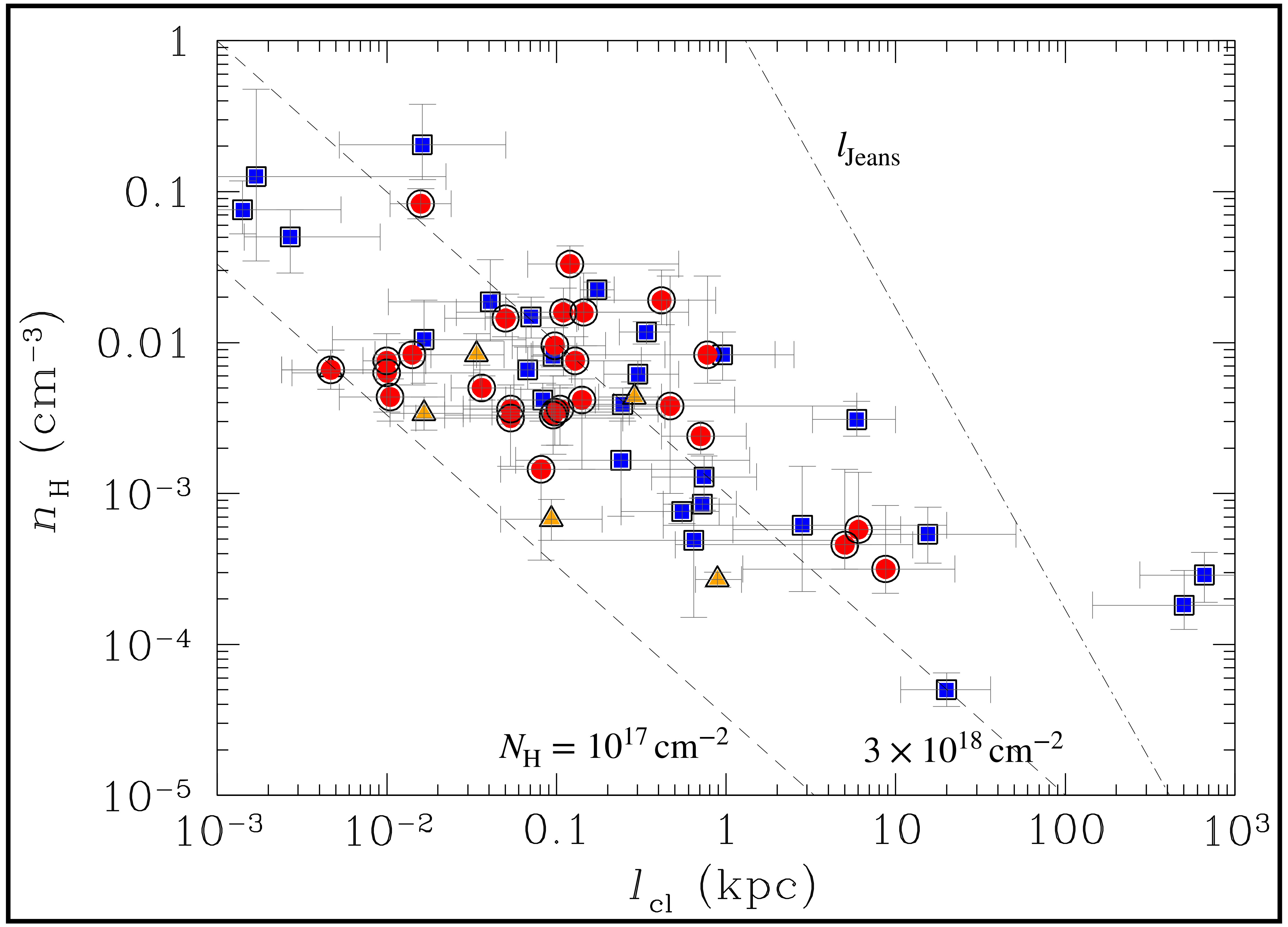

The velocity-size relation shows that the turbulence is subsonic with a constant energy transfer rate of 0.001 cm²/s³ from ~ 1 kpc to ~ 1 pc

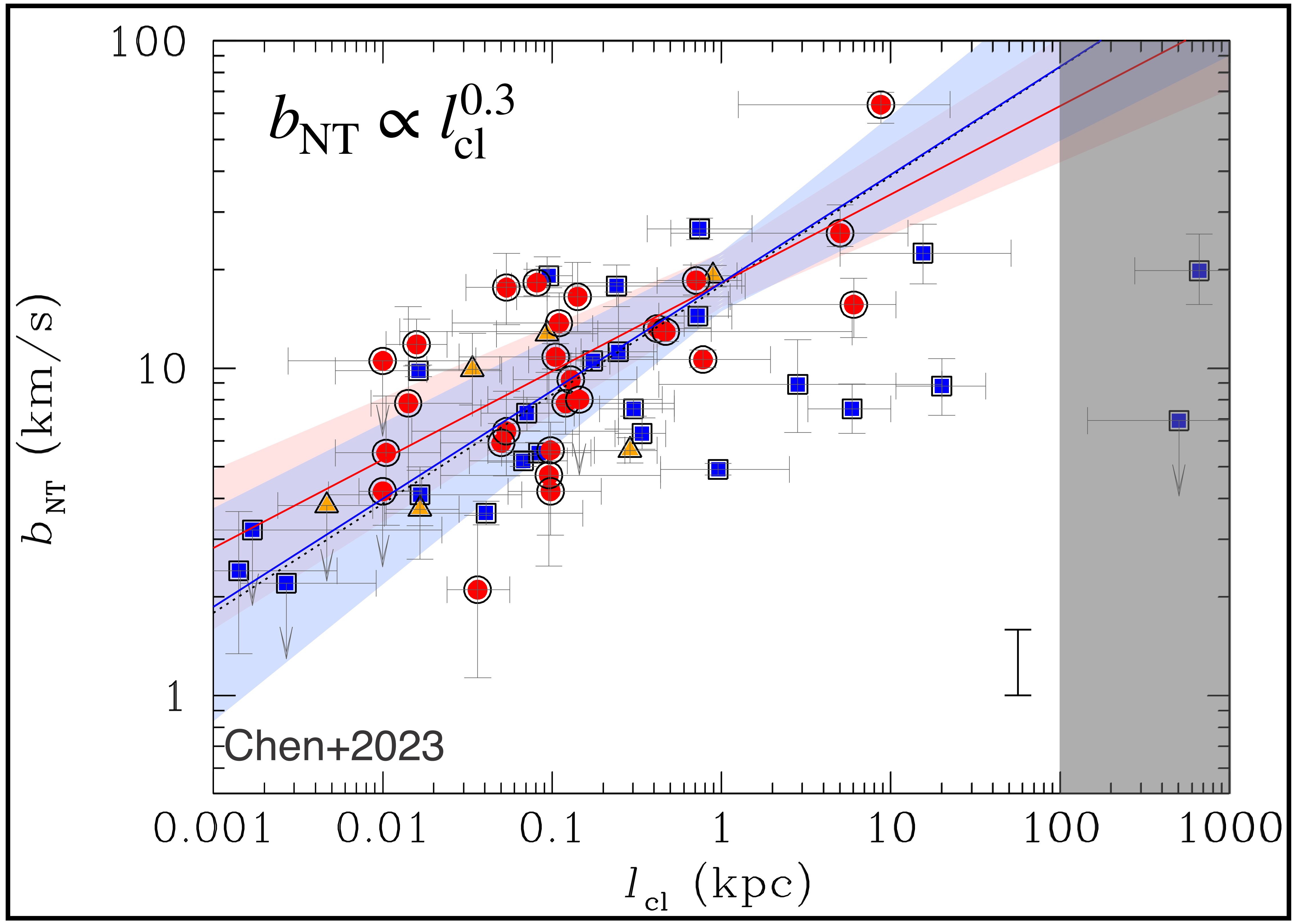

Summary on CGM Absorption

1. Great details have been learned from cross-section studies but a deeper understanding of the gas physics still relies on resolved absorption component studies

2. High-resolution absorption spectra of distant QSOs provide unsurpassed sensitivities for probing the physical, thermodynamic, and chemical conditions of the diffuse multiphase CGM

3. Large variations in density, metallicity, and abundance pattern are directly seen between individually-resolved components arising in the same galactic halo and must be accounted for in ionization models.

4. Local fluctuations in the ionizing radiation field are possible, though no often.

5. Chemically evolved gas is seen in the low-metallicity CGM, indicating a mixture of chemically-enriched outflows and accreted low-metallicity gas

6. The CGM is turbulent, and the turbulence is subsonic with a energy transfer rate at the level of 1% of what is seen in star-forming regions. In addition, massive quiescent halos show a higher fraction of turbulent energy than star-forming halos.